

**R-02-04**

# **Strategy for a Rock Mechanics Site Descriptive Model**

**A test case based on data from  
the Äspö HRL**

John A Hudson (editor)  
Rock Engineering Consultants

June 2002

**Svensk Kärnbränslehantering AB**

Swedish Nuclear Fuel  
and Waste Management Co  
Box 5864  
SE-102 40 Stockholm Sweden  
Tel 08-459 84 00  
+46 8 459 84 00  
Fax 08-661 57 19  
+46 8 661 57 19



# **Strategy for a Rock Mechanics Site Descriptive Model**

## **A test case based on data from the Äspö HRL**

John A Hudson (editor)  
Rock Engineering Consultants

June 2002

This report concerns a study which was conducted for SKB. The conclusions and viewpoints presented in the report are those of the author(s) and do not necessarily coincide with those of the client.

# Preface

This edited and standalone Report focuses on the Test Case undertaken during the development of the Rock Mechanics Site Descriptive Model strategy. The Report has been compiled by collating and compacting the Test Case elements of the associated SKB reports and other contributions which supported the work. Linking narrative has been added to provide introductory material, continuity and conclusions.

The main contributions are from the companion SKB reports listed below.

<i><b>SKB report</b></i>	<i><b>Authors</b></i>	<i><b>Title</b></i>
TR 02-01	Andersson J, Christiansson R, Hudson J. A.	Site Investigations: Strategy for Development of a Rock Mechanics Site Descriptive Model
R 02-01	Röshoff K, Lanaro F, Jing L.	Strategy for a Rock Mechanics Site Descriptive Model: Development and Testing of the Empirical Approach
R 02-02	Staub I, Fredriksson A, Outters, N.	Strategy for a Rock Mechanics Site Descriptive Model: Development and Testing of the Theoretical Approach.
R 02-03	Hakami E, Hakami H, Cosgrove J.	Strategy for a Rock Mechanics Site Descriptive Model: Development and Testing of an Approach to Modelling the State of Stress.
R 02-11	Makurat A, Løset F, Hagen A W, Tunbridge L, Kveldsvik V, Grimstad E.	Äspö HRL: A Descriptive Rock Mechanics Model for the 380–500 m level

The reports listed above, R 02-01, R 02-02, R 02-03 and R 02-11, are reports from the respective contracting organizations: BBK, Golder Associates, Itasca and NGI.

Additionally, information from the following sources has been used in the preparation of this report.

- SKB TR 97-06. Rhén I, Gustafson G, Stanfors R, Wikberg P. Äspö HRL – Geoscientific evaluation 1997/5: Models based on site characterization 1986–1995.
- Unpublished report by Andersson J. and Hudson J. A. on the Project Plan for the Test Case.
- Unpublished report by Andersson J. and Stigsson M. on the comparison of predicted and ‘best estimate’ rock properties, see the figures in Section 4.5.
- RVS modelling information provided by Stigsson M.
- Minutes of various meetings written by Andersson C, Andersson J, and Hudson J A.

The report has been edited by J A Hudson, with assistance from R Christiansson and J Andersson.



# Summary

In anticipation of the SKB Site Investigations for radioactive waste disposal, an approach has been developed for the Rock Mechanics Site Descriptive Model, as described in /Andersson et al, 2002/. This approach was tested by predicting the rock mechanics properties of a 600 m × 180 m × 120 m rock volume at the Äspö Hard Rock Laboratory (HRL) using limited borehole data of the type typically obtained during a site investigation. These predicted properties were then compared with ‘best estimate’ properties obtained from a study of the test rock volume using additional information, mainly tunnel data. The exercise was known as the Test Case, and is the subject of this Report.

Three modelling techniques were used to predict the rock properties:

- the ‘empirical approach’ – the rock properties were estimated using rock mass classification schemes and empirical correlation formulae;
- the ‘theoretical approach’ – the rock properties were estimated using numerical modelling techniques; and
- the ‘stress approach’ – the rock stress state was estimated using primary data and numerical modelling.

These approaches are described separately and respectively in /Röshoff et al, 2002; Staub et al, 2002; Hakami et al, 2002/. The work describing the ‘best estimates’ of the actual rock conditions based on all available information from the Äspö HRL is described in /Makurat et al, 2002/.

Following an explanation of the context for the Test Case within the strategy for developing the Rock Mechanics Site Descriptive Model, conditions at the Äspö HRL are described in Chapter 2. The Test Case organization and the suite of nine Protocols used to ensure that the work was appropriately guided and co-ordinated are described in Chapter 3. The methods for predicting the rock properties and the rock stress, and comparisons with the ‘best estimate’ properties of the actual conditions, are presented in Chapters 4 and 5.

Finally, the conclusions from this Test Case exercise are given in Chapter 6. General recommendations for the management of this type of Test Case are also included.



# Sammanfattning

Inom ramen för SKB:s förberedelser för platsundersökningsprogrammet har en strategi utvecklats för bergmekanisk platsmodellering, som beskrivits av /Andersson m fl, 2002/. Strategin testades genom att prognostisera de mekaniska egenskaperna i en 600mx180mx120m stor bergvolym vid Äspö Hard Rock Laboratory (HRL), genom att använda en begränsad mängd borrhålsinformation, med data typiska för vad som avses insamlas under platsundersökningarna. Sedan jämfördes de prognostiserade egenskaperna med de "bästa" bedömda egenskaperna baserad på ytterligare information, främst data från tunnarna. Tillämpningsövningen kallades Test Case (praktikfall), och avrapporterades i denna rapport.

Tre modellerings tekniker användes för att prognostisera bergegenskaper:

- det empiriska angreppssättet – bergets mekaniska egenskaper bedömdes med stöd av empiriska klassningssystem och empiriska korrelationer.
- det teoretiska angreppssättet – bergmekaniska egenskaper bedömdes genom numerisk modelleringsteknik.
- spänningsmodell – bergets spänningstillstånd bedömdes med stöd av primärdata och numerisk modellering.

Dessa angreppssätt beskrivs separat av /Röshoff m fl, 2002; Staub m fl, 2002; Hakami m fl, 2002/. Den "bästa" bedömningen, baserad på all tillgänglig information beskrivs av /Makurat m fl, 2002/.

Efter beskrivning av hur detta praktikfall var en del av utvecklingen av strategin för platsbeskrivande bergmekanisk modellering beskrivs platsförhållandena vid Äspö HRL i kapitel 2. Strukturering av praktikfallet och implementering av nio protokoll för att leda och samordna arbetet beskrivs i kapitel 3. Metoderna för att prognostisera bergmassans mekaniska egenskaper och spänningstillstånd beskrivs i kapitlen 4 och 5.

Avslutningsvis ges de specifika slutsatserna från praktikfallet i kapitel 6. Där ges även rekommendationer för genomförande av denna typ av praktikfall.





# Contents

<b>1</b>	<b>Introduction</b>	13
1.1	SKB Site investigations	13
1.2	Development of the Rock Mechanics Site Descriptive Model strategy and the Test Case	13
1.3	The Test Case objectives and work programme	17
<b>2</b>	<b>The Äspö Hard Rock Laboratory (HRL) and the Test Case site</b>	19
2.1	Äspö HRL location and geological overview	19
2.2	The Äspö HRL Test Case location	21
2.3	Rock types, geometrical scales, fracturing, mechanical properties and stress state at the Äspö HRL site	22
2.3.1	Rock types	22
2.3.2	Geometrical scales	23
2.3.3	Fracturing	23
2.3.4	Mechanical properties	26
2.3.5	Rock stress conditions	27
2.3.6	Further information	28
<b>3</b>	<b>Test Case organization and procedure</b>	29
3.1	The Test Case Project Plan	29
3.2	Test Case phases	30
3.2.1	Phase 1 – Development of a plan for the Test Case	30
3.2.2	Phase 2 – Preparation of data sets	30
3.2.3	Phase 3 – Predictions and evaluation	31
3.2.4	Phase 4 – Documentation	31
3.3	The Use of Protocols	31
3.3.1	Listing of parameters – Protocol 1	32
3.3.2	Representation of uncertainty – Protocol 2	35
3.3.3	Specification of the parameter ‘ranges’ – Protocol 3	35
3.3.4	Input data to be used for the Test Case – Protocol 4A	36
3.3.5	Predictions – Protocols 4B and 5	39
3.3.6	The ‘best estimate’ of rock properties for the 380–500m level model – Protocol 6	41
3.3.7	Evaluation of results – Protocols 7 and 8	42
3.3.8	Documentation – Protocol 9	45
3.4	Information supplied to the Teams and block numbering specification	45
3.4.1	Information supplied to the teams predicting the rock properties	45
3.4.2	Additional information supplied to the Team establishing the ‘best estimate’ of the rock properties.	47
3.4.3	Numbering of the individual blocks in the target volume	48
<b>4</b>	<b>Modelling the mechanical properties</b>	49
4.1	The empirical approach	49
4.1.1	Equations for determining strength and modulus of deformation	51
4.1.2	Confidence levels	51

4.1.3	Initial stress field and groundwater issues	52
4.1.4	Dealing with uncertainty and variability issues	52
4.1.5	The division of the core sections and the nested data processing forms	54
4.1.6	Results for the 380–500 m model	56
4.1.7	Quantification of the uncertainty in the characterization ratings and parameters	58
4.2	The theoretical approach	59
4.2.1	Methodology	59
4.2.2	Input data to the theoretical approach	63
4.2.3	Set-up of the numerical model	63
4.2.4	Sensitivity analyses using the model	65
4.2.5	Set-up for the fracture zones	67
4.2.6	Distribution of the parameters – Monte Carlo simulations	68
4.2.7	Review of the input data	71
4.2.8	Data uncertainty	72
4.2.9	Output data from the Test Case modelling	73
4.3	The empirical-theoretical consensus approach	75
4.4	‘Best estimates’ of the actual rock conditions	76
4.4.1	Methodology	76
4.4.2	Fracture zones	77
4.4.3	Model A – based on conventional rock mass classification	77
4.4.4	Model B – based on a characterization approach	78
4.4.5	Comparison of the Model A and Model B ‘best estimates’	79
4.5	Comparison of the empirical and theoretical model results with the ‘best estimate’ reference model results	80
4.5.1	Presentation of results	80
4.5.2	Deformation modulus	81
4.5.3	Rock mass strength parameters	83
<b>5</b>	<b>Modelling the state of stress</b>	<b>87</b>
5.1	Initial stress prediction from database information	87
5.1.1	Stress magnitudes	87
5.1.2	Stress orientations	91
5.1.3	Description of uncertainty and spatial variability parameters	92
5.1.4	Initial prediction for the 550 m block	93
5.1.5	Initial prediction for the Target Block	93
5.2	Site specific information	94
5.2.1	Geological information from the Test Case site	94
5.2.2	Stress measurement from the Test Case site	95
5.3	Numerical analysis of in situ stress	100
5.3.1	Geometry of the 3DEC model	100
5.3.2	Examples of results from 3DEC models	102
5.4	Final in situ stress prediction	104
5.4.1	Prediction of the stress field in the 550 m block	104
5.4.2	Stress prediction for the 380–500 level Target Block	107
5.5	Comparison with the ‘best estimate’ reference results	108
<b>6</b>	<b>Conclusions</b>	<b>109</b>
6.1	Test Case conclusions	109
6.1.1	Overall conclusions	109

6.1.2	Characterizing, modelling and predicting the mechanical properties	110
6.1.3	Modelling and predicting the state of stress	113
6.1.4	The ‘best estimate’ of the actual conditions	113
6.2	Recommendations for general rock mechanics site characterization and Test Case work	114
<b>7</b>	<b>References</b>	<b>115</b>
	<b>Appendix – Test Case Protocol 4B for Individual Model Predictions</b>	<b>119</b>



# 1 Introduction

The Test Case work described in this report was undertaken as one of the components in developing the approach to the Rock Mechanics Site Descriptive Model for the site investigations to be carried out by the Swedish Nuclear and Fuel Waste Management Company (SKB). The development of the work items is presented, together with the associated conclusions and recommendations. The content of the report should not be interpreted as necessarily being SKB's view of a recommended approach to the rock mechanics aspects of site characterization.

## 1.1 SKB Site investigations

SKB is responsible for managing Sweden's nuclear waste and is currently planning to carry out site investigations for the deep repository for spent fuel /SKB, 2001a/. These site investigations are comprehensive studies of the bedrock and the surface ecosystem using surface and borehole data. During this phase, detailed studies will also be made on how the available generic design of a KBS-3 Deep Repository could be sited, and the associated transport accommodated, as well as assessing the environmental consequences of construction and operation and the subsequent closure of the repository. The investigations are planned at different granitic rock sites in Sweden.

Work on the Design and Safety Assessment, as well as studies of the Environmental Impact Assessment, will be carried out in parallel and will therefore allow feedback to the characterization programme /SKB, 2001b/ which defines the different characterization stages and describes the interaction needed between different disciplines. The selection of information to be considered during the site characterization program will depend on several assessments of what is required for use in the safety assessment and design.

## 1.2 Development of the Rock Mechanics Site Descriptive Model strategy and the Test Case

The rock mechanics features at each site will be described with a Rock Mechanics Site Descriptive Model. During 2001, the approach to the Model structure was developed and a series of associated reports have been prepared, as shown in Table 1-1 with the current report highlighted in the shaded row.

**Table 1-1. Reports describing and supporting the development of the Rock Mechanics Site Descriptive Model (also see Preface).**

<i>SKB Report Number</i>	<i>Report Title</i>
TR 02-01	Site Investigations: Strategy for Development of a Rock Mechanics Site Descriptive Model
R 02-01	Development and Testing of the Empirical Approach
R 02-02	Development and Testing of the Theoretical Approach
R 02-03	Development and Testing of an Approach to Modelling the State of Stress
R 02-04	A Test Case based on Data from the Äspö HRL (this report)
R 02-11	Äspö HRL: A Descriptive Rock Mechanics Model for the 380–500 m Level

In /Andersson et al, 2002/, the first report listed in Table 1-1 describing the strategy used in developing the Rock Mechanics Site Descriptive Model, it is explained that three parallel approaches were used: the Empirical, Theoretical and Stress approaches. These are described in the next three reports in Table 1-1. A key component of the work involved the testing of these three approaches, both individually and through harmonization of the Empirical and Theoretical approaches. This was the Test Case, as described in the present report, in which predictions were made mainly for the rock mechanics properties in a volume of rock at the 380 – 500m level of the Äspö HRL. These predictions were compared with the ‘best estimate’ of conditions, as described in the last report listed in Table 1-1 The ‘best estimate’ of conditions was based on access to all site information at the Äspö HRL.

The development of the strategy for the Rock Mechanics Site Descriptive Model is shown in Figure 1-1, and the context for the Test Case is illustrated in the flowchart in Figure 1-2. Increasing confidence was developed as the Empirical, Theoretical and Stress Models were formulated, as the harmonization of the approaches was accomplished, as the Test Case work was undertaken, and the overall approach then modified according to the Test Case conclusions.

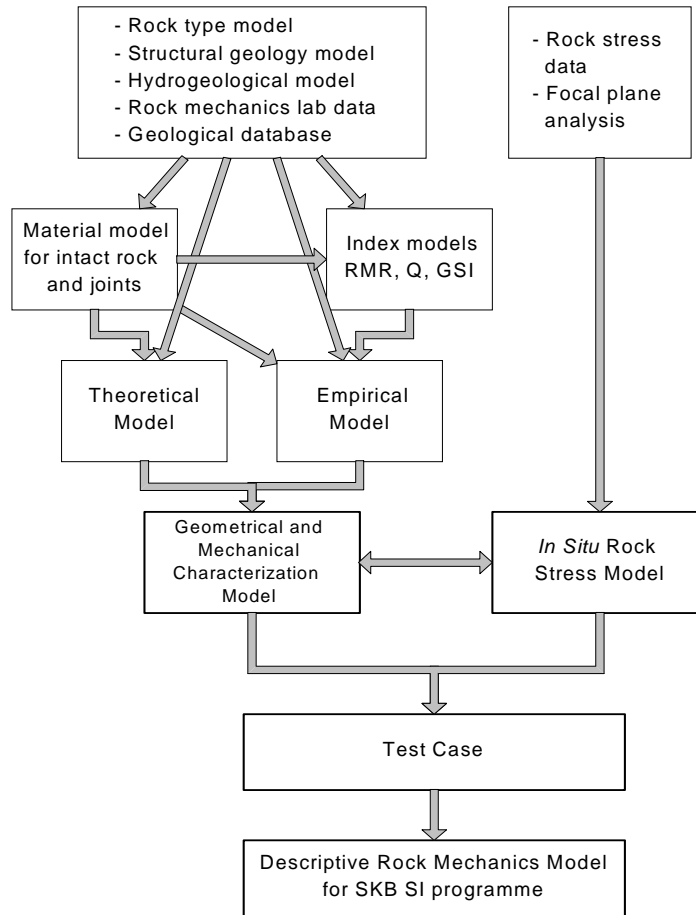


**Figure 1-1.** The development of the strategy for the Rock Mechanics Site Descriptive Model.

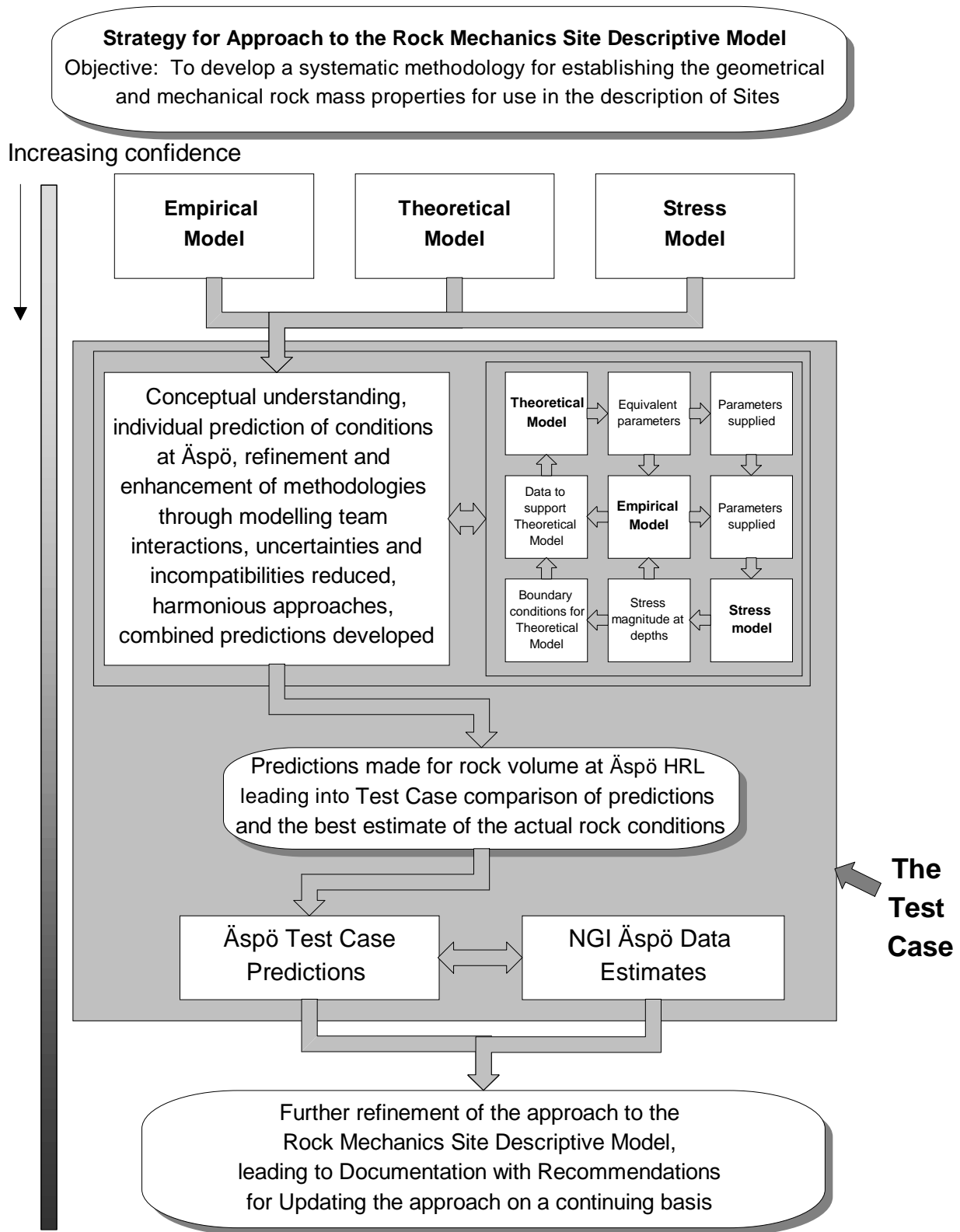


**Figure 1-2.** The context for the Test Case at the Äspö Hard Rock Laboratory – in developing the approach to the Rock Mechanics Site Descriptive Model.



The Test Case was thus an essential component of the development work. It provided a test of the approach using real data with a level of detail commensurate with that which will be obtained during the planned Site Investigations. Moreover, the work involved dealing with uncertainties, the implementation of Quality Control instruments including protocols, calibrating the methodology, and understanding what was required for further development of the strategy.

### **1.3 The Test Case objectives and work programme**

The overall objectives of the Test Case were to

- test and, if possible, verify the proposed rock mechanics site characterization strategy,
- identify and address any unresolved issues,

and thus establish the state-of-the-art, what is practically achievable, and how far the characterization can be practically developed.

The Test Case was also a benchmarking procedure. Before embarking on the Site Investigations, it was necessary to ensure that the structure and procedures for the rock mass characterization had been fully understood and tested.

Specific objectives of the Test Case included the following.

- Given different modelling procedures, establishing whether it is possible to harmonize these into one unified modelling strategy.
- Given limited site data, establishing how well the overall rock mass properties can be predicted.
- Establishing how many data are required to make adequate predictions and hence characterize a site.
- Checking the use of Quality Control instruments for such site characterization,
- Providing a benchmark example for characterization of a volume of the Swedish bedrock,
- Demonstrating the application of the proposed Rock Mechanics Site Descriptive Model strategy and producing an associated report.

The results of the Test Case characterization of a rock mass volume at the Äspö HRL thus provided additional information for developing the approach to the Rock Mechanics Site Descriptive Model. As the Site Investigations develop, the associated ideas, techniques, and results will assist in improving the strategy.



## 2 The Äspö Hard Rock Laboratory (HRL) and the Test Case site

In this Chapter, the Äspö Hard Rock Laboratory, which hosted the Test Case work, and the specific rock mass location are described. Information on the site, geology, geometry, rock stress, mechanical conditions, and the available underground data are presented.

### 2.1 Äspö HRL location and geological overview

The Äspö Hard Rock Laboratory operated by SKB is located on the coast of SE Sweden, see Figure 2-1 . The red lines in the Figure indicate in plan view the ramp and tunnels comprising the laboratory. There is also shaft access on the Äspö island.



*Figure 2-1. The location of the Äspö Hard Rock Laboratory /from Rhén et al, 1997/.*

A cut-away view of the shaft, spiral ramp and lower level experimental tunnels is shown in Figure 2-2, and the geology of the host rock with the main fracture zones is shown in Figure 2-3.

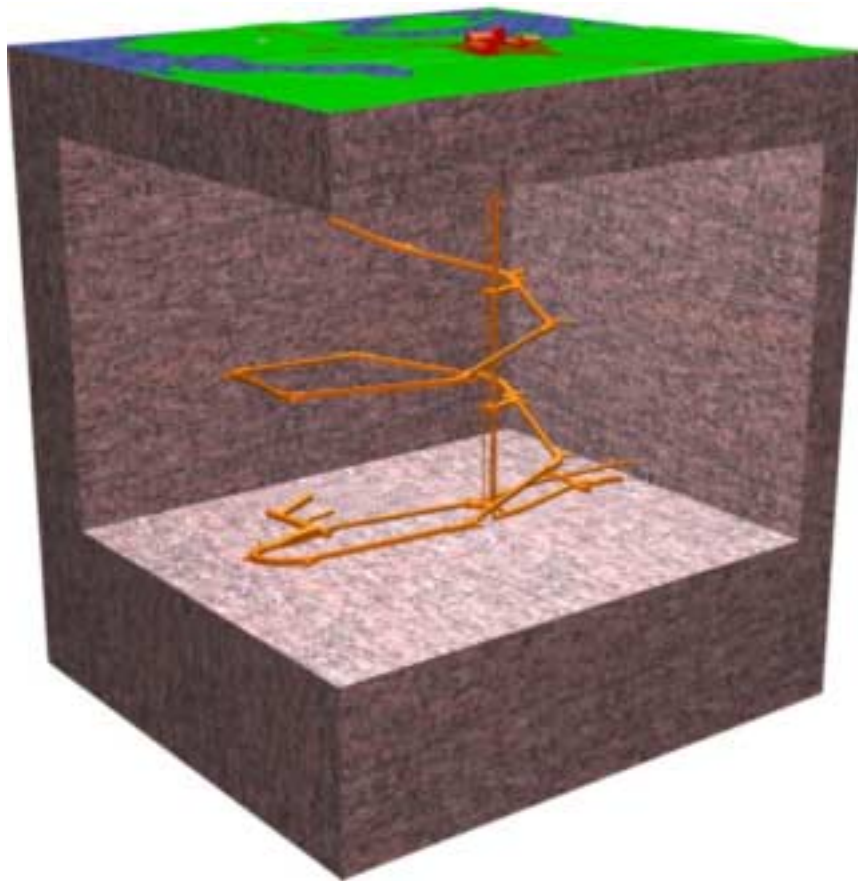


**Figure 2-2.** The geometry of the underground shaft, ramp and tunnels at the Äspö HRL /from Rhén et al, 1997/.

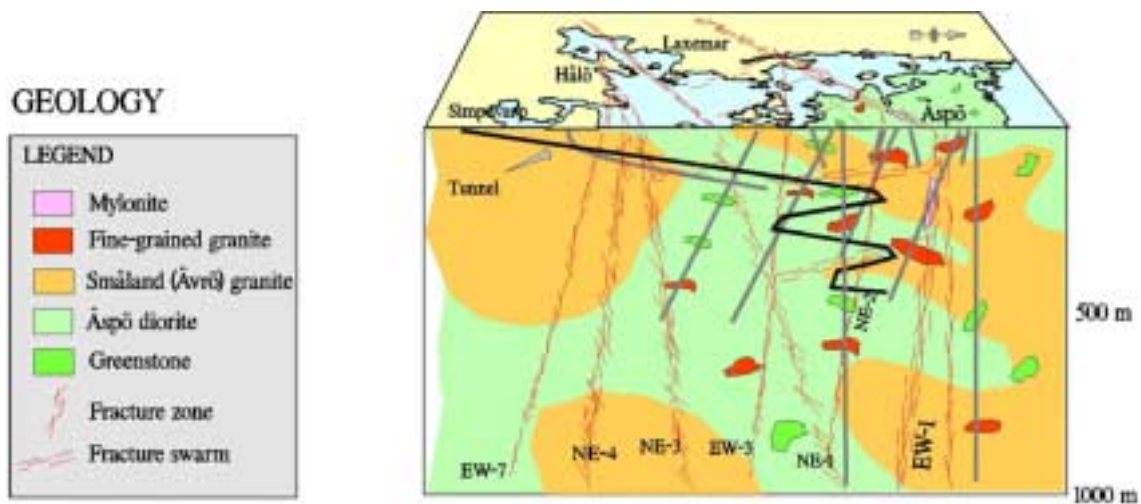


**Figure 2-3.** The geology and main fracture zones at the Äspö HRL. The access ramp is shown in black and the labelled fracture zones are shown in brown hatching. /From Rhén et al, 1997/.

## 2.2 The Äspö HRL Test Case location

The 550 m rock block and the target volume of rock, 600 m × 180 m × 120 m chosen for the Test Case are shown in Figure 2-4.

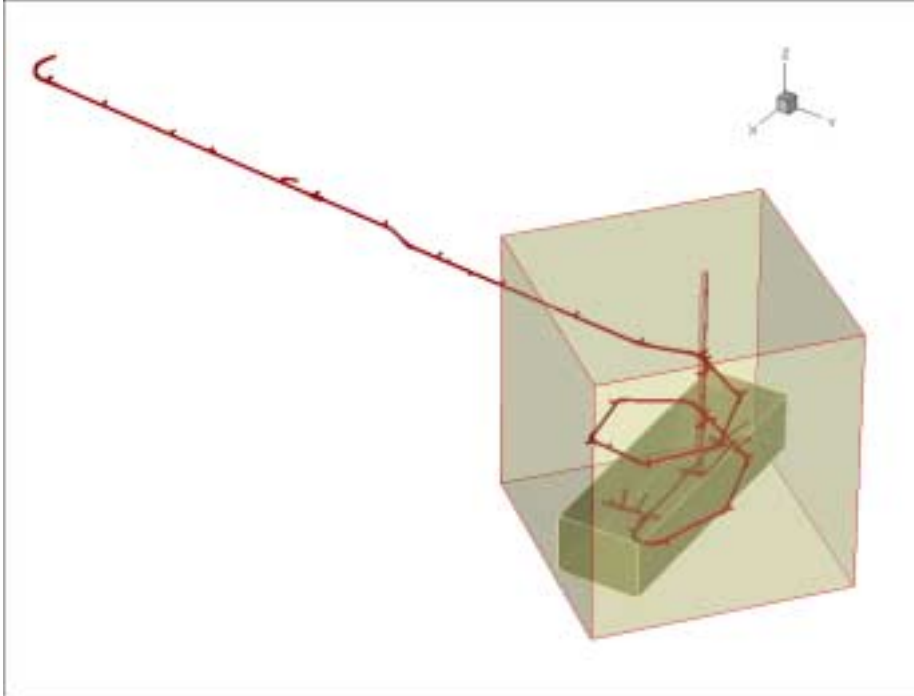


*Figure 2-4. 3-D view of the two rock volumes used for the Test Case, showing the access tunnel and the shaft (X: East, Y: North), from /Staub et al, 2002/.*

The reasons for choosing this location for the Test Case were that it is an SKB site, there has been a history of testing rock at the Äspö HRL, the geology and fracture zones had been characterized but a detailed rock mechanics characterization did not already exist, and some published reports and other information were available. Also, the Test Case work would lead to an enhanced understanding of the ‘typical’ bedrock rock mass block at Äspö and hence contribute to the rock characterization.

Three boreholes (explained later in Section 3.4) were used to provide information on the rock variability and, as highlighted in Figure 2-5, two boreholes drilled from within the tunnel gave further information, especially on oriented fractures. Also, the three boreholes were logged with procedures that will be used in the future SIs. Furthermore, a borehole was close to the tunnel so there was the opportunity to compare equivalent borehole and exposed rock conditions.

It was hoped that the Test Case work would not only assist in methods of characterizing variability in mechanical properties, but also assist in interpreting variations in the in situ stress state. The models developed earlier /Rhén et al, 1997/ did not explain the variation in mechanical properties and stress.

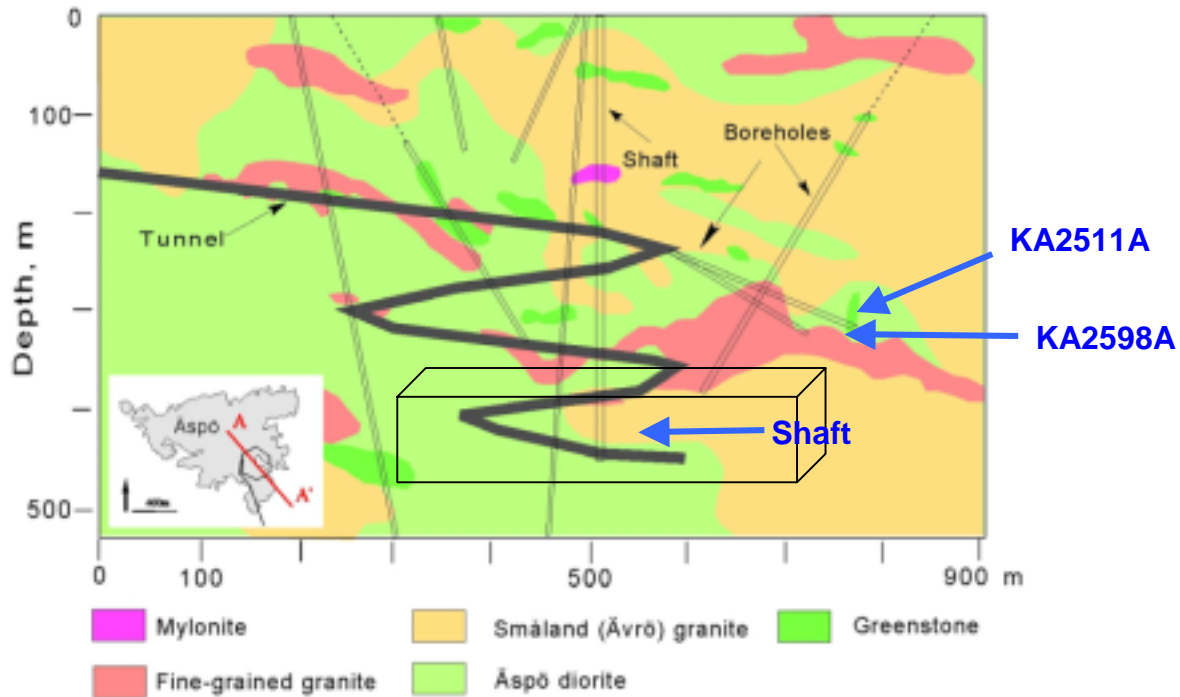


**Figure 2-5.** The Test Case rock mass volume at the 380–500 m level (based on /Rhén et al, 1997/). The shaft and two boreholes from the tunnel are indicated by the blue arrows.

## 2.3 Rock types, geometrical scales, fracturing, mechanical properties and stress state at the Äspö HRL site

A description of the Äspö HRL rock types, fracturing, stress state and mechanical properties is given in Rhén et al, 1997, and summarized here.

### 2.3.1 Rock types

The four main rock types, as indicated in Figure 2-5, are

Äspö diorite	The most commonly encountered rock on the Äspö island surface and in the tunnels.
Småland (Ävrö) granite	Cuts the Äspö diorite and is a more homogeneous rock type.
Greenstone <sup>1</sup>	Occurs as inclusions within the granitoids and dioritoids.
Fine-grained granite	Thought to be ancient dikes and are younger than the more coarse-grained Småland granites.

<sup>1</sup> The term ‘Greenstone’ is used for convenience and is not intended to be a precise technical term.

The distributions of these four main rock types at different depths are quite similar, except near the surface where the Småland granite is more frequent than the Äspö diorite, and at the 400–460 m bottom level where only Äspö diorite has been mapped. Figure 2-5 shows that most of the Test Case rock volume was in the Äspö diorite, but some parts of the block were composed of the other rock types.

### 2.3.2 Geometrical scales

Four geometrical scales are used in the site description, as shown in Figure 2-6. Thus, the choice of a target volume of rock  $600 \text{ m} \times 180 \text{ m} \times 120 \text{ m}$  for the Test Case was within the regional scale and encompassed the site and block scales because the Test Case block elements were  $30 \text{ m} \times 30 \text{ m} \times 30 \text{ m}$  blocks. However, the Test Case did not go down to the local/detailed scale of 0–10 m because this was too fine a resolution for the study.

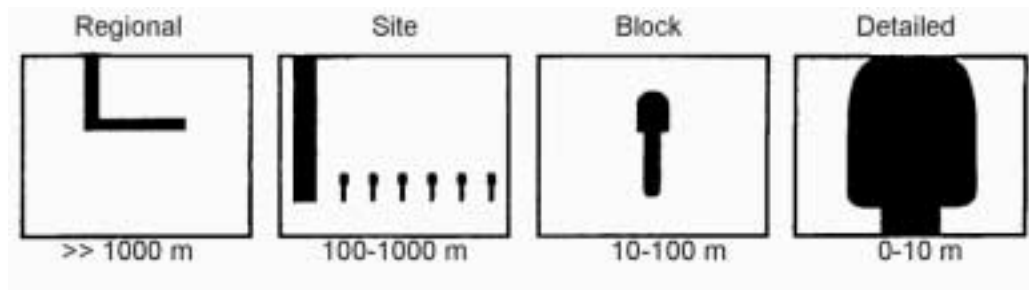


**Figure 2-6.** Terms used for the geometrical scale considerations in the description of the Äspö rock volume /from Rhén et al, 1997/.

### 2.3.3 Fracturing

It was anticipated that the fracture zones, as defined for the Äspö site /Rhén et al, 1997/<sup>2</sup>, would have a significant effect on both the mechanical properties and stress state in the rock, so it was important to understand these. The fracture zones illustrated in Figure 2-7 were defined for the Äspö site /Rhén et al, 1997/ as having an intensity of natural fractures at least twice that of the surrounding rock, and then classified as major or minor according to their size: major fracture zones being more than 5 m wide and extending several hundred metres; and minor fracture zones being less than this.

This gave fracturing characteristics on the different scales as follows:

- Regional scale: Major fracture zones
- Site scale: Major fracture zones, minor fracture zones, fracture swarms, small scale fracturing
- Block scale: Minor fracture zones, fracture swarms, and small scale fracturing
- Local/detailed scale: Small scale fracturing.

<sup>2</sup> The description of the fracture zones is evolving and the nomenclature is expected to change to 'deformation zone'.

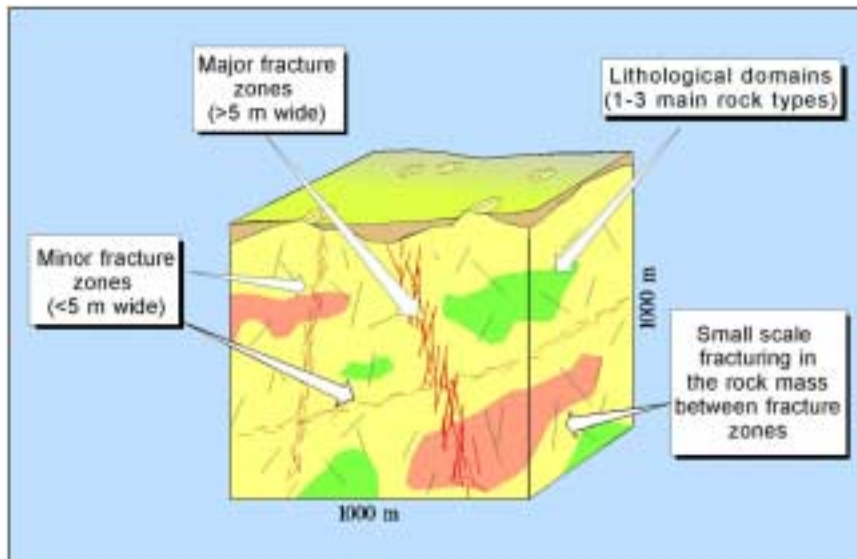


**Figure 2-7.** Fracture zones more than 5 m wide are considered as major fracture zones. Minor fracture zones and smaller scale individual fractures are also present. /from Rhén et al, 1997/.

The type of fracturing encountered in the block scale elements of the Test Case is illustrated in Figure 2-8.

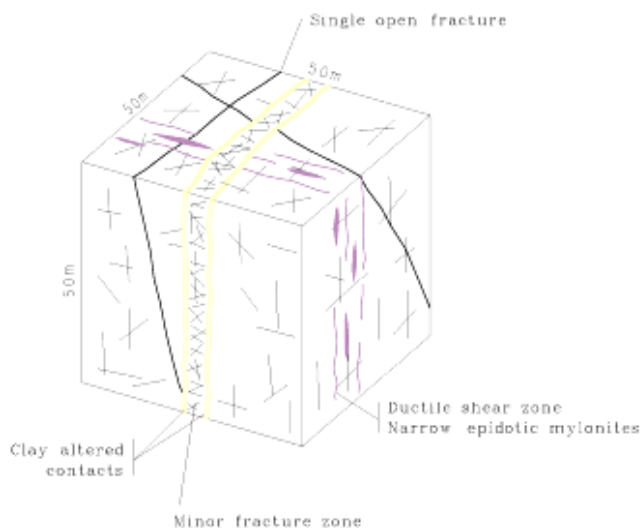


**Figure 2-8.** Type of fracturing anticipated on the 50 × 50 × 50 m block scale /from Rhén et al, 1997/.



The rosette histograms and contoured lower hemisphere projections in Figure 2-9 show that the main orientations of the fractures at the Test Case block depth are horizontal and sub-vertical striking SE-NW and NE-SW.

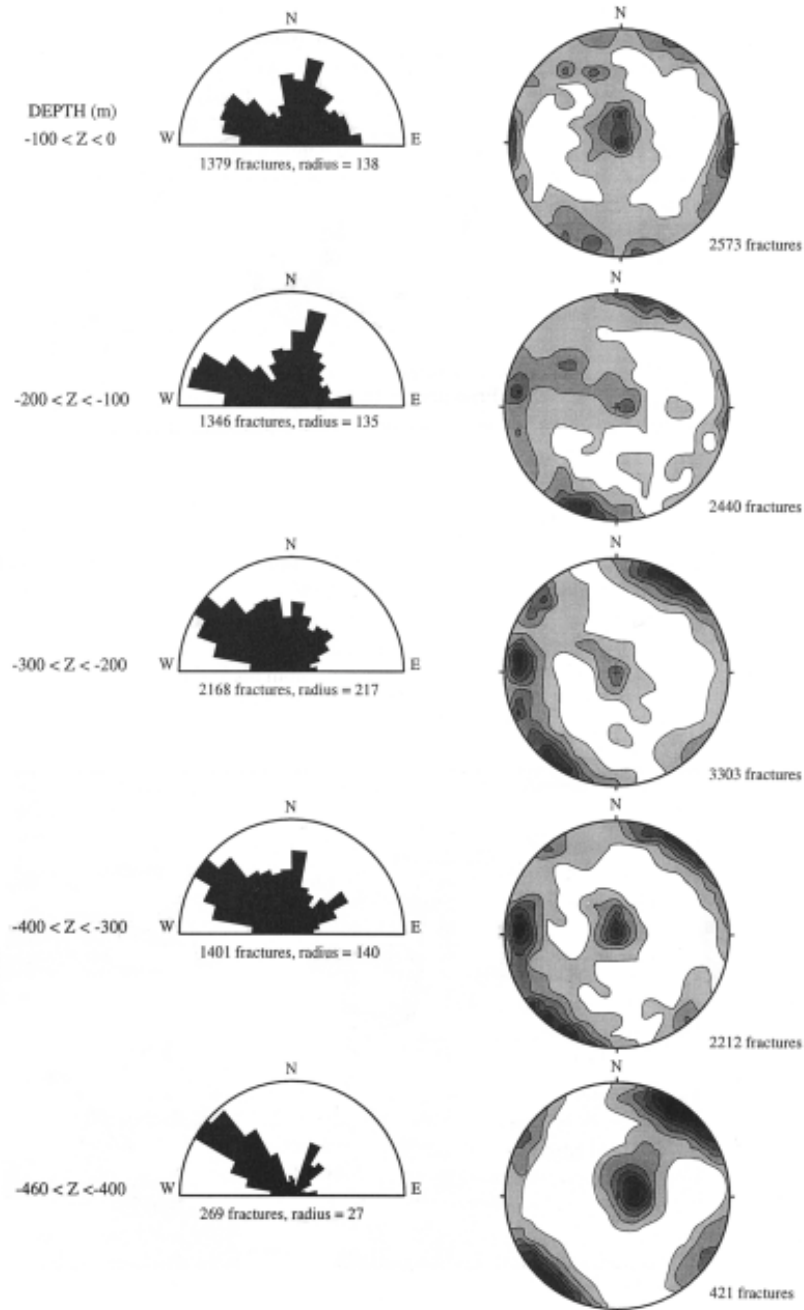


**Figure 2-9.** Lower hemisphere poles of fractures (to the right) encountered at different depths in the tunnel. The rosette diagrams (to the left) are for fractures with dips from 70° to 90° /from Rhén et al, 1997/.

### 2.3.4 Mechanical properties

Mechanical property data from the tunnel boreholes are shown in Table 2-1.

**Table 2-1. Summary of mechanical rock property data from tunnel borehole samples /from Rhén et al, 1997/.**

	Greenstone	Fine-grained granite	Åspö diorite	Småland granite
Compressive strength, MPa, mean and range	207 121–274	258 103–329	171 103–210	255 197–275
Young's modulus, GPa, mean and range	78 71–96	77 72–80	73 65–80	74 63–79
Poisson's ratio mean and range	0.24 0.18–0.31	0.23 0.21–0.25	0.24 0.22–0.29	0.23 0.20–0.26
Brittleness	Brittle	More brittle	More brittle	More brittle

It is evident from these data that the rock strengths are all high, although the Åspö diorite has the lower mean strength. Also, the Young's moduli for the four rock types are similar, as are the Poisson's ratios. Thus, it was to be expected that significant variations in the mechanical properties of the rock in the Test Case block were likely to occur in the vicinity of fracture zones, rather than in the intervening rock mass intersected only by individual fractures.

The Rock Mass Rating (RMR) system had been used to assess the rock quality during tunnelling. Five rock properties are used to compile the RMR value. The profile of RMR values along the access tunnel in Figure 2-10 shows that, although the major fracture zones are clearly strongly affecting the RMR values, there is also significant variation occurring between these zones.

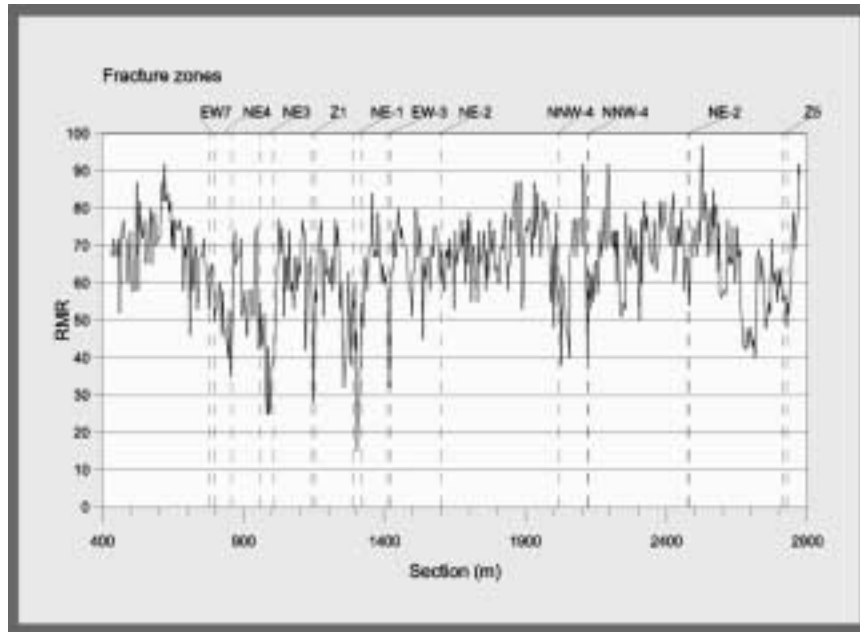


**Figure 2-10.** Profile of RMR values along the tunnel with the major fracture zones indicated /from Rhén et al, 1997/. This tunnel length is from ca 50 m depth to ca 380 m depth.

### 2.3.5 Rock stress conditions

It is known that the orientation of the maximum principal stress in NW Europe is horizontal and orientated SE-NW. Measurements made at the Äspö HRL have confirmed that, indeed, this is the case in the rock mass there. The magnitude of the maximum horizontal stress component is shown in Figure 2-11. In general, the vertical stress is expected to increase at a rate of 1 MPa for every 40 m depth. Thus, at 400 m, the vertical stress would be expected to be 10 MPa. From Figure 2-11, the maximum horizontal stress at 400 m depth is of the order of 20 MPa, giving a horizontal to vertical stress ratio of about 2.

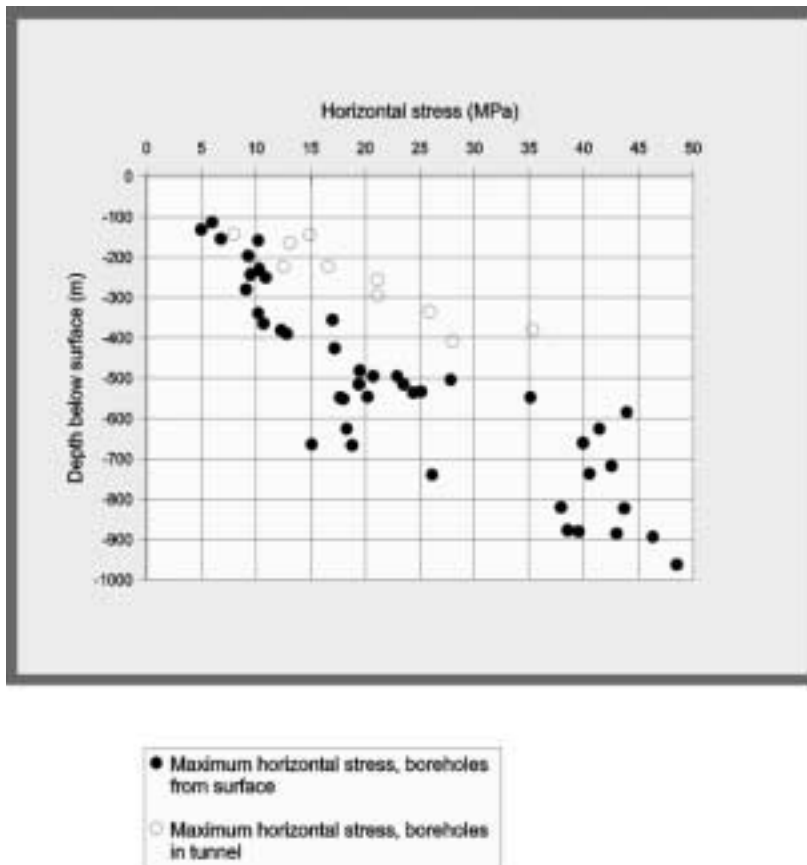


**Figure 2-11.** Magnitude of the maximum horizontal stress as a function of depth at the Äspö HRL /from Rhén et al, 1997/.

Figure 2-11 also shows some evidence that the horizontal stress component may not be smoothly increasing in value with depth and that perhaps there is a ‘stress jump’ at about 500 m depth.

### 2.3.6 Further information

The information summarized in this Chapter has been taken from /Rhén et al, 1997/ which is based on site characterization in 1986–1995, and provides an overview of the conditions as recorded in 1997. Many additional SKB and other reports are available on the Swedish bedrock in general and the Äspö HRL in particular. Some of this information has been published since 1997.

## 3 Test Case organization and procedure

The basic Test Case plan was to use restricted information to predict the rock properties for a 550 m cube model, concentrating on the 30 m × 30 m × 30 m sub-blocks within a 600 m × 180 m × 120 m target volume within the larger 550 m cube volume, and compare these target volume predictions with the ‘best estimate’ values determined using additional information. Given the specific objectives for the Test Case listed in Section 1.3 and the information regarding the Test Case location in Chapter 2, it was necessary to generate a Project Plan for the work and ensure that appropriate Quality Control measures were in place.

### 3.1 The Test Case Project Plan

The Project Plan involved the use of three approaches to predict the rock properties in the Test Case volume (see Figure 1-1 and Figure 1-2).

- an empirical model – which includes evaluation based on the geological description, using existing rock mass classification system schemes, empirical formulae, and experiences from similar areas.
- a theoretical model – which is a description and characterization based on measured data (usually on the small scale) from the field (boreholes) or laboratory (analyses of borehole cores) and the properties typically used in analyses.
- a stress model – for studies and interpretation of the rock mass stress distribution in the light of the tectonic history, geological structure and fracture properties.

In addition to the overall objectives listed in Section 1.3, the Test Case was also geared to the following.

- Test the draft modelling manuals developed within the project (see Section 1.2), to the extent that these manuals were available at the time of the Test Case, and thereby establish a reference point for future improvements of the methodology.
- Trigger the development of practical means for representing uncertainty (even if this was already considered in the draft modelling manuals).
- Explore confidence in the modelling technique, by evaluating to what extent theoretical and empirical models arrived at similar conclusions and to what extent they were in agreement with observation (bias and precision).
- Evaluate both the practical experiences of the model application and the confidence in its application and thereby document potential problems/difficulties and suggest improvements and adjustments of the modelling technique.
- Explore to what extent increased input data density enhanced predictions.

The Test Case thus produced results to be considered in the final approach to the Rock Mechanics Site Descriptive Model Strategy. In addition, the conclusions from the Test Case exercise were documented separately, i.e. in this report, with the aim of demonstrating that SKB has successfully tested an appropriate methodology.

## **3.2 Test Case phases**

The Test Case was organized in four phases with the components as listed in the next four sub-sections.

### **3.2.1 Phase 1 – Development of a plan for the Test Case**

Phase 1 involved the following.

- Establishing objectives and scope of the Test Case
- Selecting a set of limited available data to be used for the Test Case, simulating a Site Investigation (SI)
- Defining what was to be predicted
- Defining strategy for comparing model predictions with the 550 m rock block and the detailed 380–500 m target volume
- Outlining the suite of protocols necessary for implementation of the Test Case predictions and their evaluation
- Ensuring compatibility of the technical auditing output of the Phase 1 rock mechanics model work with the Test Case protocols
- Estimating of resources needed for the entire Test Case
- Making decisions on scope and finalisation of project plan

### **3.2.2 Phase 2 – Preparation of data sets**

Phase 2 involved the following.

- Definition of co-ordinate systems
- Updating Äspö structure model and put it into MicroStation (the software SKB is using for rock visualization)
- Preparing rock type model and put it into MicroStation
- Confirmation that the information in Table 3-3 and Table 3-4 is available in SICADA or elsewhere
- Initial development of the 380–500 m level model
- Further development of the protocols

### 3.2.3 Phase 3 – Predictions and evaluation

Phase 3 involved the following.

- First step predictions of parameters in the 380–500 m level model (see Table 3-5) from the 550 m block model and documentation of results
- Second step combined predictions of parameters in the 380–500 m level model from the combined 550 m block model and documentation of results
- First comparison of results – comparison between predictions and the actual values of the 380–500m level model
- International review meeting
- Second evaluation of results, establishing reasons for discrepancies, upgrading of protocols to improve the prediction methodology.
- Consideration of the possible need for a third iteration of predictions using more data in order to explore the potential improvement by using more data and evaluation of results of third iteration
- Conclusions and initial recommendations

### 3.2.4 Phase 4 – Documentation

Phase 4 involved the following.

- Outlining the report
- Drafting the report
- Reviewing draft report
- Production of Final Report (i.e. this report SKB R 02-04)

## 3.3 The Use of Protocols

It was necessary to establish protocols for the procedures to be applied. Each of the nine main components of the Test Case work was guided by a separate protocol, as illustrated in Figure 3-1.

Each Protocol consisted of three sections:

- **Objectives:** Listing of the one or more objectives associated with each step of the Test Case work
- **Procedures:** Listing of the procedures to be adopted to achieve the objectives
- **Products:** The products that will be generated by each step of the Test Case work

An example protocol sheet, 4B Individual Model Predictions, is presented in the Appendix. A description of the work associated with each protocol is given in the following sub-sections. Although the protocols were developed for the Test Case, with modification similar protocols may also be envisaged for describing the overall modelling procedures in the Rock Mechanics Site Descriptive Model.

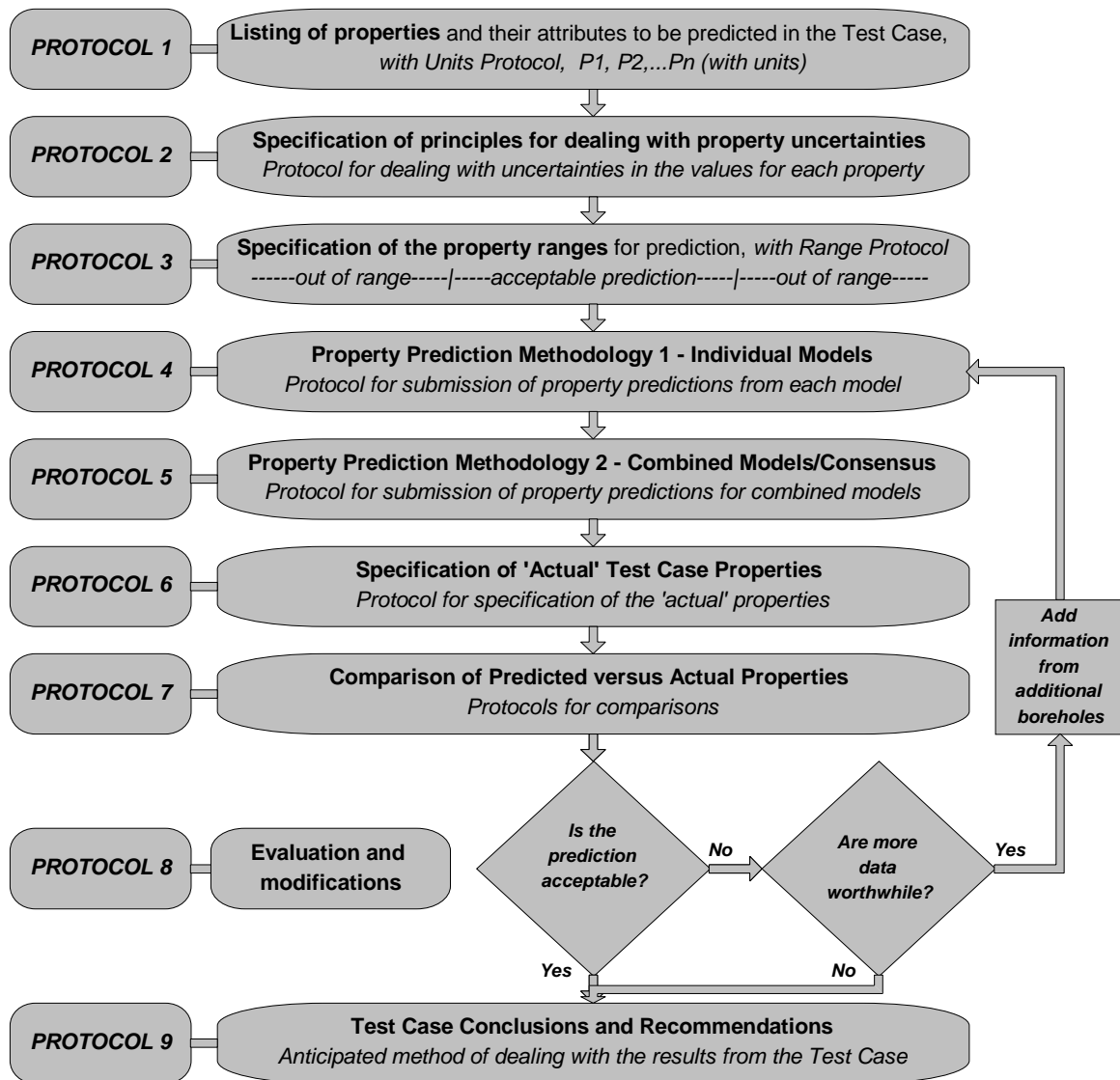


Figure 3-1. The nine main components of the Test Case work.

### 3.3.1 Listing of parameters<sup>3</sup> – Protocol 1

Protocol 1 outlines the procedures for identifying which parameters are to be predicted by the modelling. The SKB selection of parameters to be explored during the site characterization rests on several assessments of what is required to be determined for use in safety assessment and design. The general objectives of the rock mechanics analysis in support of the design activity during the site investigation phase are outlined in /SKB, 2000b/. When the site investigations are finished, the design activity shall have:

<sup>3</sup> Although the Test Case work has finished, in the text in Section 3.3 describing the protocols, the future tense is used in some places because that is the form in which the protocols were written and used.



- presented one site-adapted deep repository facility among several analyzed and proven its feasibility,
- identified facility-specific technical risks, and
- developed detailed design premises for the detailed characterization phase.

The general site characterization programme /SKB, 2000b/ lists relevant rock mechanics parameters (Table 4-5 in /SKB, 2000b/). A more specific table, Table 3-1, has been developed listing the rock mechanics properties to be provided by the Rock Mechanics Site Descriptive Model.

The Table also indicates which scale is needed for describing the parameter. This scale should be consistent with the intended use of the parameter. Accordingly, the scale in focus is the tunnel scale, i.e. around 30 m. The Table also contains an indication of the accuracy/precision required in their estimation. Starting from an initial listing, the properties and acceptable estimation values have been assessed primarily by the input from the modelling teams according to Protocols 1–3.

The Test Case focussed on a subset of the parameters listed in Table 3-1. This subset, is described in more detail in Table 3-5. It should also be understood that the properties used in this Test Case are those related to site characterization and anticipated repository design and Performance Assessment/Safety Assessment (PA/SA) considerations, but have been limited in scope by the availability of actual data with which to compare the predicted properties. It is anticipated that there will be more properties in the final Model as recommended for use for site characterization.

For the engineering problems, the main focus of the parameters in Table 3-1 is the intact rock strength and the rock mass properties. Both the intact rock properties and fracture properties are used as input for determining the rock mass properties. Also, the rock mass properties are required for safety assessment applications. For traceability, modelling groups should provide information on which values were used in determining the rock mass properties. The required resolution in describing the three-dimensional distribution of, e.g. intact rock strength, has yet to be developed. This lies outside the scope of the Test Case.

In order to estimate the data in Table 3-1, there is also a need to use data and model predictions provided by other disciplines. A general overview of such data is provided in Table 3-2, based on Table 5-3 in the general site characterization programme, /SKB, 2001b/.

**Table 3-1. Listing of mechanical rock parameters to be eventually incorporated in the Rock Mechanics Site Descriptive Model, with initial suggestions on acceptable uncertainty values (builds on Table 5.2 in /SKB, 2001b/). Only a subset of these parameters will be predicted for the Test Case, as specified in Table 3-5.**

<b>Rock mass</b>			
<b>Parameter (generally a function of space)</b>	<b>Scale</b>	<b>Units</b>	<b>Acceptable estimation *</b>
Orientation of in situ principal stresses	tunnel scale (30 m)	degrees, azimuth/dip	$\pm 20^\circ$ (if anisotropic otherwise less strict)
Magnitude of in situ principal stresses	tunnel scale (30 m)	MPa	$\pm 20\%$ but high precision is required for judging whether $\sigma_1 < 60$ MPa
Rock mass modulus, $E_m$	tunnel scale (30 m)	GPa	$\pm 15\%$ if $15 \text{ GPa} < E_m < 45 \text{ GPa}$ , less than $10\%$ if $E_m > 45 \text{ GPa}$
Rock mass strength (H-B, M-C failure criteria)	tunnel scale (30 m)	various	Conclusions whether there is risk for substantial rock failure (.e.g. spalling) should be accurate. Such evaluations may e.g. be made using the diagram 5-1 in Andersson et al, 2000.
Rock Quality Designation (RQD)	tunnel scale (30 m)	%	$\pm 20\%$
<b>Intact rock and fractures</b>			
<b>Parameter</b>		<b>Units</b>	<b>Acceptable estimation *</b>
Intact rock modulus, E		GPa	Not discussed in current project
Intact rock compressive strength, $\sigma_c$		MPa	See rock mass strength
Intact rock tensile strength, $\sigma_t$		MPa	Not discussed in current project
Condition of fractures & alteration			Not discussed in current project
Fracture roughness			Not discussed in current project

See Section 3.3.3 for motivation.

**Table 3-2. Parameters needed for rock mechanics, but obtained from other subject areas (from Table 5-3 in /SKB, 2001b/).**

<b>Parameter</b>	<b>Determined in subject area</b>
Position and direction of regional and local large fracture zones	Geological programme
Statistical description of local minor fracture zones	Geological programme
Discrete fracture statistics (size, orientation, density of different fracture sets)	Geological programme
Lithological characterization of different rock units	Geological programme
Thermal properties of different rock units	Thermal programme
Hydraulic properties of fracture zones and fractures	Hydrogeological programme
Hydraulic properties of different rock units	Hydrogeological programme
Regional seismic activity	Geological programme

### 3.3.2 Representation of uncertainty – Protocol 2

Protocol 2 outlines procedures for dealing with uncertainty in rock mechanics parameters. In general, a means of representing uncertainty for each parameter in Table 3-1 (and as further specified in Table 3-5 for the Test Case) is needed.

All parameters listed in these Tables are functions of space and thus exhibit spatial variability. The properties will be spatially specified by block number location and the uncertainty methods will thus be linked to location. Currently, it is thought that spatial variability and uncertainty can mainly be described as a range over the appropriate scale within each geometrical unit in the model, but during the course of development more elaborate descriptions may be envisaged.

In the general Rock Mechanics Site Descriptive Model methodology, the approaches need to be able to handle uncertainty in the Geological and Geometrical Model, given as input to the rock mechanics modelling. Because the procedures for handling such uncertainties and their characterization are being developed in another SKB project, this means that uncertainty management will not be fully tested in the Test Case.

### 3.3.3 Specification of the parameter ‘ranges’ – Protocol 3

The Test Case involved making predictions and comparing the predictions with ‘best estimate’ reference values of the actual conditions. When assessing the results of this comparison, there is a need for some guidance on the magnitude of deviations between prediction and reality which would indicate a significant difference. The procedures are outlined in Protocol 3.

The following overall principles apply when specifying property ranges and when dealing with property uncertainties.

- There is no need for absolute certainty: it is only an adequate prediction that is required, not an exact prediction. If uncertainties are bounded and shown to be acceptable for the relevant performance issues, the model may be sufficient.
- It is the engineering and safety assessment impact of the property range that is the key consideration – through asking questions of the type, “What engineering or safety assessment *decisions* would be altered if the rock mass properties or stresses take on different extreme values within the predicted uncertainty (ignorance) range?” Specific attention should be given to considering whether the predicted uncertainty ranges are too wide to be of any engineering value.
- The Test Case predictions should be made bearing in mind the use to which the property values are to be put and the practicalities of prediction. The predictions only need to be adequate in the sense that they are commensurate with the purpose of obtaining the property value. For example, if the uniaxial compressive strength is only being obtained for use in the RMR rock mass classification scheme, then the estimation accuracy should be tailored to the ranking divisions of <1, 1–5, 5–25, 25–50, 50–100, 100–250, >250 MPa, as used in the RMR system.

Table 3-1 provides an initial estimation of the acceptable differences between predicted and ‘actual’ or ‘best estimate’ values for use in the Test Case and its context for the Rock Mechanics Site Descriptive Model. However, these estimates will need re-evaluation, if they are to be applied for a general methodology. In particular, it can

be questioned if the ‘acceptable’ range can be described as a range only. The acceptability will be conditioned by the specific values of the parameters. For example, if principal stress values are of similar magnitude, there is no need to put strong demands on the principal stress directions; conversely, in a strongly anisotropic stress field, the principal stress directions are important.

These issues should be evaluated for the different properties to be predicted by discussion within the three modelling groups, so that the Test Case is sensible and practical. Additionally, the same property may be used by the theoretical model, empirical model and stress model groups for different purposes – so that a baseline property range will be established satisfying the three modelling requirements.

### **3.3.4 Input data to be used for the Test Case – Protocol 4A**

Protocol 4A concerns specification of the input data and the major assumptions used for making predictions. For the Test Case, supplying the input data required use of the existing data from the Äspö HRL. The data should be obtained through the routes anticipated in the overall Site Descriptive Modelling Procedures /see SKB, 2001b/, i.e. geological data are to be obtained from the Geological Model rather than from independent interpretation of geological/geophysical measurements. The Äspö database is extensive, ranging from measurements obtained during the pre-construction stages, experiences during construction and the detailed mapping of the deeper parts of the tunnel systems and its surroundings.

In view of the listing of basic rock properties in Table 3-1 and the practicalities of the available data, it is suggested that the following data should be used as the basis for model construction:

- a geological model (structures, rock types, geological history),
- mechanically relevant borehole logs in some boreholes,
- rock stress measurements made in boreholes,
- mechanical properties estimated from rock samples (borehole cores) tested in the laboratory.

During the coming Site Investigations, it is expected that such information will be available in SICADA and the appropriate version of the site descriptive models in RVS. However, for the present test case, the data were not fully compiled in this form.

### **Co-ordinate system**

It is essential that all three-dimensional information is represented and presented in the same co-ordinate system. The RVS-standard is the RT-90 system. However, most of the Äspö information is in the local Äspö system; so, for practical reasons, the local Äspö system will be the co-ordinate system for the Test Case. Careful attention to co-ordinate systems is required. In particular, measured fracture orientations are usually measured with a compass and related to magnetic north. All such data, if used, need to be converted to the Äspö local system. Processed data provided (e.g. geometrical model, lithology and DFN-parameters) will all be in the local Äspö system.

## Geological and geometrical data

According to the detailed Site Investigation programme, SKB, 2001b, the (statistical) description of fracture zones and fractures and distribution of rock types should be obtained from the geological modelling. This, therefore, includes some of the fracture properties in Table 3-2. However, there are no plans to develop an entirely new geometrical or geological model of Äspö based on the information from only few boreholes. Instead it was suggested to moderately update the best currently available geometrical and geological model as input to the exercise.

Even if this was unrealistic, the decision also had some advantages:

- The procedure is resource efficient as there will be no need to develop an entirely new geometrical/geological model.
- It will be an opportunity to practice the procedure of abstracting rock mechanics parameters from a model, rather than ‘directly’ from data – which is important because this will be the anticipated data transfer during the site investigations, i.e. through an interface between different groups. It is particularly important that rock mechanics experts do not develop ‘their own’ geological model, but use the official geological model.
- Uncertainties connected to the geometrical and geological model will be reduced, which means that it will be possible to focus more on the specific rock mechanics uncertainties.
- Procedures for estimating and representing uncertainty in the geometrical and geological models are being developed. Ultimately the rock mechanics methodology needs to incorporate the fact that geometry and geology are uncertain, and make use of the representation of the uncertainty methods being developed. However, due to the current development stage of the geometrical modelling, it would be premature to test such aspects in the Test Case.

The geological model of the geometry of fracture zones and the suggested geological evolution model are described in /Rhén et al, 1997/. An update of the model was prepared, and the model was available in a general CAD-format.

Also, the rock type model was updated. A special geometrical unit representing greenstone was made available. Greenstone is now judged to be the only rock unit estimated to have significantly different mechanical properties, compared to the bulk volume at the site. The geometrical unit was made available in CAD-format.

Smaller scale fractures were described statistically via the input parameters to a DFN (discrete fracture network model), essentially comprising the parameters of fracture density ( $P_{32}$ ), orientation distributions for the different fracture sets, size distributions for the different fracture sets, underlying statistical model, and fracture termination characteristics. These parameters were taken from the DFN model developed for the prototype repository at Äspö (to be delivered as a data sheet). In addition, statistics of the fracture orientations, as measured along the shaft, was made available because the boreholes used did not provide logs of fracture orientation.

The geometrical data to be used are summarised in Table 3-3.

**Table 3-3. Geological and geometrical data to be used for the Test Case.**

Type of data	Description	Source
Geometrical units (fracture zones)	Updated version of geometrical model as given in SKB TR 97-06	CAD-file
Lithology	Updated version of Greenstone distribution	CAD-file
Small scale fracture density	DFN-estimate fracture density $P_{32}$ , for the prototype drift	Number
Small scale fracture orientation	DFN-estimate for different sets for the prototype drift. Statistics of the fracture orientations measured along the shaft	Table with the statistical parameters and stereoplots
Small scale fracture size	DFN-estimate for different sets for the prototype drift	Table with the statistical parameters
Additional fracture statistics	Underlying statistical model and fracture termination properties in the DFN-model of the prototype drift	Table with the statistical parameters

### Rock mechanics data

Rock mechanics data and rock stress measurements were taken from a number of different borehole or borehole core measurements. Since few mechanical measurements were made in boreholes drilled prior to tunnel construction, some measurements were taken from boreholes drilled from the tunnel. This may be seen as unrealistic in terms of a conventional site investigation, but was judged to be acceptable – because such data could have been obtained from a borehole drilled from the surface. This assumes that the borehole orientation is not important and that the borehole core will not have been too disturbed by the tunnel. The information was sampled from different boreholes according to Table 3-4. The actual data are available in the SKB database SICADA.

**Table 3-4. Rock mechanics data to be used for the Test Case modelling.**

Type of data	Boreholes				
	KAS02	KA2511A	KA2598A	KA3579G <sup>4</sup>	Optional boreholes for a third iteration
<i>Q (and RQD) in specific directions</i>	200 – 600 m	yes	yes	–	yes
<i>RMR (and RQD) in specific directions</i>	350 – 550 m	400 m – bottom	400 m – bottom	–	yes
<i>Stress tensor</i>	yes (HF and OC)	–	–	yes (OC)	yes
<i>Mechanical properties of intact rock, seismic velocity, etc</i>	<i>E-modulus for intact rock where there are OC-data</i>	–	–	yes	yes

HF – hydraulic fracturing; OC – Overcoring

<sup>4</sup> If there are rock mechanics data from other holes in the prototype repository, these may be used as well.

In addition to the data specified above, modelling teams were allowed to use any non-site specific data concerning e.g. general stress patterns in south Sweden or to use other data sets to test out specific ideas relating to their modelling tools, e.g. information from the CLAB site, /Fredriksson et al, 2001/. The only restriction in data use was that no other deep information from Äspö should be used.

### 3.3.5 Predictions – Protocols 4B and 5

The three models developed within the rock mechanics modelling project predict the rock mechanics properties as specified in Table 3-5 over a volume called the ‘550 m block model’, from the surface and down mimicking a Site Model, see Figure 3-2. The predictions should be made in steps. Protocol sheet 4B is given in the Appendix.

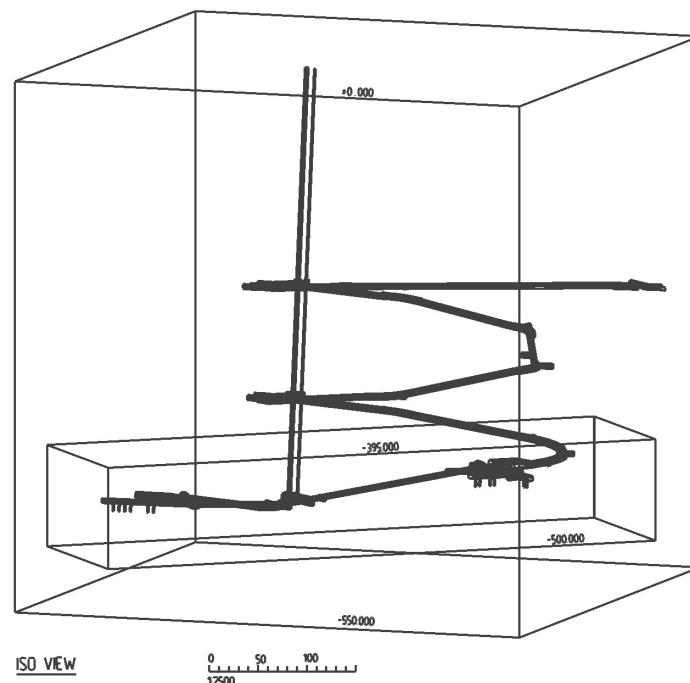


**Figure 3-2.** The Rock Mechanics model will make predictions for a large model, starting from ground surface (the larger block in the diagram), but the comparison between the predictions and the ‘best estimate’ results will only be made for the 380–500 level region (the smaller block in the diagram).

**Table 3-5. Parameters\* provided by the 380–500 m level model and parameters to be predicted in blocks of about 30 m scale along the tunnel.**

<b>Detailed mechanical properties</b>	<b>Empirical indices</b>	<b>Rock mass properties</b>	<b>In-situ stresses (i.e. stresses prior to tunnel construction)</b>
Intact rock modulus	Q, RMR, GSI	Strength parameters for Hoek-Brown, and Mohr-Coulomb criteria.	Magnitudes of the principal stress components $\sigma_1$ , $\sigma_2$ , $\sigma_3$ (MPa),
Intact rock compressive strength		Rock mass deformation modulus, $E_m$	Directions (trend and plunge) of the principal stress components.
Fracture deformation characteristics		Rock mass Poisson's ratio $\nu_m$ ,	

*The prediction of the properties refers, not only to the mean value, but also to the standard deviation of values, and anisotropy/inhomogeneity estimates where appropriate. Trends in spatial variation (if any) should be indicated. The anisotropy is built into the nature of the stress tensor, but the stresses can still be inhomogeneous. For most of the parameters, however, both anisotropy and inhomogeneity are an issue and will be built into the prediction Protocols. A related issue is the influence of the sampling directions and locations on the measured values.*

The models should provide information on the values used (spatial distribution) of intact rock strength and deformation characteristics and values used of fracture deformation and strength characteristics, even if this information should be regarded as ‘input’ rather than output parameters. The assumed spatial variation (if any) of these properties is still a modelling decision.

For example, the description of the rock mass strength will be made in terms of the parameters of the Hoek and Brown /Hoek and Brown, 1997/ failure criterion, i.e.

$$\sigma_1' = \sigma_3' + \sigma_{ci} \left( m_b \frac{\sigma_3'}{\sigma_{ci}} + s \right)^a$$

The values should be provided at the ‘tunnel scale’, i.e. in blocks of a 30 m edge length cube. The division of blocks should reflect the geometrical units of the geological model. Fracture zones should be handled as specific units, even if they may not be as wide as 30 m. However, if a unit is larger than the 30 m block size, it should be divided into blocks, but different blocks may be given the same statistical description.

Within each block, the model provides the parameters as a mean and a measure of the uncertainty (such as standard deviation or an interval). The description of uncertainty should be in line with the Protocols established.

### **First step predictions – Protocol 4B**

In the *first step*, the three different approaches should make individual predictions of parameters relevant to their modelling studies. The precise content of the predictions should be decided by discussions with the three modelling group (see Protocol 4A).



It was anticipated that predictions would be made in line with Table 3-5 with the following exceptions:

- Rock mass properties will only be predicted by the theoretical model and by the empirical model. The theoretical model has, as yet, no well defined procedure for calculating rock mass strength, but should nevertheless try to do it.
- Empirical indices will only be predicted by the empirical model.
- Stresses will only be predicted by the stress model.

In addition, the values of intact rock strength and deformation characteristics used and values of fracture deformation and strength characteristics used should be provided. (This information could be important later if there is a need to discuss discrepancies between models).

The information should be provided at the same scale and with the same spatial resolution as in the 4–500 m level model, but it is not expected that the models will provide different values for different blocks in a similar geometrical unit. Furthermore, predictions will be made over a much larger region (the ‘550 m block model’) than covered by the 380–500 m level model, but comparison of results would, of course, only be possible for the region covered by the 380–500 m level model. The predictions should be in terms of expected value and uncertainty – expressed by some acceptable statistical model (such as standard deviation or interval). The modeller should indicate to what extent the uncertainty concerns spatial variability (i.e. if the different blocks will take different values in ‘reality’) and to what extent the uncertainty concerns ‘ignorance’. If sensitivity analyses have been used to provide the error bars, the methods should be indicated in supporting text.

### **Second step predictions – Protocol 5**

In the *second step*, all three modelling teams will co-operate and use their combined information and know-how to revise the predictions. These second stage predictions will concern all parameters in Table 3-5. The procedures for this joint re-evaluation will be established during the course of the exercise, but should preferably involve more than a consensus meeting (see Protocol 5). Using a rock mechanics numerical model, the rock mass parameters predicted should be used to calculate, stresses from assumed stress history, the geometrical/geological model and measured stresses. The exact methodology will be developed, based on the protocol structure listed in Figure 3-1. For the combined model predictions, it is especially important to indicate how individual model predictions have been modified to the combined model prediction by interaction with the other modelling groups. Also, the way in which individual error estimates have been modified should be noted.

#### **3.3.6 The ‘best estimate’ of rock properties for the 380–500m level model – Protocol 6**

Protocol 6 concerns the need to provide the information with which to compare the rock mechanics model predictions, i.e. to provide the ‘best estimate’ of the actual rock properties. As a special project, SKB will develop a detailed model at about the 30 m scale along the direction of the deepest tunnel of Äspö HRL /Makurat et al, 2002/.

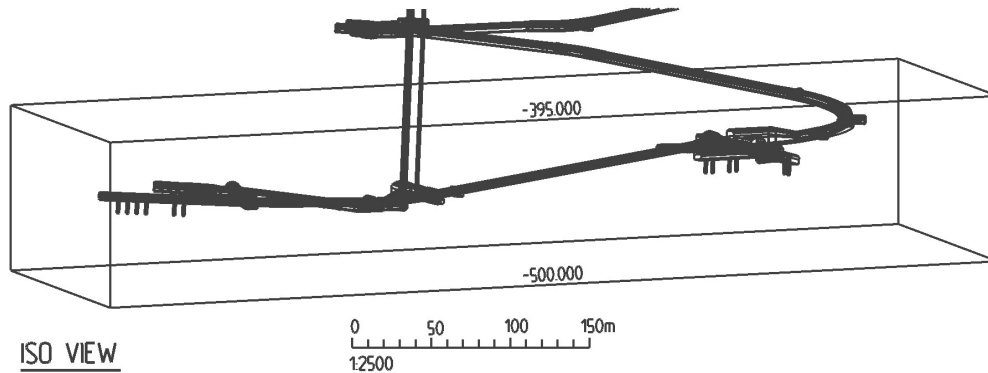


**Figure 3-3.** Location of the 380–500 m level Test Case rock block volume at Äspö HRL.

The model, called the 380–500 m level model, will use all available rock mechanics information on the Äspö HRL, including the information used for the Test Case. It covers the region around the tunnel at the 380–500 m level, see Figure 3-3, and provides the rock mechanics properties defined in Table 3-5.

The exact co-ordinates of the 380–500 m level model will be provided and the volume will be included in a CAD file. The producers of the detailed model have been instructed to use any information that they deem appropriate in estimating the actual properties. It is essential that all data and other assumptions used are carefully documented.

### **3.3.7 Evaluation of results – Protocols 7 and 8**

There is a need to develop fixed procedures for evaluation of results, as indicated by Protocols 7 and 8 listed in Figure 3-1. In particular, it is important to anticipate that some predictions will not be correct and that the reasons for the discrepancies need to be established. Thus, the Protocol has to include an anticipated method for dealing with such discrepancies, and hence improving the rock mechanics model prediction methodology.

The comparison of predictions (Protocol 7) will aim at

- identifying the differences between i) the individual predictions as compared to the actual properties, and ii) the combined predictions as compared to the actual properties,
- studying the influence of property location on the prediction quality.

The evaluation of the comparison (Protocol 8) will aim at

- tracing the origin of successful, inconclusive and unsuccessful predictions,
- evaluating the possible reasons for inconclusive and unsuccessful predictions, and
- establishing whether ‘re-prediction’ is a useful exercise, or whether the objectives of the Test Case have been achieved.

## Strategy for comparing results

When comparing predictions made by different models, it is necessary to realise the following.

- The true answer is not available and the 380–500 m level model is also a prediction. However, it will be based on much more detailed information and should provisionally be regarded as reality, in the sense of a ‘best estimate’ or a ‘reference estimate’.
- There is no need for absolute certainty: it is only an adequate prediction that is required, not an exact prediction. If uncertainties are bounded and shown to be acceptable for the performance issues at stake, the model may be sufficient.
- Inability to make ‘adequate’ predictions should not necessarily be seen as an ‘error’; it may just be an indication that the required accuracy and precision in predictions simply cannot be obtained using the limited set of input data made available for the task.
- It is generally not possible to define strict numerical criteria for what can be regarded as an ‘acceptable fit’. Differences need to be evaluated and discussed. However some criteria are essential and ‘rules-of-thumb’ may be applicable in given instances.

For *each geometrical* unit (i.e. essentially fracture zone intersections, regions with higher greenstone content, and the remaining rock) the rock mechanics model predicted values (with uncertainty) of the parameters in Table 3-5 should be compared with the values (with uncertainty) of these parameters in the 380–500 m level model. Comparisons between results should be made on the following basis.

- The uncertainty range of the predictions should include the values of the 380–500 m level model. If this is not the case, there is a need to explore the possible origin of such misleading predictions.
- The (potentially) increased precision of the 380–500 m level model should be assessed in relation to the engineering significance of the difference between predictions and 550 m block model values. The following rules-of-thumb show how the logic will be developed:
  - Rock properties that are functions of the fractures are more difficult to characterise and predict than those of the intact rock.
  - Properties measured or estimated on a small scale are generally subject to greater variation than those measured/estimated on a larger scale.
  - For these reasons, generally the mechanical properties of intact rock and the empirical RMR and Q indices can be estimated more accurately than the properties of the fractures and the rock mass.
  - Rock stress values are particularly difficult to measure and predict accurately.

- It is not necessary to make accurate predictions of properties whose precise values are not important for site characterization, repository design, and PA/SA calculations. Thus, deviations in best estimate ‘design value’ of, for example,  $E_m$  of less than 25% will have little engineering implications; whereas for  $\sigma_{mc}$ , or the magnitude of stresses, such a deviation could be significant in a region of high stress where the ratio of maximum stress to compressive strength was one of the main design parameters.
- Similarly, deviations should be interpreted within the context of the parameter itself. For example, if the stress field is close to isotropic deviations in stress directions have no significance.
- The protocols to be developed will establish the acceptable deviations for the purposes of the Test Case.
- To the extent that the predicted uncertainty range represents spatial variability, it should be assessed whether the predicted spatial variability, in a statistical sense, is in agreement with the spatial variability of the 380–500 m level model. For example, if the 380–500 m level model states that 10% of all 30 m blocks have a strength below a certain value, it would be interesting to see if the predictions come close to a similar ratio of blocks with such low strength. Ideally, more formal statistical significance tests could be utilised, but this can only be judged when the actual forms of the uncertainty presentation of the rock mechanics models are decided.
- The engineering impact of the predicted uncertainty representing ignorance should also be assessed, by asking questions of the type, “What engineering decisions would be altered if the rock mass properties or stresses take different extreme values within the predicted uncertainty (ignorance) range?” Specific attention should be given to considering whether the predicted uncertainty ranges are too wide to be of any engineering value.

The assessment should first be made for the individual team predictions made in Step 1 and then for the ‘consensus’ type predictions made in Step 2 (see Figure 3-1 and Section 3.3.5).

### **Potential actions as a result of the evaluation**

The evaluation will be made in a report, discussing the findings, exploring the origins of discrepancies, discussing whether problems (if any) are due to the limited data available or if they depend on the modelling technique applied (see Protocol 8). The documents should also suggest potential improvements to the modelling technique.

One option to consider, in case there is a poor agreement between the detailed 380–500 m level model and the 550 m block model, is try a third step of model predictions where additional data are obtained to allow more input data to be used for the 550 m block model. Additional data should primarily be the optional data indicated in Table 3-4, i.e. additional boreholes with rock mechanics characterization. However, a decision to make such an additional iteration must rest on the evaluation conclusions. There would be no point in executing it if it is obvious that the available input data density is not the reason for the difference.

### 3.3.8 Documentation – Protocol 9

The Test Case will be documented in a special report, Protocol 9 (overviewed in /Andersson et al, 2002/, see Table 1-1, and this current report.

## 3.4 Information supplied to the Teams and block numbering specification

### 3.4.1 Information supplied to the teams predicting the rock properties

The information supplied to the teams making the predictions is listed below. The borehole and tunnel locations are shown in Figure 3-4.

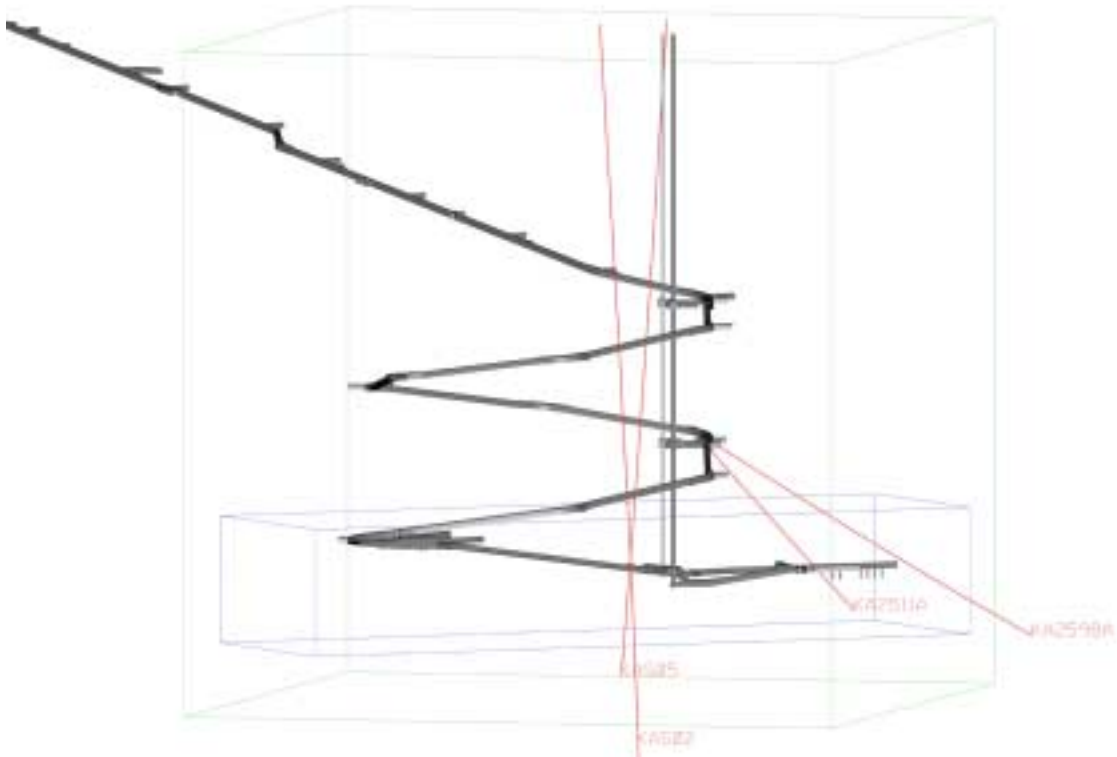


**Figure 3-4.** Location of the boreholes at the Äspö HRL from which the data were obtained and supplied to the teams. The green block is the 550 m block; the blue block is the 380–500 target block.

### *Digital data*

Äspö surface grid resistivity

Äspö surface grid total magnetic field

Äspö SICADA mineral codes (key for interpreting the borehole database)

TMS codes (Tunnel Mapping System, codes for interpretation)

Äspö block presentation/block model 010515 (Rev. 2, showing rock units)

### *Borehole data*

KAS 02: Rock type mapping, sonic logging, normal resistivity measurements, magnetic susceptibility, RQD, Q and RMR values, hydraulic fracturing stress data

KAS 05: Overcoring stress data

KA2598A: Rock type mapping, RQD, detailed hydraulic characterization in different packed-off intervals, Q and RMR values

KA2511A: Rock type mapping, packer flow logging, Q and RMR values

KAS02, KA2598A, KA2511A

Vein mapping, sealed joints mapping, natural joints mapping, fracture frequency, interpretation of crushed zones in boreholes

KAS02, KAS05, KA2598A, KA2511A

Surveying of borehole collars and borehole orientations

### *Shaft data*

Rock type mapping, fracture mapping (to assist in fracture orientation because boreholes were logged without fracture orientation), mapcells (sections where sampling was made), ACAD drawing (visualization of tunnel mapping in 3-D)

### *SKB Reports available*

In the list of Reports, IPR refers to an International Progress Report, and PR refers to a Progress Report. For full references to the Reports, see the entries in the references section of this document, Section 7.

HRL IPR-99-25 Mechanical properties of the diorite in the prototype repository

HRL IPR-25-88-03 Borehole radar measurements

HRL IPR-25-88-06 Geophysical laboratory measurements

HRL IPR-25-89-09 Geological core mapping and geophysical bore hole logging

HRL IPR-25-89-10 Results from borehole radar measurements

HRL IPR-25-89-17 Rock stress measurements in boreholes

HRL IPR-25-91-11 Identification of water conductive oriented fractures in the boreholes

HRL PR-25-88-16 Ground level geophysical measurements on the island of Äspö

HRL PR-25-89-12 Ground surface radar measurements at Äspö

HRL PR-25-88-12 The rocks of the Äspö island.

HRL PR-25-89-22 Ground level geophysical measurements

HRL PR-25-92-10 Reflection seismic profiling

HRL PR-25-87-15 Seismic refraction investigation at Äspö

HRL PR 25-87-03 Natural fractures in the Simpevarp area

HRL PR 25-88-10 Fracture mapping study on Äspö island.

HRL PR 25-88-08 Radon and radium concentrations in ground- and surface water

### *Further information*

The three teams also took part in a site visit which included the rock exposures.

### 3.4.2 Additional information supplied to the Team establishing the ‘best estimate’ of the rock properties.

In addition to all the information listed above, the team establishing the ‘best estimate’ reference rock properties were provided with the following.

Full access to the Äspö HRL which included underground site visits, discussions with Äspö HRL personnel, tunnel maintenance records, and access to all reports. Also, in connection with the Zedex project in 1994/1995, the following boreholes had been logged by NGI previously:

KXZA1-KXZA7 length	266.91 m
KXZB1-KXZB8 length	155.11 m
KXZC1-KXZC7 length	352.65 m
KXZRD and KXZRT length	71.85 m

In total, 1886 m of core at Äspö was logged for Q and RMR. In Boreholes KA2511A 3.28–293 m, KAS02 160.92–612.95 m and KA2598A 2.34–300.77 m, tilt testing and profiling of joint roughness were also carried out.

In addition, data from the following boreholes logged by SKB were used:

KA3065A02, KA3067A, KA2563A, KA3110A, KA3105A, KA3590G02, KA3554G02, KA3566G02, KA3542, KA3600F, KA3573A, KA3590G0, KA3548A01, KA3542G01, KA3510A, KA3385A, KA2563A, KG0048A01, KG0021A01, KI0023B, KI0025F03, KI0025F, KI0025F02, KJ0050F01, KJ0052F02, KJ0052F03, KJ0044F01.

For these boreholes RQD values only (no Q or RMR) were given for each metre of core, plus some other geological information.

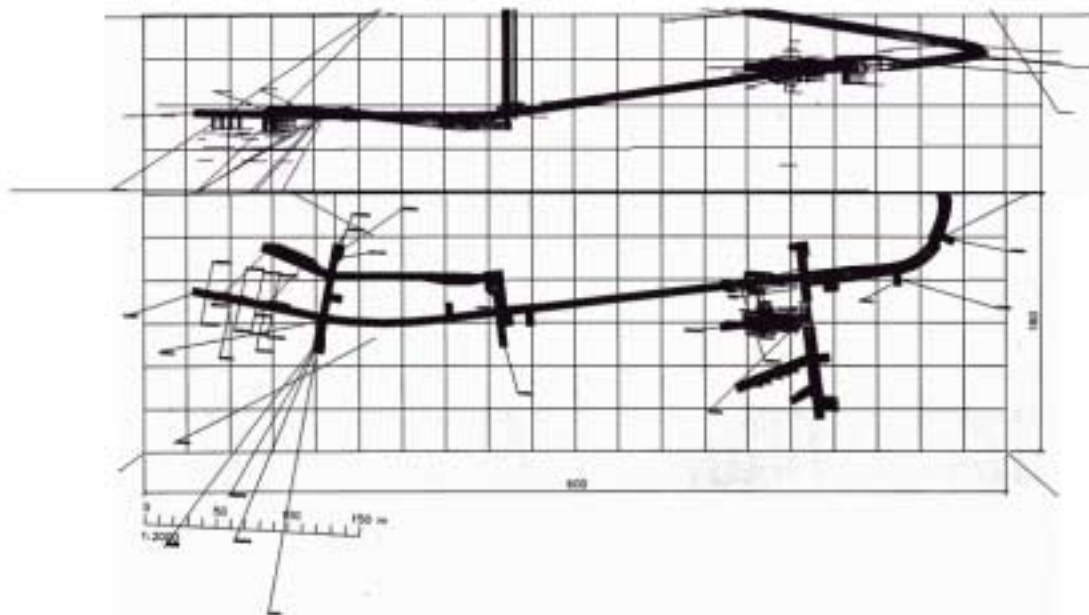


**Figure 3-5.** Vertical cross-section and plan of the Test Case rock volume. The grid lines correspond to the 30 m × 30 m × 30 m blocks.

The tunnel system within the model area is shown in Figure 3-5. The Zedex tunnel (38 m) and the first 50 m of the TBM tunnel were mapped by use of the Q and RMR systems. The rest of the tunnels had been mapped by SKB with the RMR system. The tunnel system inside the model consists of the 400 m long TBM tunnel, about 170 m of the access tunnel, 60 m of lift shaft and several test tunnels.

**3.4.3 Numbering of the individual blocks in the target volume**

The target volume of the Test Case rock block was located between elevation -380 and -500m. The area encompassing the model is 600 m long and 180 m wide and the resulting volume has been divided into 30 m x 30 m x 30 m cubes (blocks). The model thus contains 480 blocks, which were numbered from 1 to 480 starting at the top layer with No.1. These blocks are the smallest units for presentation of the data. This meant that there were four block layers, see Figure 3-6, as follows:

- Layer 1: -380 to -410 m
- Layer 2: -410 to -440 m
- Layer 3: -440 to -470 m
- Layer 4: -470 to -500 m

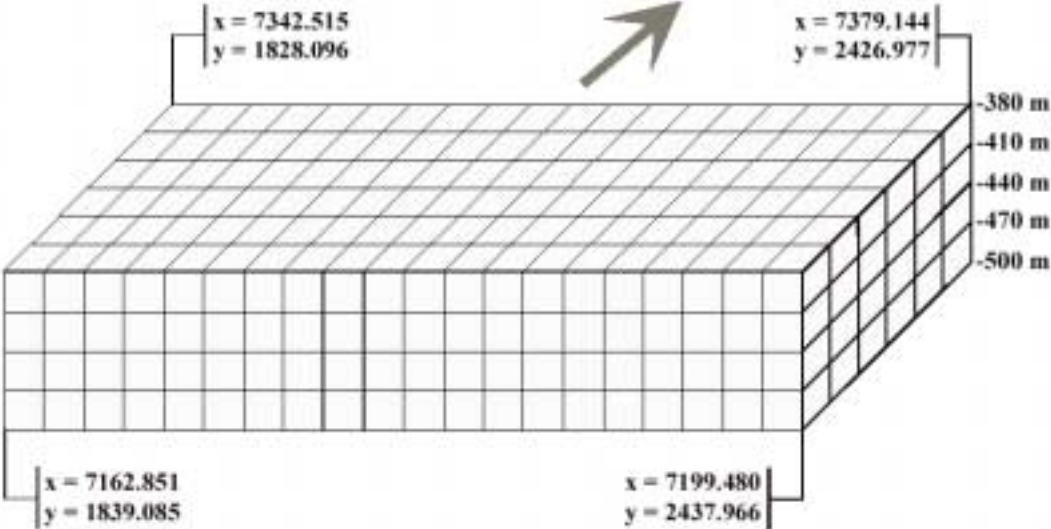


**Figure 3-6.** The Test Case rock volume, 600 m x 180 m x 120 m, sub-divided into individual rock cubes, each with a 30 m edge length. Corner co-ordinates are also shown.

This Test Case target volume is cut by the Äspö tunnel system, and the central part of the underground laboratory is inside the volume, see Figure 3-5.



## 4 Modelling the mechanical properties

As described in Chapter 1, the mechanical properties were estimated by two different approaches: the empirical approach and the theoretical approach. In this Chapter, these individual methodologies are explained first. Then the empirical-theoretical consensus approach is discussed. These approaches provide both the individual and combined predictions for the Test Case rock volume. The comparisons between the predictions and ‘best estimates’ of the actual conditions as mentioned in the previous Chapter are then illustrated. Finally conclusions are drawn concerning the mechanical property component of the Test Case work.

It should be noted that this Chapter describes the specific approaches adopted for the Test Case work. Since then, some modifications have been introduced in developing the wider rock mechanics modelling strategy, Andersson et al, 2002, but these modifications are not reflected in the current Chapter.

### 4.1 The empirical approach

Full details of the empirical approach are given in Röshoff et al, 2002, which presents the methods and results of deriving the required mechanical properties of the fractured rock masses at the Äspö area for a volume of 550 m × 550 m × 550 m, and a smaller volume near the Prototype Repository area between the level of –380 to –480 m, called the Target Volume, using mainly the empirical rock mass classification systems of Q and RMR. Due to the lack of a more direct approach and difficulties in numerical homogenisation models, the rock mass classification systems, typically Q and RMR, are very often used as a means of determining an initial estimation of mechanical properties (such as deformation modulus) and strength parameters (such as internal friction angles and cohesion, uniaxial compressive strength) of the rock mass, based mainly on engineering experiences and judgement. Rock mass classification systems can also be used as an empirical approach to homogenisation and up-scaling for deriving equivalent properties of fractured rocks.

#### The rock unit system

The first step for any rock mass classification system is the division of the rock into units of qualitative lithological and structural homogeneity. These were delineated using the main geological and geometrical information, see Figure 4-1. The rock mass was divided into a number of units by the following structural features and mechanical properties:

- Contact zones of lithology that divide the rock mass into a number (N) of rock units, in both vertical and horizontal directions. *Data source: geological model.*
- Major fracture zones (D1-D2) larger than 500 metres in length, which divide each rock formation into a number ( $K_{i,j} = 1, 2, \dots, N$ ) of basic units, Unit i-j (i-formation number, j – unit number), in both vertical and horizontal directions; *Data source: direct input from the geological model.*

- Fracture zones themselves, due to their large size and possibly large width, with probably complex internal structural, mineralogical and mechanical compositions and properties, are treated as independent basic units. *Data source: direct input from the geological model.*
- Major differences in minor (D3-D4) fracture density, such as differences in fracture set numbers may divide individual rock units into sub-units (e.g. no fractures and one set of fracture is a large difference, but 4 sets and 5 sets with no significant differences in orientation can be treated as minor differences). *Data source: borehole logging data (RQD, set number and orientations along depth (borehole length), surface and shaft mapping results, DFN data at the test area.*
- Major differences in representative mechanical properties of rock matrices and fractures (such as the uniaxial compressive strength,  $\sigma_c$ , of the intact rock and the residual friction angle,  $\phi$ , of the fractures) may divide basic rock units into subunits.

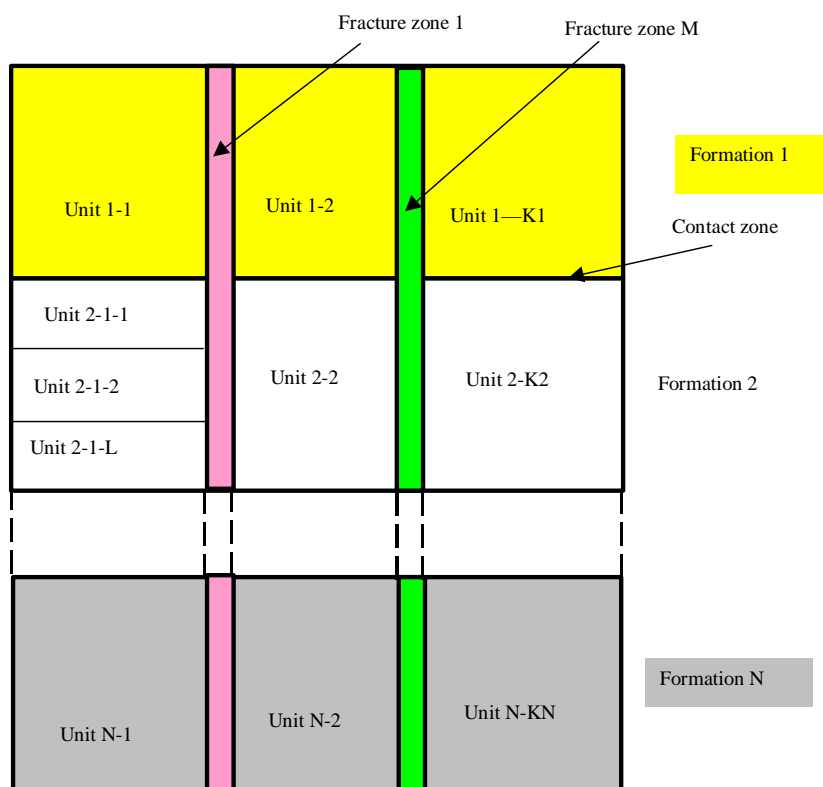


**Figure 4-1.** Conceptual geological model of the site and rock unit division by rock formations (lithology), major fracture zones (D1-D2), fracture properties (Set number, RQD) and main mechanical properties of rock matrix ( $E$ ,  $\nu$ ,  $\sigma_c$ ).

The above unit delineation divides the rock mass of the site into a number of working units (basic and sub-units) of homogeneity in terms of lithology, structure and main mechanical properties. These units served as the basis for implementing the empirical model using Q, RMR, GSI and RMI rating systems.

#### **4.1.1 Equations for determining strength and modulus of deformation**

A variety of equations were used to relate the rock mass classification index values with the required properties. A fuller description is given in /Röshoff et al, 2002/.

#### **4.1.2 Confidence levels**

The confidence levels to be assigned were

- 1- Ratings and properties are obtained by local data support
- 2- Ratings and properties are obtained by interpolation/reasoning
- 3- Ratings and properties are obtained through pure guesswork .

To define these confidence levels, rules-of-thumb were defined as below:

- i) the cells which have one or more boreholes passing through will have confidence 1.
- ii) cells will have confidence level 1 if they have nearly equal distances to a vertical borehole as a nearby cell which contains the vertical borehole; this applies to the borehole KAS02;
- iii) cells immediately surrounding cells of confidence level 1, within the same unit/block, will have confidence level 2;
- iv) the rest of the cells have confidence 3.

These rules consider the confidence level according to the distance of the cells from boreholes.

Data sources – core logging and surface/shaft mapping

Seven types of data sources were available for use in the Q/RMR-rating systems.

- 1) The RVS geology/geometry models for the block system definition, supplied by SKB for the project.
- 2) Borehole logging records for three boreholes: KAS02 which passes through blocks H, I and J; KA2598A which passes through blocks G, H and E, and KA2511A which passes through block H, supplied by SKB for the project.
- 3) Surface mapping data about fracture orientations and trace lengths, which covers all blocks except for blocks K and M, reported in /Ericsson, 1988/;
- 4) Mechanical shear test data with fracture samples taken from the Prototype Repository area, with samples taken from the cells 263, 264, 281–283, and 302–303, at layer 2, and testing for uniaxial compressive strength of intact rock with samples taken from cell 283, reported in /Lanaro, 2001/.

- 5) Shaft mapping data containing orientation and traces of fractures with trace lengths larger than 1.0 m, located within block/unit H, supplied by SKB for the project.
- 6) Mechanical testing of samples of intact rock and fractures, reported in /Stille and Olsson, 1990/. The properties produced included uniaxial compressive strength, Young's modulus and Poisson's ratio for greenstone, aplite, diorite and granite, and the friction angles of steep and gently dipping fractures, with rock types not reported. The locations of the intact rock samples were also not reported.
- 7) Mechanical testing of rock fractures and intact rock samples reported in /Nordlund et al, 1999/, with samples taken near the Prototype Repository area at Äspö. The rock type is diorite and the mechanical properties produced include the uniaxial compressive strength, tensile strength, Young's modulus, Poisson's ratio, cohesion, internal friction angle, strength parameter  $m$  in the Hoek-Brown strength criterion, and other cracking-related properties.
- 8) Measured in situ stress results at the Äspö area reported by /Hakami et al, 2002/.

#### **4.1.3 Initial stress field and groundwater issues**

Initial stress field and groundwater flow behaviour affects the Q and RMR ratings to a significant extent, as represented by the ratio ( $J_w / SRF$ ) in Q and  $RMR_{water}$  in RMR rating systems. However, water and stress were not considered in the empirical classification methods for the Test Case as discussed below.

The measured in situ stresses are used to determine the major and minor principal stresses according to the largest depth of the location under consideration, for example, at the bottom end of a core section which is used to determine Q and RMR ratings along a borehole. The stress field is therefore basically uniform without considering possible changes due to changes in rock types, and fracture zones.

For the groundwater issue, it is assumed that a hydrostatic pressure field should be used to determine the water pressure at different depths, with zero pressure at the ground surface. In reality, water flows are controlled by connected fracture networks and are not uniform, as can be seen from the Äspö HRL tunnels. However, this effect cannot be incorporated properly within the rating systems at this stage of the project and the fracture system effect on water pressure has to be ignored. This may cause overestimated water pressure at some (unknown) locations, whose effect on the overall ratings cannot be properly evaluated. Some inflow rate data are available for boreholes KA2598A and KA2511A. However, it is not so straightforward to transform these data into inflow rate per 10 m of a tunnel and therefore only the pressure is used for RMR ratings, and engineering judgement for the descriptive flow condition (dry, dripping, large flow, etc) for the Q ratings.

#### **4.1.4 Dealing with uncertainty and variability issues**

##### **The main uncertainty issues and their treatment**

The main limitations of the empirical approach were:

- a) The empirical approach of the rating systems makes it impossible to check whether they will obey basic laws of physics, such as conservation laws. The deformation

modulus derived does not come from properly defined constitutive models, but is an empirical estimate with the assumption of an equivalent elastic gross mass behaviour.

b) Strength parameters in the RMR system are based on a failure criterion, which may or may not meet site specific rock conditions.

c) The estimated rock mass deformation modulus and strength parameters based on the empirical approaches cannot be explicitly made stress-dependent and ‘fracture-system’ – ‘geometry-dependent’. However, the SRF factor in the Q system provides a means to compare results with the stress-dependent deformation modulus produced by the theoretical approach, although indirectly. The properties produced by the RMR approach are stress-independent.

The main uncertainty sources considered at present in this project are:

a) **Uncertain size distribution of the fractures:** this uncertainty comes from the fact that most of the fracture information comes from three boreholes, KAS02, KA2511 and KA2598A, and one shaft near the centre of the 500 m level model, for orientations. The main source for fracture size, which is needed for RMR rating, comes from surface mapping results for regional structural geology purposes rather than site characterization, with no information regarding unit/block structures.

The treatment of this uncertainty was to assume that the mean value (about 1.0 m) of the fracture length from the surface mapping was valid for the whole model area. This basic value was then modified locally at different borehole depths when calculating local  $RMR_{fracture\ condition}$  values along borehole sections. The modification was done with engineering judgement based on the numbers of larger fractures appearing on the shaft walls (whose size is certainly larger than 4.5 m, the diameter of the shaft), where the shaft is in the concerned unit and core sections.

This treatment put the mean fracture length in the category of 1–3 m level for most cases, and 3–10 m level in a few cases, according to the RMR rating system.

b) **Uncertain spatial distribution of mechanical properties of intact rock and fractures:** The required mechanical properties of intact rock for the Q and RMR ratings are the Uniaxial Compressive Strength (UCS) of the intact rock, Joint Wall Compressive Strength (JCS), residual friction angle  $\phi_r$ , and Joint Roughness Coefficient (JRC) of fractures. These properties were tested in a number of units but not all. Except for the shear tests reported in /Lanaro, 2001/, sampling locations were not reported in other early technical reports, such as the rock mechanics testing and evaluation by /Stille and Olsson, 1990/. This lack of proper documentation made the unit rating and estimation of spatial variability of the properties difficult.

The treatment of this uncertainty was to assume that the mean values of these properties were valid for the whole block where samplings and tests were reported.

c) **Uncertain block information:** This uncertainty comes from the fact that a large number of blocks, A, B, C, D, F, K, L, M and N are almost ‘blank’ blocks where no data from borehole, shaft, or mechanical testing were available. The only data source available was the surface mapping data about fracture sets and trace lengths, and indications from seismic velocity records over the whole Äspö site, which was divided

into two areas, the North Domain area (covering Blocks A, B, C, D, E and F) and the South Domain Area (covering Blocks H, I, L and N). The blocks K and M were totally 'blank' blocks where no information is available at all.

d) **Uncertain effect of rock types on block unit division:** It was decided the blocks A – N, formed by the fracture zones as represented in the 550 m model, should be taken as the unit system, and no further division of blocks according to different rock types, mechanical properties and fracture density should be considered. Therefore, these blocks had mixed major rock types. During processing of the borehole data for the rating systems, it was found that distinct, large zones of different rock types with different mechanical and fracture characteristics existed in the same blocks. Sometimes these zones were over 100 m in one direction. Thus, the block system model defined for this project did not properly represent the site geology, at least in view of rock lithology.

e) **Uncertain Greenstone formations:** There are an unknown number of lenses of greenstone in the model area, but their exact locations and extensions are largely unknown. A general estimation is that these greenstone lenses may occupy about 5% of the total volume of the model area. It was assumed that effect of the greenstone on the ratings could be ignored because of their small volume.

f) **Uncertain fracture surface condition:** The surface condition of the fractures, such as roughness, weathering, in-filling, coating, flow, wall strength and aperture, are important indices for both Q and RMR rating systems. Among these parameters, the wall strength, roughness and coating were relatively better characterized, using Schmit hammer tests and borehole observations, but the weathering, in-filling and aperture were largely unknown.

g) **Uncertain fracture orientation relative to tunnel orientation:** Since no tunnel was concerned, it was assumed that a general 'fair' index for the fracture orientation should be adopted for all RMR ratings as a general condition. This produced a reduction of total RMR rating by 5, and may be a relatively conservative estimation.

h) **Uncertain validity of the empirical coefficients used for determining mechanical properties using Q and RMR ratings:** The empirical coefficients, which are used for determining mechanical properties using Q and RMR have been established over long periods of practice. However, they still may not be suitable for the site-specific conditions of the model area in this project.

#### **4.1.5 The division of the core sections and the nested data processing forms**

Each borehole in each block unit was divided into a number of core sections along its length of homogeneous RQD and fracture frequency values. The difference in rock type was not considered in the current RVS geological unit system model. The difference in fracture set numbers was treated as variation within the block, without splitting blocks into sub-units. Figure 4-2 illustrates the technique of division of borehole sections and the data files created for each core section.

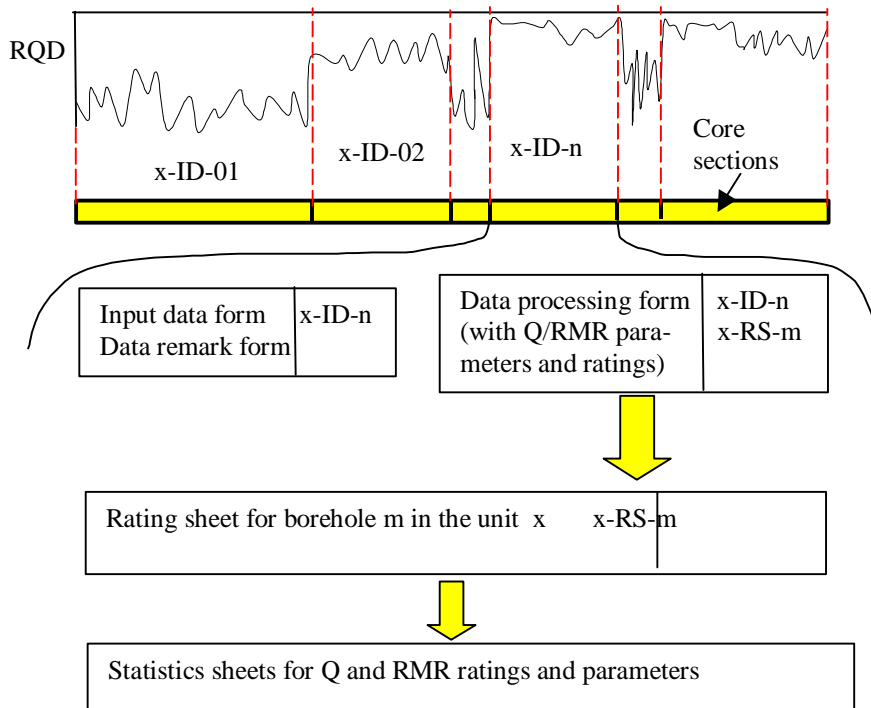


**Figure 4-2.** An example of division of borehole sections for Q/RMR parameterisation /from Röshoff et al, 2002/.

For each core section, three data processing sheets are created

- 1) Input data form: This sheet contained all basic information for parameterization of both Q and RMR systems,
- 2) Data remark form: This sheet contained mainly the information and file sources and comments on the fracture conditions.
- 3) Data processing form: This sheet was the parameterization form for both Q and RMR with all necessary parameters.

The Q/RMR parameters and ratings from the data processing sheet for all core sections from the borehole were collected into a 'Rating sheet'. From this rating sheet, statistical analyses of Q, Q' and RMR ratings and all associated parameters were performed to produce two additional data sheets, the 'statistics analysis sheet' of ratings and similarly of parameters.

The above data processing sheets formed a nested data file system for storage and cross-reference of all the input data, parameterization, ratings, comments and sources for each borehole in each block, as shown in Figure 4-3.

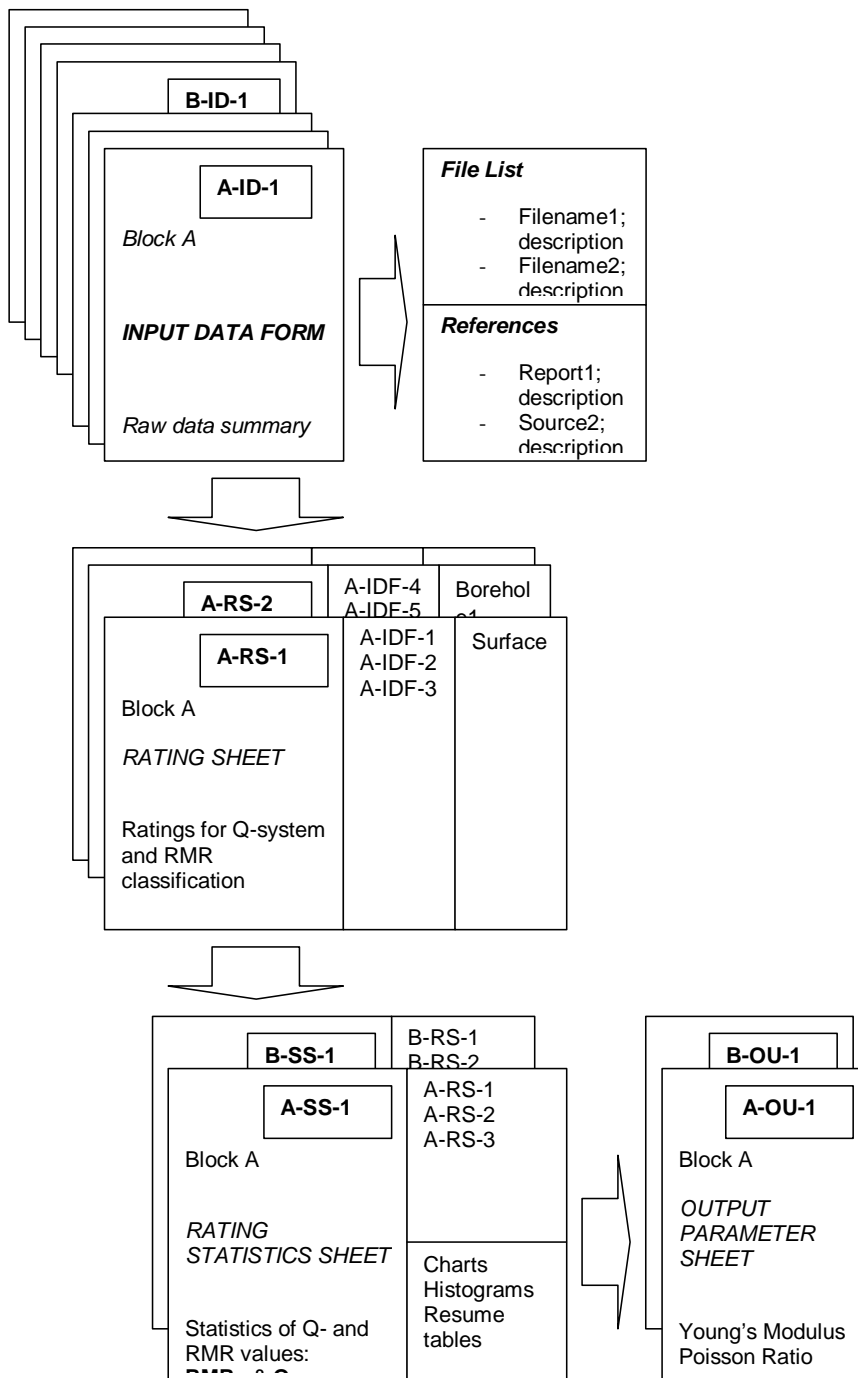


**Figure 4-3.** The nested data processing forms and sequences for Q/RMR ratings /from Röhshoff et al, 2002/.

#### 4.1.6 Results for the 380–500 m model

The Q and RMR ratings, and the deformation modulus (mean value and standard deviation, or ranges) estimated from Q and RMR, were produced for each cell. For cells filled with mixed rock types, with competent rocks and fracture zones, two sets of values were presented.



The ratings of the cells were produced according to the following rules-of-thumb (see Section 4.1.3):

- For cells of confidence level 1, the Q and RMR ratings and their associated parameters were all calculated directly from local core sections and mechanical test results on samples taken from these cells. Therefore, these results may be different from the mean values of the blocks/units.
- For cells of confidence level 2, the Q and RMR ratings and their associated parameters were given as the same as that of the confidence 1 cells which they surround.
- For the cells of confidence level 3, the Q and RMR ratings and their associated parameters were given as the mean values of the block/unit.

**The results are presented in**

Table 4-1 and Table 4-2.

**Table 4-1. Characterization: Q- and RMR-ratings for the target cells and the deformation modulus obtained using /Grimstad and Barton, 1993/ from Q and /Serafim and Pereira, 1983/ from RMR.**

Cube ID	Rock Unit	Northing [m]	Easting [m]	Z depth [m]	Q Mean	RMR Mean	Em Mean Q [GPa]	Em StDev Q [GPa]	Em Mean RMR [GPa]	Em StDev RMR [GPa]
4	E	7333.953	1933.815	-395	3.9	72	15	-	35	-
	H				7.68	71	22	-	33	-
5	H	7335.785	1963.759	-395	6.45	67	20	3	28	13
50	H	7285.054	2117.142	-395	14.76	76	29	2	45	12
105	H	7186.065	1972.916	-395	15.92	75	30	-	42	-
124	E	7333.953	1933.815	-425	2.81	72	15	-	35	-
150	H	7314.998	2115.311	-425	16.2	78	30	-	50	-
170	H	7285.054	2117.142	-425	16.67	80	31	-	56	-
270	H	7314.998	2115.311	-455	15.83	77	30	0	47	4
389	H	7313.167	2085.367	-485	15.81	77	30	1	49	6

**Table 4-2. Characterization: Cohesion and friction angle via /Hoek, 1990/ for two levels of the confining pressure for the target cells.**

Cube ID	Rock Unit	Northing [m]	Easting [m]	Z depth [m]	c 0–5 MPa [MPa]	c 10–20 MPa [MPa]	$\phi$ 0–5 MPa [deg]	$\phi$ 10–20 MPa [deg]	$\sigma_{c(H-B)}$ [MPa]	RMR char.
4	E	7333.953	1933.815	–395	4	17	61	48	30	72
	H				4	16	61	47	28	71
5	H	7335.785	1963.759	–395	4/2	15/3	59/3	44/4	22/14	67
50	H	7285.054	2117.142	–395	5/2	17/3	60/2	47/4	35/14	77
105	H	7186.065	1972.916	–395	5	17	60	47	35	75
124	E	7333.953	1933.815	–425	4	17	61	48	30	72
150	H	7314.998	2115.311	–425	6	18	61	48	41	78
170	H	7285.054	2117.142	–425	6	18	61	49	46	80
270	H	7314.998	2115.311	–455	6/0	17/0	61/0	48/0	39/0	77
389	H	7313.167	2085.367	–485	6/1	18/1	61/0	48/1	40/5	77

#### 4.1.7 Quantification of the uncertainty in the characterization ratings and parameters

A technique was created to quantify the uncertainties in parameters, see /Röshoff et al, 2002/. The principle of the technique was a ranking of the characterization ratings according to:

- the kind of information (published SKB reports, data files, on site observations, personal communication, engineering judgement and reasoning);
- different biases for a particular parameter (measurement techniques, personal perspectives, different time of measurement);
- size of sampling and data population;
- different evaluation techniques for the same parameter (e.g. UCS, JCS, roughness, JRC, Q from seismic velocity, visual evaluations, estimations during logging, availability of comments concerning logged parameters);
- confidence in the estimation of the difficult parameters (e.g. aperture, fracture surface roughness, coating, weathering, and trace length/persistence);
- ambiguity in descriptions in certain classification codes;
- engineering/expert judgement for difficult situations, such as lack of data;
- mismatching between the geological and engineering definitions.

Three classes of uncertainty were defined for each rating as:

- **CERTAIN:** the classification was made by using exactly the value of the parameter/rating supported by reliable sources: all variations in the data were computed for spatial variation and sampling bias;

- **PROBABLE:** The classification was based on engineering judgement and reasoning to a certain extent, with very limited support from reliable data sources. There was a possibility that the chosen classification class may have certain variation margins, but not more than one rank higher or lower than the estimated values;
- **GUESSWORK:** the classification was based on engineering judgement/reasoning without the support of reliable data sources, and variation in the rating/parameter could be large. A margin of two ranks higher or lower than the estimated values, within a reasonable limit, was given to quantify this class of uncertainty.

More detail concerning the empirical approach to the estimation of rock properties is given in /Röshoff et al, 2002/.

## **4.2 The theoretical approach**

In order to consider how the rock mass properties can be estimated from the component items, intact rock and rock fractures, a numerical model is needed /Staub et al, 2002/. The model provides the rock mass response under different loading conditions.

### **4.2.1 Methodology**

The methodology is presented by /Staub et al, 2002/ and summarized in the flow chart in Figure 4-4. It was considered possible to model the mechanical behaviour of a fractured rock mass in two dimensions by considering rock sections in different directions. For this purpose, the 2-D numerical code UDEC was selected as the calculation tool. The computations of the mechanical properties of the rock mass were based on multiple stochastic realisations. Multiple realizations reflected the variability and possible distribution of the input parameters to the model and permitted a statistical analysis of the results. Each simulation was treated independently in UDEC. This meant that for a single set of input parameters, UDEC had to be run several times to obtain the expected set of results.

#### **DFN model**

This was the base for the fracture definition in the UDEC model. It defines mainly the spatial density of the fractures within a given volume and the statistical distribution of the fracture orientation and size.

#### **FracMan® DFN modelling**

FracMan® was used to generate fractures in three dimensions (3D) within a given rock volume, whose size could be modified according to the size of the required model. For the purpose of this study, the DFN model was generated in rock volumes of 50 m × 50 m × 50 m.

#### **Generation of 2-D fracture trace sections**

The three dimensional discrete fracture network (DFN) generated by FracMan® had to be reduced to fracture traces to fit the assumptions of a two-dimensional UDEC model. Since the boundary conditions of the UDEC model are preferably set to normal loading only (no shear conditions), fracture traces were obtained in planes aligned with the in situ principal stresses at the investigated site.

Three different fracture trace planes of size  $30\text{ m} \times 30\text{ m}$  aligned with the in situ principal stress field were identified. These planes cut the DFN model at its centre. The DFN model size was set large enough to avoid any truncation of the fracture traces at the boundaries of the trace planes: the edges of the trace planes were always located within the volume of the 3-D DFN models.

Full details of the methodology and its constraints are reported in Staub et al, 2002.

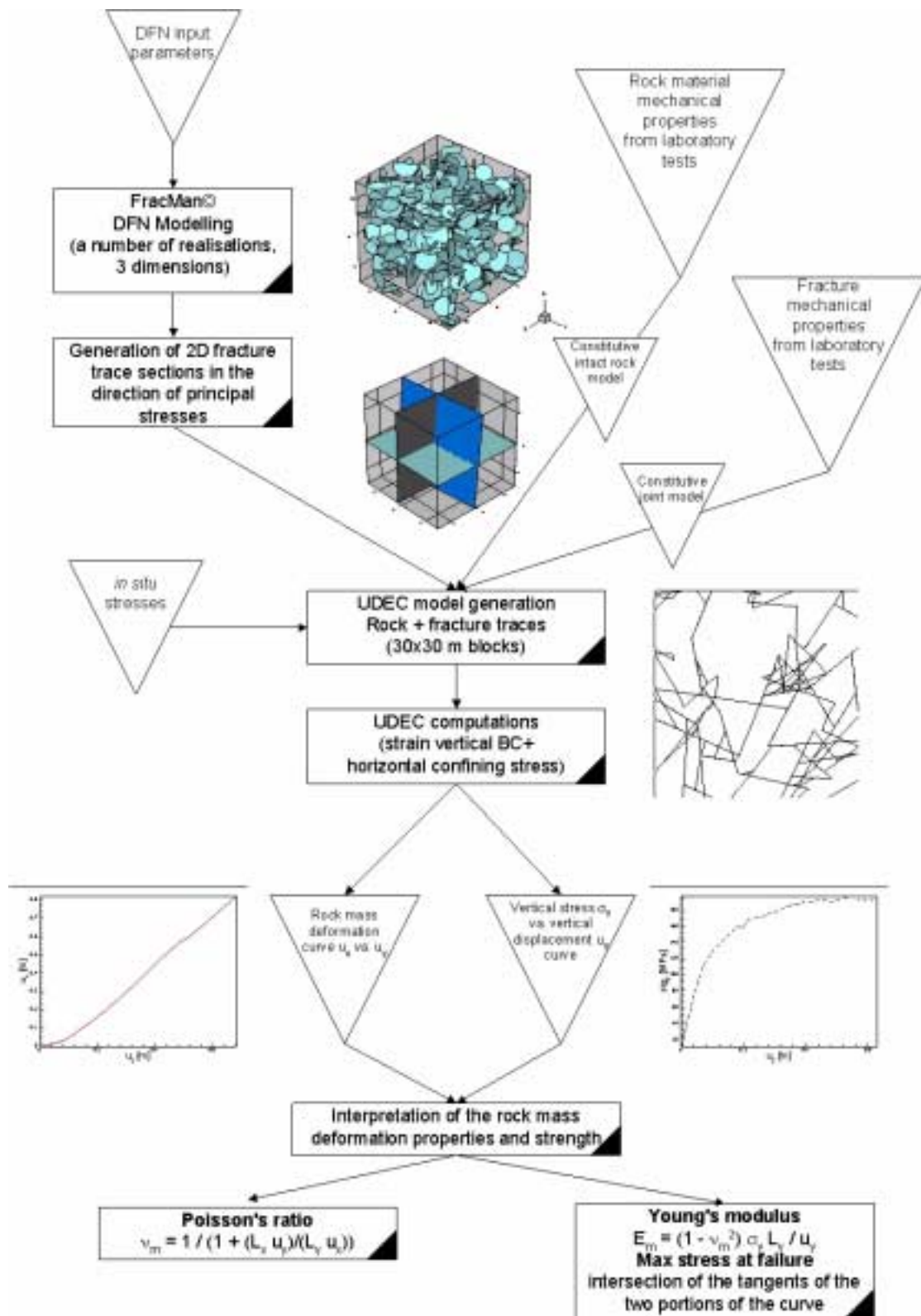


Figure 4-4. Flowchart for the theoretical approach /from Staub et al, 2002/.

## **Constitutive models for intact rock and fractures**

Different constitutive models are available in UDEC that can be used to model the behaviour of the intact rock and of the fractures.

The models chosen for this project were:

- The Mohr-Coulomb plasticity model for the intact rock
- The Barton-Bandis model for rock fractures (and occasionally for numerical reasons the continuously yielding model).

The influence of the constitutive models used in this project was also studied.

## **In situ stresses**

The in situ stress conditions were reproduced in the UDEC model. Orientations of in situ stresses were considered by means of 2-D sections generated in the directions of the three principal stresses. The in situ stress magnitudes and orientations were provided by the Stress Model group /Hakami et al, 2002/.

## **Boundary conditions**

Stress and velocity boundary conditions were applied to the block model. Since the block model test in UDEC is similar to a plane strain test, confining stresses were applied on the vertical and upper boundaries of the model. Horizontal deformations were set to zero at the left vertical side of the model, and vertical deformations were set to zero at the lower boundary of the model. A constant velocity boundary was then applied to the top of the model for computations of the plane strain test.

## **UDEC computations**

The mechanical testing was simulated with a vertical loading applied on top of the model by means of a constant velocity boundary displacement. Even if the boundary conditions were such that the model is in an initial force-equilibrium state before alteration, the equilibrium state was checked before performing vertical loading. The vertical loading was applied to the model beyond the elastic behaviour of the components of the model (rock material and fractures) so that the estimation of the rock mass strength could be assessed.

The following parameters were monitored during the loading test.

- Vertical displacement along a horizontal profile at the top of the model
- Vertical stress along a horizontal profile at the top of the model
- Horizontal displacements along a vertical profile at the right boundary of the model

The monitoring profiles consisted of 25 monitoring points that were equally distributed along a reference line. The value at a computing node was attributed to the nearest monitoring point on the reference lines. The mean value of the monitored variable at the twenty five points was then calculated at each loading step.

## **Rock mass deformation properties and strength**

The deformation properties of the rock mass were evaluated from two curves drawn by respectively plotting of: (1) horizontal displacement,  $u_x$ , vs. vertical displacement,  $u_y$ , and (2) vertical stress,  $\sigma_y$ , vs. vertical displacement,  $u_y$ . The first curve was used to evaluate the Poisson's ratio of the rock mass. The deformation modulus and the rock strength were determined from the second curve.

### **4.2.2 Input data to the theoretical approach**

#### **Geometry of fractures**

The main issue was to characterize features that are 3-dimensional but represented by limited, often 2-D, exposures on outcrops, in boreholes and in tunnels. Three different approaches that have been developed to simulate fracture networks are Stochastic Continuum (SC), Channel Network (CN) and Discrete Fracture Network (DFN). In the framework of this project, realistic simulation of the fracture network in the area of investigation represented the main interest, and DFN models were used. The fracture pattern for each developed DFN model was characterised by the following parameters: orientation of the fracture sets, spatial intensity of each fracture set – expressed as the area of fractures/volume, and size distribution of the fractures in each set.

#### **Mechanical properties of intact rock**

The mechanical properties of the different types of rock materials considered were obtained from laboratory tests.

#### **Mechanical properties of fractures**

Numerical modelling of practical problems with fractures may take fractures through rather complex load paths. In UDEC, two fracture/joint models are available for modelling such load paths. The models are the Continuously Yielding joint model and the Barton-Bandis joint model.

### **4.2.3 Set-up of the numerical model**

The numerical model simulates a plane strain load test of the rock mass with constant confining stress, see Figure 4-5. The rock mass was loaded by means of a loading block that was pushed down with a constant velocity, and the confining stress was then gradually reduced. High mechanical properties were assigned to the loading block to make it essentially rigid, i.e non-deformable. The interface between the loading block and the rock mass block was assumed to have no friction.

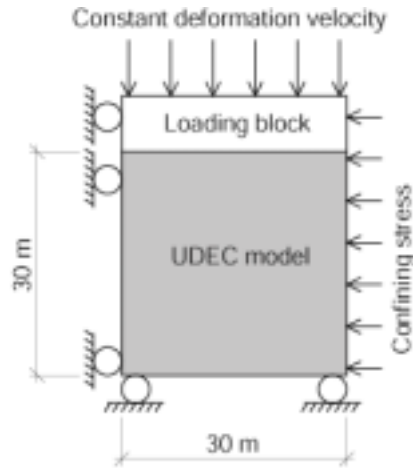


**Figure 4-5.** The numerical UDEC model /from Staub et al, 2002/.

### Evaluation of the rock mass deformation properties from the model

During the numerical loading test, the vertical stress,  $\sigma_v$ , and horizontal deformation,  $u_x$ , were recorded as a function of the vertical deformation,  $u_y$ . The Poisson's ratio,  $\nu_m$ , and the deformation modulus,  $E_m$ , of the rock mass were calculated according to the following equations:

$$\nu_m = \frac{1}{1 + \frac{(L_x \cdot u_y)}{(L_y \cdot u_x)}} \quad E_m = \frac{(1 - \nu_m^2) \cdot \Delta\sigma_y \cdot L_y}{u_y}$$

where  $L_x$  and  $L_y$  are the length over which  $u_x$  and  $u_y$  are measured.

### Evaluation of the rock mass strength from the model

In geotechnical software, a failure criterion is used to describe the rock mass strength. Two well known failure criteria are the Hoek-Brown and Mohr-Coulomb criteria. The constants in the generalised Hoek-Brown failure criterion for jointed rock masses are determined by statistical analysis of sets of stresses ( $\sigma_1$  and  $\sigma_3$ ) at failure. The range of minor principal stress values,  $\sigma_3$ , over which these combinations of stresses are given is critical in determining reliable values for the constants. The Mohr-Coulomb failure constants can also be fitted to pairs of principal stresses at failure. In order to restrict the number of numerical simulations, the Mohr-Coulomb failure criterion was used to evaluate the strength of the rock mass for these Test Case simulations.

The evaluated rock mass properties were intended to be valid for a 30 m  $\times$  30 m  $\times$  30 m rock volume around the anticipated deposition tunnels. The confining stress around the tunnels will range from zero at the tunnel wall to the horizontal in situ stress at a distance of about five radii from the tunnel (about 15 m). To obtain an average, it was decided to run two loading tests in the numerical model. The first test was initially consolidated to the in situ stresses and then loaded in vertical compression to failure. The second test was initially consolidated to the in situ stresses, then unloaded to a



horizontal stress value one quarter of the in situ value (valid for a distance of about 0.2 radii from the tunnel wall) and then loaded in vertical compression to failure. From these numerical loading tests, two sets of principal stresses at failure,  $\sigma_{1a}$ ,  $\sigma_{3a}$  and  $\sigma_{1b}$ ,  $\sigma_{3b}$ , were obtained.

#### 4.2.4 Sensitivity analyses using the model

##### Intact rock and fracture models

Three different failure criteria models for the intact rock have been tested, first the Mohr-Coulomb (M-C) failure criterion, second the Hoek-Brown (H-B) failure criterion, and third a Strain-Softening model (S-S) based on M-C. For the tests on different material models for the intact rock, the Barton-Bandis joint model – as implemented in UDEC – was used. The differences between the models were quite insignificant up to the peak value. The S-S model showed a pronounced peak at all confining stress levels. At the highest confining stress, the H-B and M-C models provided a higher stress at failure than the S-S model.

##### Influence of the boundary conditions

The set-up of the model was slightly modified to test the influence of the boundary conditions. Two different set-ups were simulated, one run with confining stresses applied on the right vertical side only, the other one with confining stresses applied on both vertical sides, all other parameters remaining constant, see Figure 4-6.

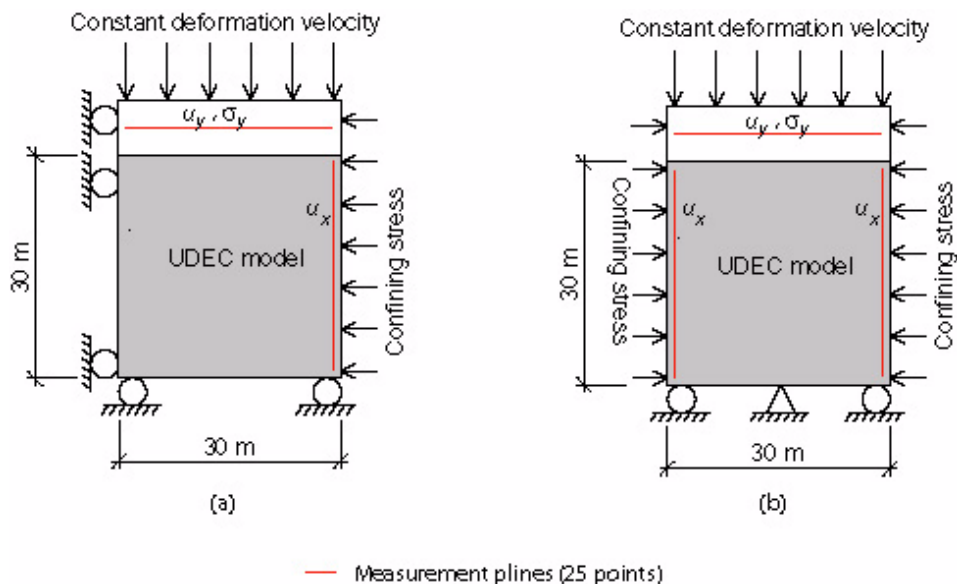


**Figure 4-6.** Set-up of the boundary conditions for the same model size; a) loading on one vertical side and b) loading on both vertical sides /from Staub et al, 2002/.

The model loaded on both vertical sides was subjected to little more deformation than the model loaded on one vertical side, and provided a lower value of stress at failure. In order to obtain some statistics on the influence of boundary conditions, the input data for fracture traces were taken randomly from different realisations of the DFN model on a vertical section of a given orientation, The 20 m × 20 m model was subjected to more deformation and provided lower values for failure at stress. Meanwhile, the values obtained from the 30 m × 30 m model were almost the same in both cases, but higher when confining stresses were applied on both vertical sides.

The conclusions were that the boundary conditions seem to have very little influence on the rock mass deformation properties and stress at failure, especially when running the 30 m × 30m model. More than the boundary conditions, the fracture pattern, which controls the generation of rock blocks in UDEC, seems to have a strong influence on the deformation properties of the simulated rock mass.

### Influence of the domain size

In order to determine the influence of the domain size on mechanical properties, models of different sizes were built. The chosen sizes were (in metres) 20 × 20, 30 × 30, 40 × 40 and 60 × 60, see Figure 4-7.

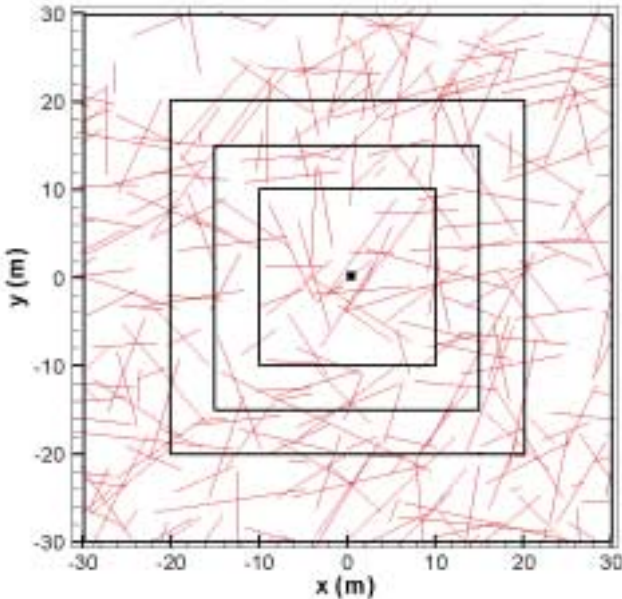


**Figure 4-7.** Generation of the fracture pattern for the different models /from Staub et al, 2002/.

It is not possible to define a trend in the rock mass mechanical properties in relation to the size of the model. For a specific geometry, the 30 m × 30 m model provided the highest deformation modulus. Nevertheless, when looking at the sample simulations, the 30 × 30m model generated the lowest mean values for the deformation modulus and stress at failure. The fracture pattern in the model had a strong influence on the deformation properties of the simulated rock mass.

### **Influence of the discarded joints**

The fracture traces that terminate in the intact rock and do not intersect with any other fracture traces were discarded when ‘meshing’ and generating the rock blocks in UDEC. In order to determine the influence of this process on the mechanical properties of the rock mass, a manual procedure was applied that enabled one to artificially maintain the fractures discarded by UDEC. The impact of the discarded fractures on the deformation properties of the rock mass seemed to be almost insignificant. The rock mass even appeared to be slightly stiffer when running with ‘artificial’ and ‘real’ fractures.

However, the procedure of prolonging and keeping isolated fractures was time-consuming, and the influence of these fractures on the deformation properties of the rock has not been highlighted by those simulations. Therefore, the models were all run by applying the ‘usual’ UDEC procedure with discarded fractures.

### **2-D simplification from the 3-D model**

The transfer of a three-dimensional fracture network into a two-dimensional trace network with the same overall mechanical properties is not trivial. For example, even if there are no blocks formed by the fractures in a three-dimensional fracture network, fracture traces in a two-dimensional cross-section may form blocks. The difference between the 3-D and 2-D model is likely to depend on the nature of the fracture network. It was unrealistic to implement 3-D simulations with real fracture networks, but some tests on simple fracture networks were performed.

The results indicated that the 3DEC model starts to soften earlier than the UDEC models. The strength of the 3DEC was only 55% of the 2-D models. With few fracture planes in the model, the difference between 3DEC and 2-D simulations is probably large. The method of gluing some part of the fracture plane, and the mechanical properties assigned to these ‘glued’ parts of fractures, can have a significant influence on the results.

## **4.2.5 Set-up for the fracture zones**

### **Assumptions related to the modelling of fracture zones**

- The model size was taken as ten times smaller than for the modelling of the rock mass, i.e. 3 m × 3 m. This set-up was adjusted to running models with higher fracture densities.
- The modelling plane is a section that is perpendicular to the fracture zones, so that the Young’s modulus can be calculated. This implies that shear displacements can occur – as the 2-D model was not oriented along the three principal stress directions.
- Confining stresses were applied on both vertical sides.

## **Geometry of fractures in the fracture zones**

The fracture pattern in fracture zones and the influence areas of these fracture zones was affected by the stresses and the deformation associated with these features. The parameters used to define the rock mass fracturing, such as fracture orientation, fracture size distribution and intensity, should be modified in accordance with the actual pattern. Specific input data are required to model the fracture pattern in the fracture zones. A DFN model, focussed on the characterization of the fracturing in the fracture zone, should be provided as necessary.

## **Mechanical properties assigned to the rock mass in the zones**

Mechanical properties of intact rock and fractures can be altered in fracture zones, and the degree of alteration will depend on the localisation from the 'core' of the zone. A detailed study and mapping of intact rock and fracture surfaces in the fracture zones enable the determination of the appropriate properties.

### **4.2.6 Distribution of the parameters – Monte Carlo simulations**

The uncertainty of a model can be separated into conceptual uncertainty, data uncertainty and spatial variability. The conceptual uncertainty originates from an incomplete understanding of the principal structure of the analysed systems and its interacting processes. This uncertainty is not discussed further here. Data uncertainty concerns uncertainty in the values of the parameters in a model. Data uncertainties may be caused by measuring errors, interpretation errors, or the uncertainty involved in extrapolation when the parameter varies in space. Spatial variability concerns the variation in space of a parameter value. Spatial variability is not an uncertainty but is, of course, often a cause for data uncertainty.

The data uncertainty and spatial variability are often expressed in statistical terms as mean value, standard deviation and type of distribution. In our case, the spatial variability can be separated into the spatial variability of the geometry of the fractures, the spatial variability of the rock type, and into the data uncertainty and spatial variability of the parameters describing the properties of the intact rock and the fractures.

The spatial variability of the fracture system is described by the DFN model. The spatial variability of the rock type is described by the percentage of different rock types in a rock block. The data uncertainty and the spatial variability of the material parameters for a specific rock type are expressed by the measured mean value and the standard deviation. A normal distribution is assumed.

A common way to obtain the statistical parameters for a model with many input parameters that can be expressed in statistical terms is to run Monte Carlo simulations. One set of parameters is chosen at random according to the statistical distributions of the parameters and the response of the model with these parameters is calculated. By running many simulations and by treating the outcome in a statistical way, the mean and the standard deviation of the outcome from the model can be estimated. This method was used.

## The large model

A model that covers the volume defined by the 550 m block was developed for the purpose of this study with RVS (Rock Visualisation System tool, developed by SKB). This model gives an overview of the position and orientation of local deformation zones in the area. In order to take into account variations of width, local orientation and undulations, the zones were assigned some thickness. The width of the modelled zones is a function of the actual observed widths and interpreted undulations of the zone.

Two different types of 'rock units' were defined: the 'ordinary rock unit' identifying the fractured rock mass, and the fracture zones. The model is then composed of 14 'rock units' block, of which 8 are fracture zones, Figure 4-9.

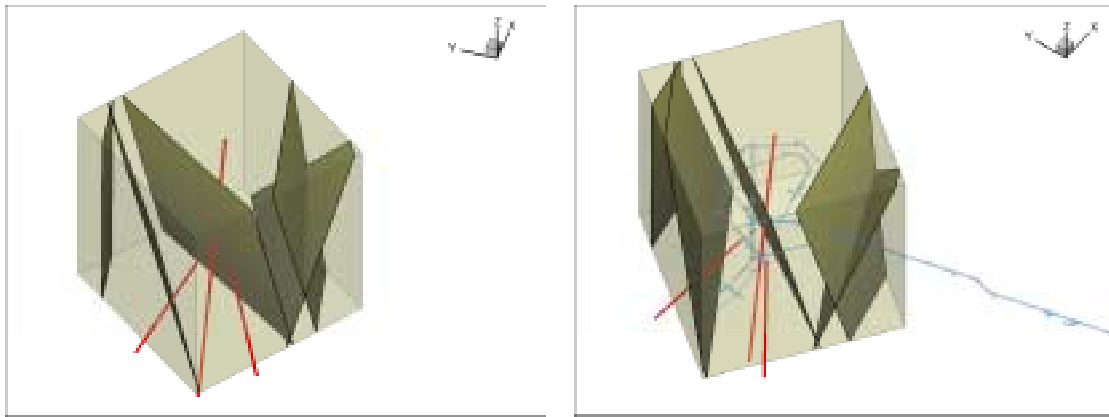


**Figure 4-8.** Two 3D views of the 550 m model, with the fracture zones (represented as planes without width), the boreholes, and the access tunnel (X: East, Y: North), from /Staub et al, 2002/.

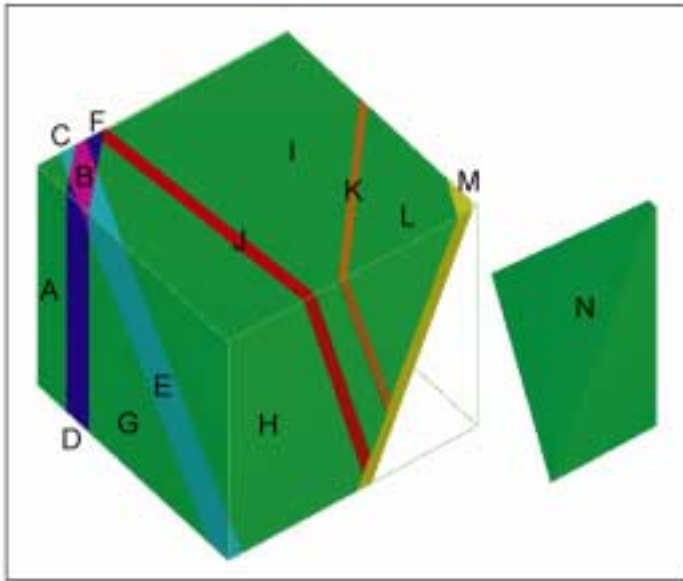


**Figure 4-9.** Presentation of the different blocks or ‘rock units’ in the RVS 550 m model, from Staub et al, 2002.

### The detailed model, or 380–500 m target area

A general view of the model illustrates that two of the three boreholes are on the side of the model Figure 4-10, and data will mostly be provided by the sub-vertical borehole going through the middle of the model. The numbering of the 30 m × 30 m × 30 m blocks is shown in Figure 4-10.

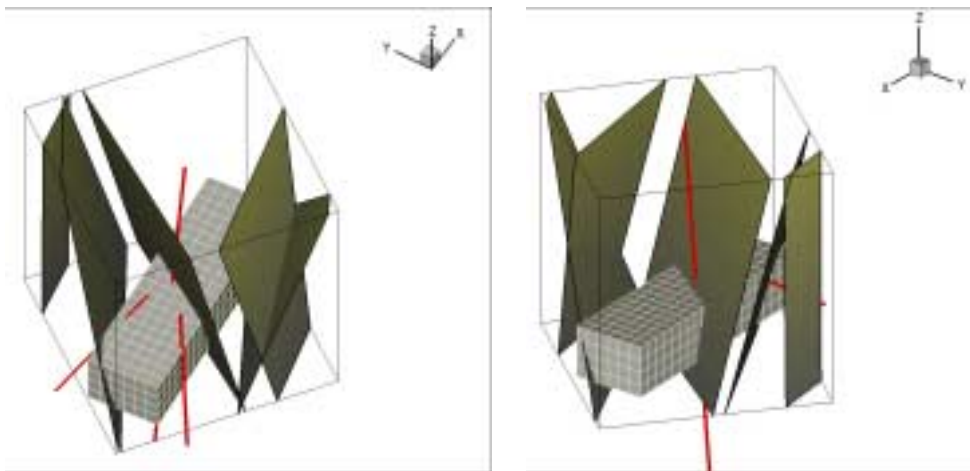


**Figure 4-10.** Two 3-D views of the detailed model, with the fracture zones and boreholes (X: East, Y: North), from /Staub et al, 2002/.

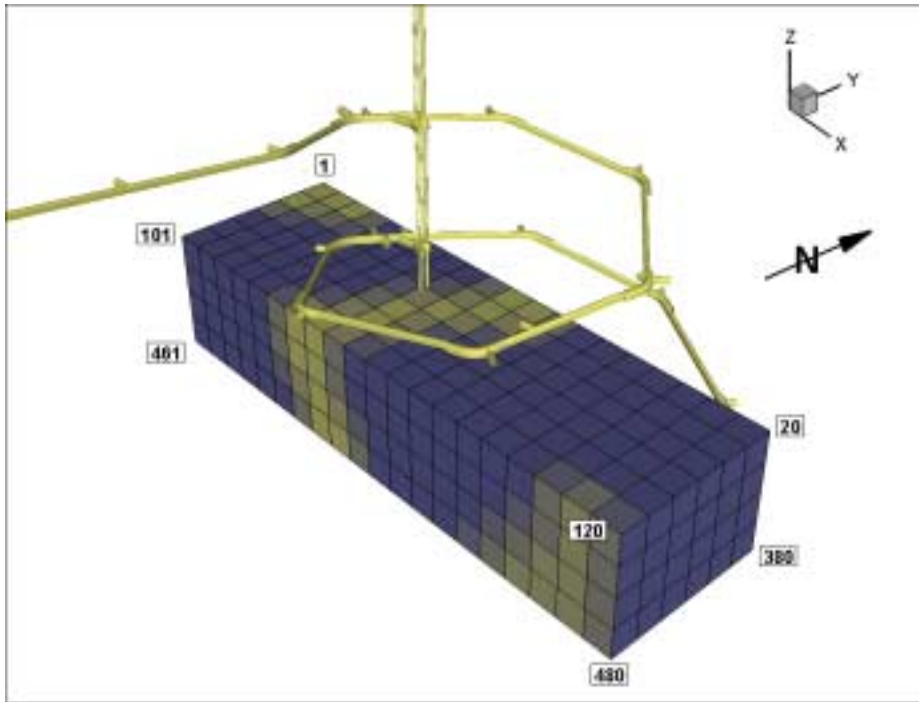


**Figure 4-11.** Numbering of the blocks in the Test Case  $600\text{ m} \times 180\text{ m} \times 120\text{ m}$  target block, from /Staub et al, 2002/.

#### 4.2.7 Review of the input data

The sets of data used for the Test Case were taken from SICADA, and obtained mainly from three boreholes, one subvertical, KAS02, that is almost 1000 m long, and two inclined boreholes, KA2598A and KA2511A, that are located on the western part of the model. The sub-vertical borehole is almost at the middle point of both models, and so no borehole data were available on the eastern side of the models. Data were also produced by geological surface mapping, laboratory tests, and geophysical measurements.

Table 4-3 presents the type of data that were used for the development of the Test Case model and for the computations, with their sources.

**Table 4-3. Review of the available and used input data, and their sources.**

Input data	Origin
Geometrical model	SwedPower
DFN model	/Hermansson et al, 1998/
Greenstone model	Golder Associates
Rocktype borehole core mapping	Sicada
Density of intact rock	/Sundberg and Gabriellsson, 1999; Nisca, 1988/
RQD borehole core mapping	Sicada
Fracture density borehole core mapping	Sicada
E-modulus	/Stille and Olsson, 1989; Nordlund et al, 1999/
Poisson's ratio	/Stille and Olsson, 1989;; Nordlund et al, 1999/
Triaxial compression tests	/Nordlund et al, 1999/
Aperture	/Lanaro, 2001/
Normal load tests on fractures	/Stille and Olsson, 1989; Lanaro, 2001/
Shear tests on fractures	/Stille and Olsson, 1989; Lanaro, 2001/
Tilt tests	/Makurat et al, 2002/
Joint wall strength	/Makurat et al, 2002/
Shaft mapping (fracture orientation and rock type)	Sicada

Additionally, information on experiences at the CLAB site was available, /Fredriksson et al, 2001/.

#### 4.2.8 Data uncertainty

Simulations were first carried out on block models constituted of homogeneous rock types. For each rock type, at one depth level, simulations were run to check the influence of the rock fracture friction angle: 20 simulations were run for  $\phi=30^\circ$ , followed by one simulation for respectively  $\phi = 25^\circ$  and  $35^\circ$ . Then, for the same depth level, and the same set-up of variation in parameters, the same number of simulations were performed for loading tests at a reduced horizontal stress. Note that the twenty simulations run on the same set-up of parameters were related to twenty different simulations of the fracture pattern when cutting a 2-D plane from the 3-D DFN model. It should be noted that up to 30% of the simulations failed because of complex fracture patterns.

Data uncertainty resulting from all these simulations was tackled in different ways, depending on the type of data.

The data uncertainty of the input parameters for the DFN model was managed through means and standard deviations of statistical functions. The influence of the spatial variability in the 3-D model was estimated by running Monte Carlo simulations on the input parameters for the model. Twenty different 3-D models were then created, and the 2-D trace section files were extracted for each of these models. Then, twenty different rock block models were generated in UDEC and run, all other parameters remaining unchanged. The variability was then statistically determined from the results of the computations.



The data uncertainty related to input mechanical properties of intact rock and fractures was tackled in two steps. First, all simulations were run by using the mean value for the parameters. The influence of one specific parameter, for example the friction angle of fractures, was estimated by changing the value of this parameter, all other parameters being the same. Then, using the calculated influence of the parameter on the outcome of the model in simplified Monte Carlo simulation, the influence of all parameters on the output data could be combined. The rock models in UDEC were always run assuming 100% of the same rock type. In order to estimate the discrepancies between the different rock types identified in the Test area, the simulations were realised four times, each time with a specific rock type. However, the 30 m × 30 m × 30 m cubes are lithologically heterogeneous. The percentage occurrence of each rock type in a cube could be estimated from borehole core mapping. This distribution was used in a simplified Monte Carlo simulation to combine the output from the lithologically homogeneous models in a way that represented the probability of occurrence of the different rock types in the cubes.

Three confidence levels were defined in the methodology as followed:

- Confidence level 1 when predictions are supported by local data
- Confidence level 2 when predictions are the result of interpolation and reasoning
- Confidence level 3 when predictions are the result of guess work.

Only two levels can be applied to this work. The confidence level was set to 1 for a rock block when a borehole or boreholes goes through it. The confidence level for all other blocks was set to 3.

#### 4.2.9 Output data from the Test Case modelling

The types of output data obtained for the 380–500 m block are illustrated in Table 4-4.

**Table 4-4. Young’s modulus and rock mass strength at different depth levels, in the granodiorite.**

GRANODIORITE	$E_m$ , GPa		$\sigma_{cm}$ , MPa	
	Mean value	Std. dev.	Mean value	Std. dev.
Level 1 (–380/–410m)	43.3	4	50.3	11.2
Level 2 (–410/–440m)	44.4	4.1	57.6	12.9
Level 3 (–440/–470m)	45.5	4.2	64.8	14.5
Level 4 (–470/–500m)	46.6	4.3	73.3	16.4

#### Mechanical properties of the rock units in the target area

The blocks with confidence level 1 are shown in Figure 4-12 according to the confidence scheme already discussed.

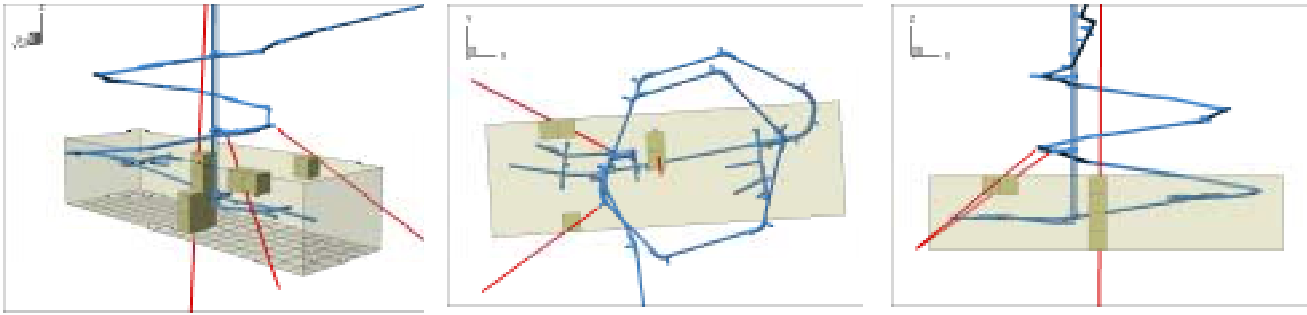


**Figure 4-12.** 3D perspective, top and profile views of the blocks with confidence 1 (X: East, Y: North), from /Staub et al, 2002/.

The mechanical properties that were estimated for the individual small blocks are indicated by the data in Table 4-5 and Table 4-6.

**Table 4-5. Young's modulus for the blocks with confidence level 1, from /Staub et al, 2002/.**

Cube ID	Rock unit Type <sup>(1)</sup>	Centre co-ordinates (m)			E <sub>m</sub> (GPa)			
					$\sigma_H$ <sup>(2)</sup>		$\sigma_{H/4}$	
		X	Y	Z	Mean	Std dev.	Mean	Std dev.
4	1	1933.811	7333.952	-395	38.8	3.61	15.95	3.37
	2				13.01	1.56	6.81	1.31
5	1	1963.755	7335.784	-395	38.8	3.61	15.95	3.37
	2				13.01	1.56	6.81	1.31
50	1	2117.138	7285.053	-395	39.22	6.13	18.15	6.15
	2				35.43	4.35	24.47	5.15
105	1	1972.912	7186.063	-395	42.57	4.38	24.13	4.26
170	1	2117.138	7285.053	-425	39.51	3.51	19.7	3.6
	2				35.43	4.35	24.47	5.15
270	1	2115.307	7314.997	-455	44.2	4.7	30.51	6.1
	2				35.43	4.35	24.47	5.15
290	1	2117.138	7285.053	-455	44.2	4.7	30.51	6.1
	2				35.43	4.35	24.47	5.15
390	1	2115.307	7314.997	-485	46.6	4.3	36	5.9
410	1	2117.138	7285.053	-485	46.6	4.3	36	5.9

<sup>(1)</sup> 1: 'ordinary rock unit'; 2: 'deformation zone unit'

<sup>(2)</sup> The values of  $\sigma_H$  are related to the depth level of each cube

**Table 4-6. Rock mass strength for the blocks with confidence level 1, from /Staub et al, 2002/.**

Cube ID	Rock unit type <sup>(1)</sup>	Centrum co-ordinates (m)			$\sigma_{cm}$ (MPa)		$c_m$ (MPa)		$\phi_{rm}$ (°)	
		X	Y	Z	Mean	Std dev.	Mean	Std dev.	Mean	Std dev.
4	1	1933.811	7333.952	-395	78.4	29.5	19	6.5	38.9	4.7
	2				47.4	17.6	11.8	4.1	36.8	4.4
5	1	1963.755	7335.784	-395	78.4	29.5	19	6.5	38.9	4.7
	2				47.4	17.6	11.8	4.1	36.8	4.4
50	1	2117.138	7285.053	-395	63.9	27.8	14.9	6.5	40.3	4.5
	2				56.1	20.4	13.4	4.7	38.9	4.4
105	1	1972.912	7186.063	-395	54.7	18.4	12.1	4.2	42.4	4.3
170	1	2117.138	7285.053	-425	82.9	32.6	19.8	7.2	38.9	4.5
	2				56.1	20.4	13.4	4.7	38.9	4.4
270	1	2115.307	7314.997	-455	70.7	22.9	15.9	5.3	41.5	4.3
	2				56.1	20.4	13.4	4.7	38.9	4.4
290	1	2117.138	7285.053	-455	70.7	22.9	15.9	5.3	41.5	4.3
	2				56.1	20.4	13.4	4.7	38.9	4.4
390	1	2115.307	7314.997	-485	73.3	16.4	16.4	3.3	41.4	3.8
410	1	2117.138	7285.053	-485	73.3	16.4	16.4	3.3	41.4	3.8

<sup>(1)</sup> 1: “ordinary rock unit”; 2: “deformation zone unit”

Similar prediction tables are supplied for the other blocks at a different confidence level. More details and conclusions relating to the theoretical approach can be found in /Staub et al, 2002/.

### 4.3 The empirical-theoretical consensus approach

The work on the empirical approach and on the theoretical approach had been contracted to two separate organizations, i.e. using the two different prediction methods. It was necessary, therefore to develop a combined consensus prediction by harmonizing the two approaches. For example, the empirical team made a more detailed rating of the weakness zones than the theoretical team. Additionally, it was necessary to harmonize with the stress approach described in Chapter 5, which had been contracted to a third organization.

Because the application of the three approaches involved a considerable amount of detailed understanding, a Workshop was held for mutual discussion and to develop an approach to a combined prediction methodology. This Workshop was held in August 2001, at Mälargården, Tammsvik, Sweden. The theme of the first Workshop day was ‘Presentation of the modelling techniques’; the theme of the second Workshop day was ‘How to develop the combined approach?’.

After the two days of discussion, some of the conclusions of the Workshop were as follows.

1. All groups should interact together more and with geological expertise in order to discuss how to extrapolate measured data into 3-D, and about the overall support for the geological model of the site.
2. The joint discussion should identify the need to characterise the site – not just to carry out the limited set of analyses discussed, which are well suited for the different approaches.
3. Stress analysis provides justification for the stress levels used in the rock property modelling (but stress levels as measured are usually sufficient for the predictions).
4. Conceptualisation of fracture zones needs to be co-ordinated and rock mechanics parameterisation of fracture zones needs to be established.
5. Comparing predicted rock mechanics parameters for the same input using the theoretical and the empirical approaches may suggest which approach is more appropriate.

#### **4.4 ‘Best estimates’ of the actual rock conditions**

The estimation of the actual rock properties, the ‘best estimate’ or ‘reference’ properties, was based on an empirical approach, but using additional tunnel and tunnel borehole information not available to the teams making the predictions, /Makurat et al, 2002/. See also Section 3.4.2.

The following parameters were estimated (except for  $\nu$  which was assumed):

$E_m$  – deformation modulus for the rock mass

$\sigma_m$  – rock mass compressive strength

$\nu$  – Poisson's ratio of the rock mass

$\sigma_1$  and  $\sigma_3$  – principal stresses

##### **4.4.1 Methodology**

The results were presented in tables and visualised by using Excel spreadsheets showing the different layers in the 380–500 m level model, i.e. four horizontal layers and six longitudinal, vertical sections. The different parameter values were given for each block in the model. The ranges in parameter values throughout the model were also visualised in the figures by use of a specific colour code. In general, Q-values were used as the basis for the estimation of the parameter values, and therefore the Q-value was estimated for each block. For some blocks, only RMR-data were available. In these cases, the parameter values were calculated directly from RMR, or the RMR-values were transformed to Q-values. For Model B (see Section 4.4.4), only Q-data have been used.

To correlate data from mapping in the tunnels and core logging with the 30 m × 30 m × 30 m blocks in the Test Case target volume, the co-ordinates for each block were calculated. Data from tunnel mapping (Q/RMR) were then transferred. For core logging data, SICADA calculated the xyz co-ordinates for each logging interval, and the data could then easily be correlated with the block locations.

The best estimate of the actual rock properties was based on existing data found in SKB reports and in the SKB database, SICADA, supported by information from the rock mechanics literature. Available data were unevenly distributed in the model. Data (Q or RMR-values) from tunnels or boreholes were available in only in 93 out of 480 blocks. Of the remaining 387 blocks, 161 shared at least one side with a block with data. For the rest of the blocks (226), no direct data were available. In Model B only the 70 blocks with Q-data have been used.

#### **4.4.2 Fracture zones**

The most distinct fault zones through the volume are striking NE-SW and ENE-WSW. The following major zones intersect the model area: EW-1, NE-1 and NE-2. Specifically the zones EW-1 and NE-1 are complex and are therefore considered as significant for the stability of underground openings. In the fault zones, crushed rocks and even clay zones are observed. In addition to these NE to ENE striking structures, NW-SE oriented fractures intersect the rock mass. These fractures have an orientation close to the major principal stress ( $\sigma_1$ ) and many of the water bearing structures have this orientation.

Based on the available data, eight minor weakness zones were identified. In the models, these zones have been named MWZ1-8 (Minor Weakness Zone). Outside the fault zones, the intensity of fracturing is usually low, and RQD values of 90–100 are usual. Generally, at least two sets of fractures are present.

#### **4.4.3 Model A – based on conventional rock mass classification**

In Model A, the existing tunnels were taken into consideration, and therefore the Q method was used in the normal way. The values of  $J_w$  and SRF were estimated from the most common values observed in the tunnels i.e.  $J_w = 1$  and  $SRF = 2$ .

The model consisted of 480 blocks from 380 to 500m depth divided into four horizontal layers, such that each layer contains 120 blocks. 93 blocks in the model contained either Q, RQD (transformed to Q) or RMR data. This meant that 387 of the blocks, or about 80%, had no data, and for these blocks the rock mass properties had to be extrapolated from blocks with data. Because of this, the uncertainty in the model is rather high. However, the rock mass quality was reasonably uniform in the total model volume, such that the rock mass properties were often near the mean value.

Some of the rock property ‘best estimates’ are shown in Table 4-7 and Table 4-8.

**Table 4-7. Summary of data from weakness zones, from /Makurat et al, 2002/.**

Weakness zone	Minimum			Maximum			Mean		
	Q	$\sigma_m$ (MPa)	$E_m$ (GPa)	Q	$\sigma_m$ (MPa)	$E_m$ (GPa)	Q	$\sigma_m$ (MPa)	$E_m$ (GPa)
EW-1	0.008	4	2	12	44	23	1.8	23	12
NE-1	0.011	4	2	12	44	23	3	27	14
NE-1 (central zone)	–	–	–	–	–	–	0.011	4	2
NE-2	1.9	24	12	8	37	20	4	30	16

In Table 4-8, the data for the different layers of the model are shown. No major differences between the different layers can be seen. It must be stated here that an SRF value of 2 was been used for the whole model. In the lower layers, the stresses might be somewhat higher than in the upper ones, and possibly this could have justified a variation in the SRF-value. This would have resulted in somewhat lower Q-values in the lower layers compared to the higher ones.

**Table 4-8. Summary of data (block values) from various layers (depth ranges), from /Makurat et al, 2002/.**

Depth	Minimum			Maximum			Mean		
	Q	$\sigma_m$ (MPa)	$E_m$ (GPa)	Q	$\sigma_m$ (MPa)	$E_m$ (GPa)	Q	$\sigma_m$ (MPa)	$E_m$ (GPa)
–380 to –410m (19 blocks)	0.3	19	7	40	97	40	11.4	67	25
–410 to –440m (33 blocks)	0.7	25	9	63	113	47	13.7	70	26
–440 to –470m (33 blocks)	4.6	47	18	34	92	38	12.6	66	24
–470 to –500m (8 blocks)	4.0	45	16	12	65	23	9.4	60	21

#### 4.4.4 Model B – based on a characterization approach

In Model B, the virgin rock mass conditions were estimated from the borehole data (i.e. without the tunnel information). This meant that some modifications in the use of the Q method had to be implemented. These modifications mainly concerned the SRF, which was given a value of 0.5 because of rather high stresses below a depth of about 250 m. The values are shown in Table 4-9.

**Table 4-9. Summary of  $Q_{cha}$ ,  $E_m$  and  $\sigma_m$  in Model B, from /Makurat et al, 2002/.**

Parameter	Block minimum	Block maximum	Block mean
$Q_{cha}$	30	82	40
$E_m$ (GPa)	34	48	38
$\sigma_m$ (MPa)	84	118	94

#### 4.4.5 Comparison of the Model A and Model B ‘best estimates’

If we compare the two models, evident differences can be seen in Table 4-10.

**Table 4-10. Comparison of mean values for Q ( $Q_{cha}$ ),  $E_m$  and  $\sigma_m$  in the 70 blocks with Q-data.**

Parameter	Block mean Model A	Block mean Model B
Q ( $Q_{cha}$ )	11	40
$E_m$ (GPa)	22	38
$\sigma_m$ (MPa)	63	94

In model B, the Q-values are 3 to 4 times higher than in Model A, but this is mainly caused by the fact that  $Q_{cha}$  is used in Model B. This means also that the values of  $E_m$  and  $\sigma_m$  are considerably higher in Model B than in Model A. Concerning the values of  $E_m$  in Model B, they are also modified by the rock compressive strength, which results in increased values.

As we can see from this, there were uncertainties in the models. These uncertainties were on two levels.

- First, there were the uncertainties concerning the data input i.e. Q ( $Q_{cha}$ ) and RMR data and the handling of these data in each of the blocks in the models. The  $J_w$ -value was based on results from the core drillings and from the observations in the tunnels. The stress measurements indicated SRF values from 1 to 2 but, in a virgin situation without tunnels, it was assumed that parameters such as  $E_m$  and  $\sigma_m$  will increase with increasing stress. Therefore, SRF = 0.5 was used in Model B.
- The other level of uncertainties concerned the methods used for estimation of the different parameter values from the available Q and RMR data. There are several equations for this estimation, and associated opinions about which of these equations provides the most reliable values.

## 4.5 Comparison of the empirical and theoretical model results with the ‘best estimate’ reference model results

In the Test Case exercise, there were three overall steps, as indicated in Figure 1-2.

- In the *first step*, the three different approaches were used to make individual predictions of parameters relevant to their modelling studies.
- In the *second step* all three modelling teams co-operated and used their combined information and know-how to revise the predictions.
- The *third step* involved comparison with predictions made by a team given access to all existing understanding/descriptions of the site.

The third step is now described for the 380–500 m level model results. The text and figures in this Section are from an unpublished report by Stigsson and Anderson.

### 4.5.1 Presentation of results

The results were presented and compared using scanlines through the target volume, histograms and tables. Figure 4-13 shows the position of example scanlines between cells 1–20 and between cells 81–100.

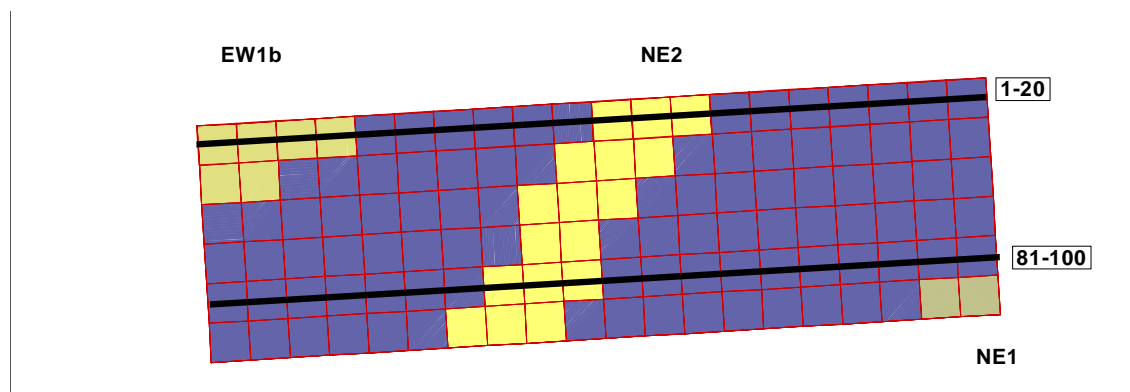


**Figure 4-13.** Position of example scanlines through blocks 1–20 and 81–100.

Scanlines (see e.g. Figure 4-14) present the value of the predicted property (deformation modulus, strength, etc) for each 30 m × 30 m × 30 m cells along the scanline. The confidence level is indicated by the size of the marker. Solid lines refer to the mean or best estimate value allocated to each 30 m × 30 m × 30 m cell. Dotted lines represent the suggested uncertainty spans (not fully comparable between teams). Different scanlines have been used to represent cells containing both rock mass and fracture zones. A typical selection of scanlines is shown below.



In addition to scanlines, results are also presented as cumulative histograms (see e.g. Figure 4-15). These plots show both mean/best estimate values (solid lines) and simulated histograms assuming a normal distribution and using the average standard deviation provided by each team (dotted lines). Each team had different ways of describing uncertainty, which means that the dotted lines are not fully comparable. The assumption of a normal distribution (added afterwards for presentation purposes only) may not be fully justified; nevertheless, the dotted lines give a fair illustration of the suggested spread predicted by the different teams.

#### 4.5.2 Deformation modulus

##### Rock mass

Figure 4-14 shows example scanline 1–20 of the rock mass deformation modulus. The diagram shows that the different teams' predictions were similar. These observations are even more evident from the histogram of the deformation modulus shown in Figure 4-15. The mean predictions for the empirical and the 'best estimates' of the actual conditions were quite close, and also matched the range of the theoretical predictions well. In contrast, the uncertainty range suggested by the empirical group was quite large.

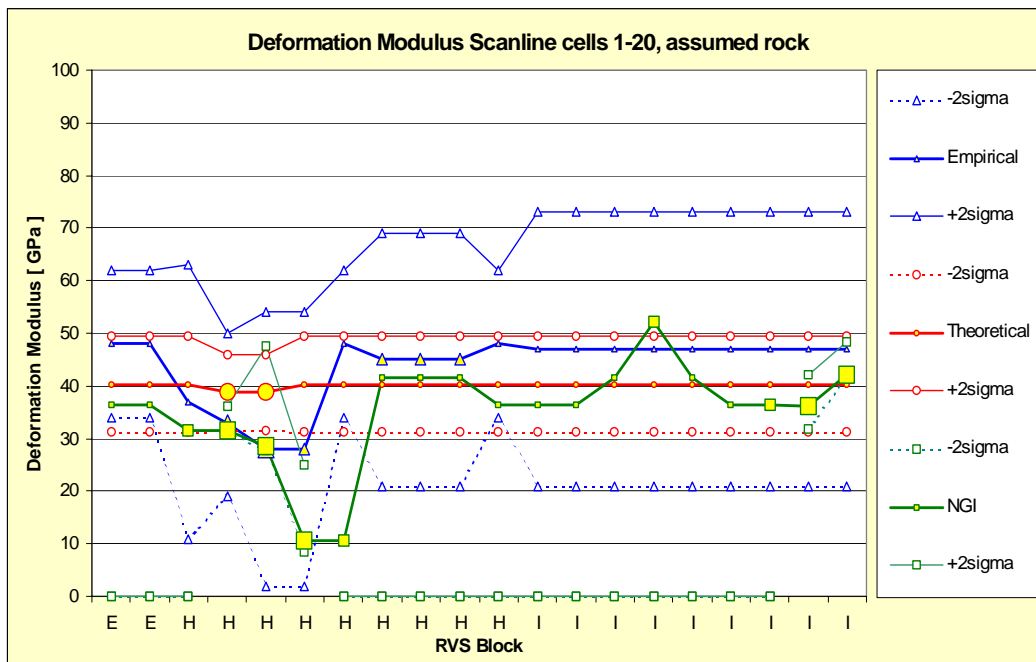


**Figure 4-14.** Scanline 1–20 for rock mass deformation modulus. Solid lines refer to values for each  $30\text{ m} \times 30\text{ m} \times 30\text{ m}$  cells. The confidence level is indicated by the size of the marker. Dotted lines represent suggested uncertainty spans (not fully comparable between teams and so should not be interpreted directly as standard deviations). Cells containing both rock mass and fracture zones are here represented by their rock mass values.

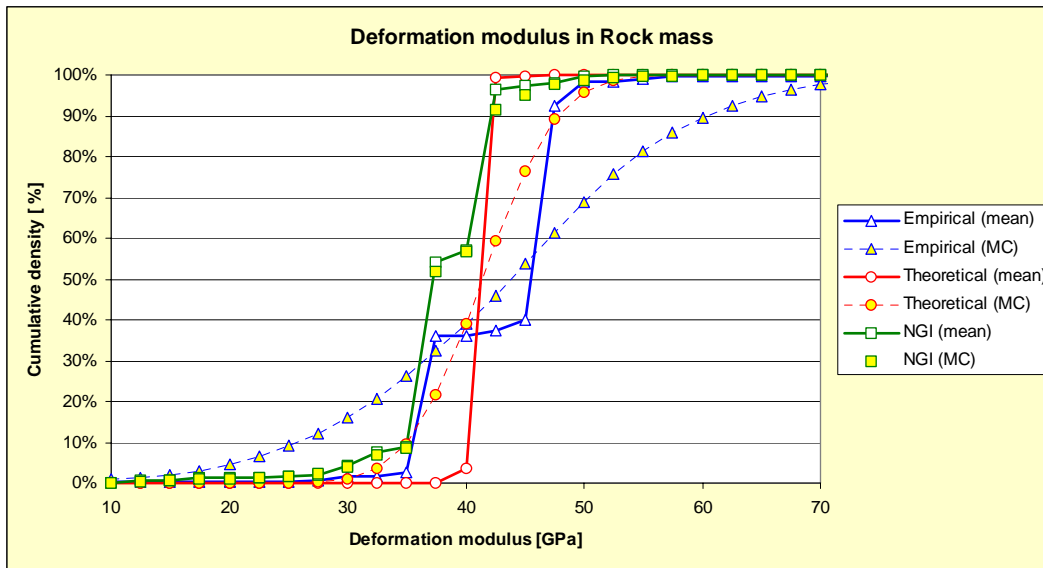


**Figure 4-15.** Cumulative histogram of rock mass deformation modulus in the rock mass cells of the 380–500 m level model. Mean/best estimate values (solid lines) and simulated histograms assuming a normal distribution and using the average standard deviation or equivalent provided by each team (dotted lines). MC refers to Monte Carlo simulation.

## Fracture zones

There was less agreement between the teams as regards fracture zones. In discussion, it seemed evident that the reason for the differences between the empirical and the theoretical models resulted from lack of data and different ideas on how to interpret the data that were available. Moreover, the two teams evaluated different fracture sub-zones. The team evaluating the ‘best estimate’ reference conditions also had more data because they were able to use the tunnel and tunnel borehole data.

## Preliminary combined predictions

Without knowing the best estimate of the actual results, the empirical, the theoretical and the stress teams tried to make a combined prediction of the rock mass deformation modulus in the 380–500 m level target volume. The results are outlined in Table 4-11.

**Table 4-11. Combined predictions for the rock mass and the fracture zones.**

<b>Rock Mass Deformation Modulus in the Target area, the 380–500 m level</b>					
Parameter	Significant deviations?	Confidence	Reasonable combined prediction	Alternate combined prediction	Notes
Median Em	No	High	42 GPa	–	
Range			35–45 GPa	18–65 GPa	If not in fracture zone
<p><i>Notes on the predictions:</i> Outside known measurements; lack of data for half the volume; 65 GPa is close to the maximum measured modulus of the intact rock: lower range may possibly be due to small scale sample; bimodal nature due to fracture zone hits (see above); the reasonable range is 35–45 GPa if not in fracture zone. The wide range is probably due to uncertainty in the geometrical model and possibly also scale effects. Measurements were made in the prototype area with an assumed scale of 15 m; there the mean modulus was 25 GPa±14 and a recovery curve of 35GPa±19.</p>					

<b>Zone EW1 – Rock Mass Deformation Modulus in the Target Area</b>					
Theoretical Model: 13 (11–15); Empirical Model: 48 (40–53)					
No overlap					
Parameter	Significant deviations?	Confidence	Reasonable combined prediction	Alternate combined prediction	Notes
Median Em	Yes	Low	T: 13 GPa E: 48 GPa		
Range	Yes	Low	T:11–15 GPa E: 40–53 GPa	5–55 GPa	
<p><i>Notes on the predictions:</i> Difficult to resolve; different input used; clay filling?; fracture formation properties; use of surface data maps may give high RQDs because the surface exposed rock is stronger than rock removed or in ‘valleys’.</p>					

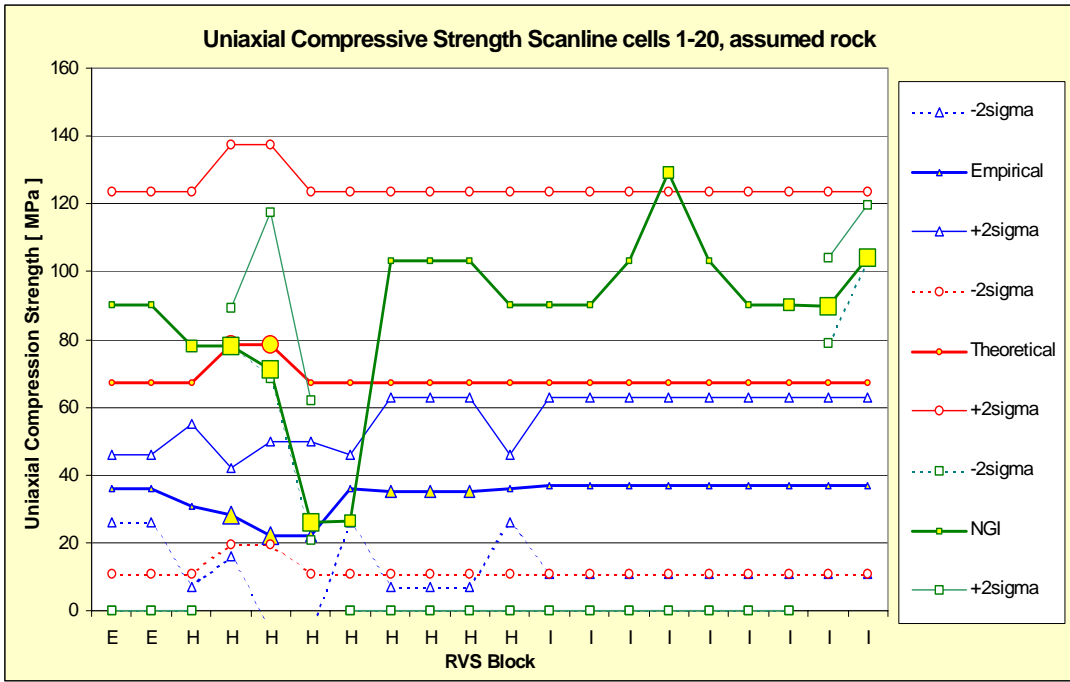
## Observations

The team results agreed quite well when the input data were similar. Deviations occurred when there were different views on how to interpret the geological model, data and how to extrapolate into 3-D.

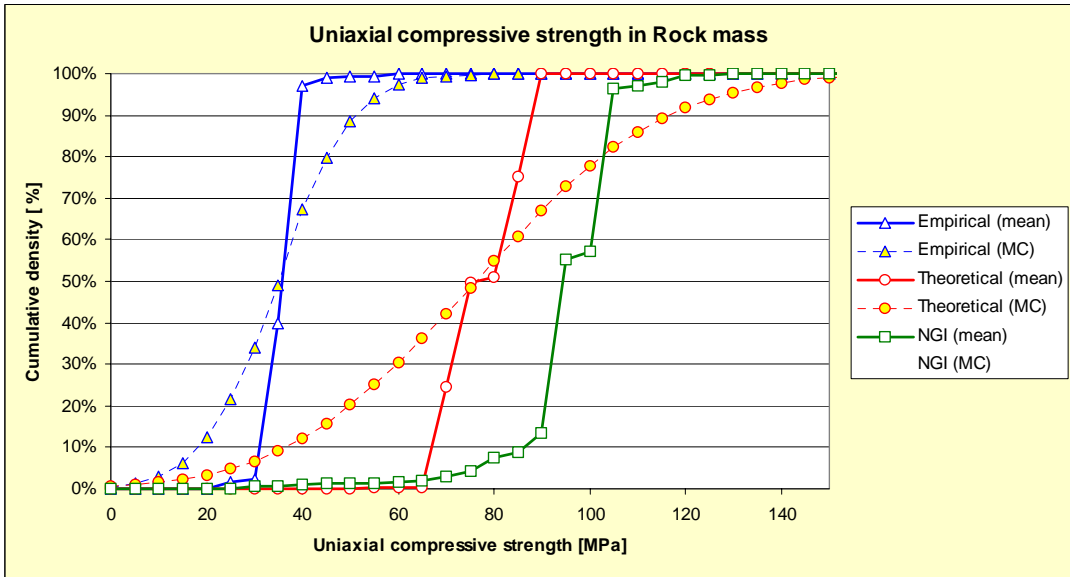
### 4.5.3 Rock mass strength parameters

Figure 4-16 shows an example scanline (cells 1–20) of predicted rock mass uniaxial compressive strength. The results are not the same, but one should note that the teams used different definitions of the strength. The empirical team used the Hoek and Brown definition; whereas the theoretical team used extrapolation of the Mohr-Coulomb relation.

Similar results were obtained for the cumulative histograms of compressive strength (Figure 4-17). In contrast, results for the Mohr-Coulomb parameters  $\phi$  and  $c$  compared much better (Figure 4-18 and Figure 4-19). It seems evident that the differences between teams related to the interpretation of the definition of the rock mass strength and differences in prediction methodology.



**Figure 4-16.** Example scanline (cells 1–20) of predicted rock mass uniaxial compressive strength. Note that the teams use different strength definitions. The empirical team used the Hoek and Brown definition; whereas the theoretical team used extrapolation of the Mohr-Coulomb relation.



**Figure 4-17.** Cumulative histogram of rock mass uniaxial compressive strength in the cells of the 380–500 m level model. Mean/best estimate values (solid lines) and simulated histograms assuming a normal distribution and using the average standard deviation or equivalent provided by each team (dotted lines). Note that teams used different strength definitions.

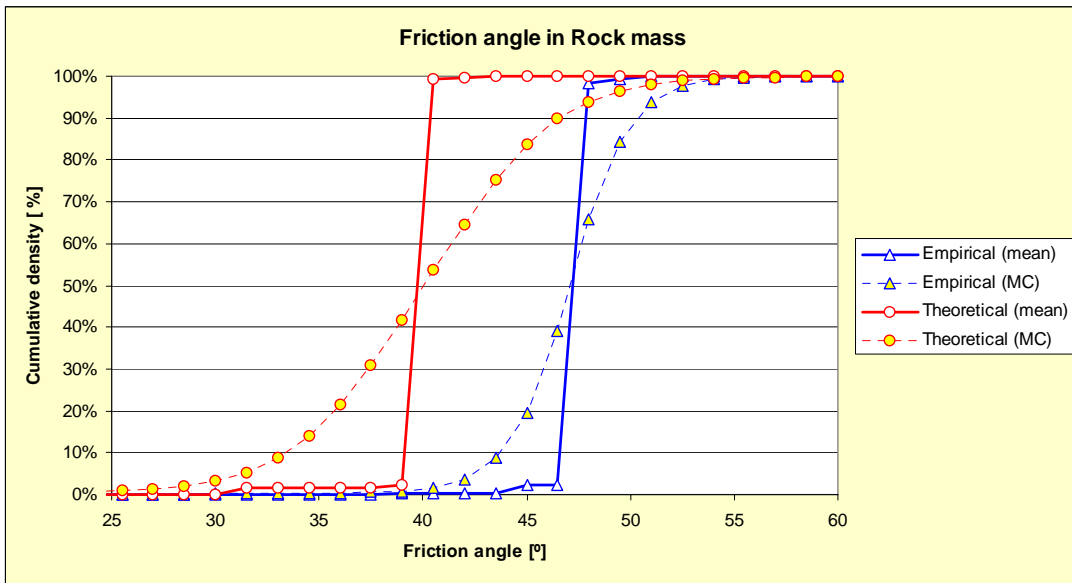


**Figure 4-18.** Cumulative histogram of friction angle (dotted lines based on Monte Carlo simulation) in the cells of the 380–500 m level model.

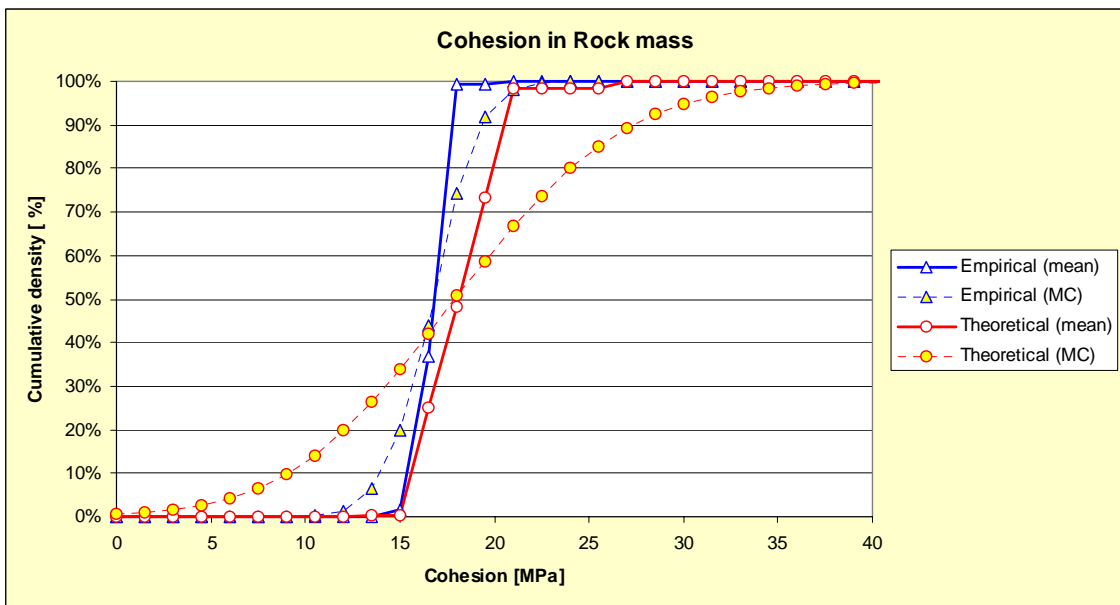


**Figure 4-19.** Cumulative histogram of cohesion (Mohr-Coulomb) in the cells of the 380–500 m level model.

It seems evident that the differences between teams relates to the definition of the rock mass strength, rather than to differences in prediction.



## 5 Modelling the state of stress

In this Chapter, the work performed in estimating the state of stress in the Test Case rock volume is presented, and is based on Hakami et al, 2002. The work included the following components.

- An initial stress prediction was made based on information that would prevail before a Site Investigation.
- Analyses were undertaken of stress measurement data and other information provided from the Test Case area, i.e. the area around the Äspö HRL. The information was constrained to mimic the type and amount of information available during a Site Investigation.
- Numerical models (3DEC) of the study area were built and the potential influence of the major fracture zones on the in situ stress field was studied.
- Comparison between different numerical models and the measurements were made
- An updated prediction was then made based on measurements, modelling and site specific information, including an estimation of uncertainty and spatial variability of the in situ stress.

### 5.1 Initial stress prediction from database information

#### 5.1.1 Stress magnitudes

##### Swedish database

The initial stress prediction was based on a Swedish stress measurement database /Martin et al, 2001/ and on data extracted from relevant literature. Figure 5-1 to Figure 5-3 show the data from /Martin et al, 2001/ for the horizontal and vertical stresses, respectively. Note that all existing data that were from ÄHRL boreholes were removed from the database because, at this stage, the estimation had to correspond to the stage before site investigations. Further, only the data in the database collected from depths between 50–600 m were included.

The reason why the very shallow and very deep data were not included was that the aim was an initial prediction for the 550 m block, and this prediction should be based on the most relevant data. There is no reason to believe that the stresses should be linearly depth-dependent to very great depths; it is more realistic to expect the depth-dependency to decrease or at least change with depth. At shallow depth, the measured stresses are more likely to be affected by topography and excavations. Also, the large amount of shallow data would have dominated the calculated linear trend. A linear trend based on the data between 50–600 m depth was therefore judged to be the most appropriate.

In Figure 5-1 to Figure 5-3 the best-fit linear trends for the data are shown with a solid line. Assuming that the database is representative for the whole of Sweden, and thus

also for the Äspö area, these average trend lines (denoted Ave.) were chosen as the most probable estimates for the mean stress magnitudes as a function of depth in the 550 m block. The pink and light blue lines correspond to the estimated uncertainty span, i.e. it is judged that the *mean* stress at a certain depth at this site will lie within the span from the pink to the blue line. Around this mean value, the stress is expected to vary from point to point within the block at the same level due to the natural stress variation caused mainly by fracturing influences at different scales. The prediction of this local spatial variation around the mean is depicted in the diagram with dashed lines in the same colour as the mean.

The ‘first initial model’ was based on this information and therefore not on any Äspö site-specific data. The stress magnitude has an ‘uncertainty and variability span’ such that 95% of the selected measurements from the database are covered by the total span.

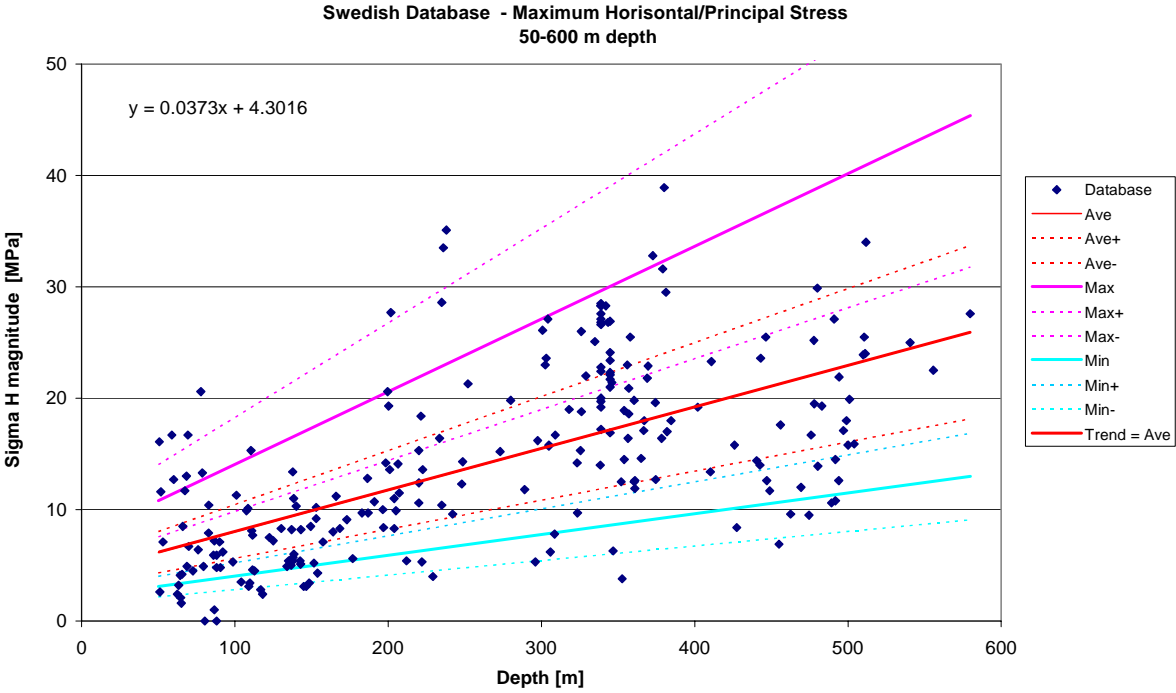


**Figure 5-1.** *Maximum horizontal stress vs. depth. Data from measurements in gneiss, granite and diorite, performed at 50–500 m depth in 27 different boreholes at different locations in Sweden (Based on /Martin et al, 2001/). The lines correspond to the selected stress model including the uncertainty span and the spatial variability span. The red line is the calculated best-fit linear trend of the data in the diagram. Dotted lines correspond to expected spatial variability around the mean.*



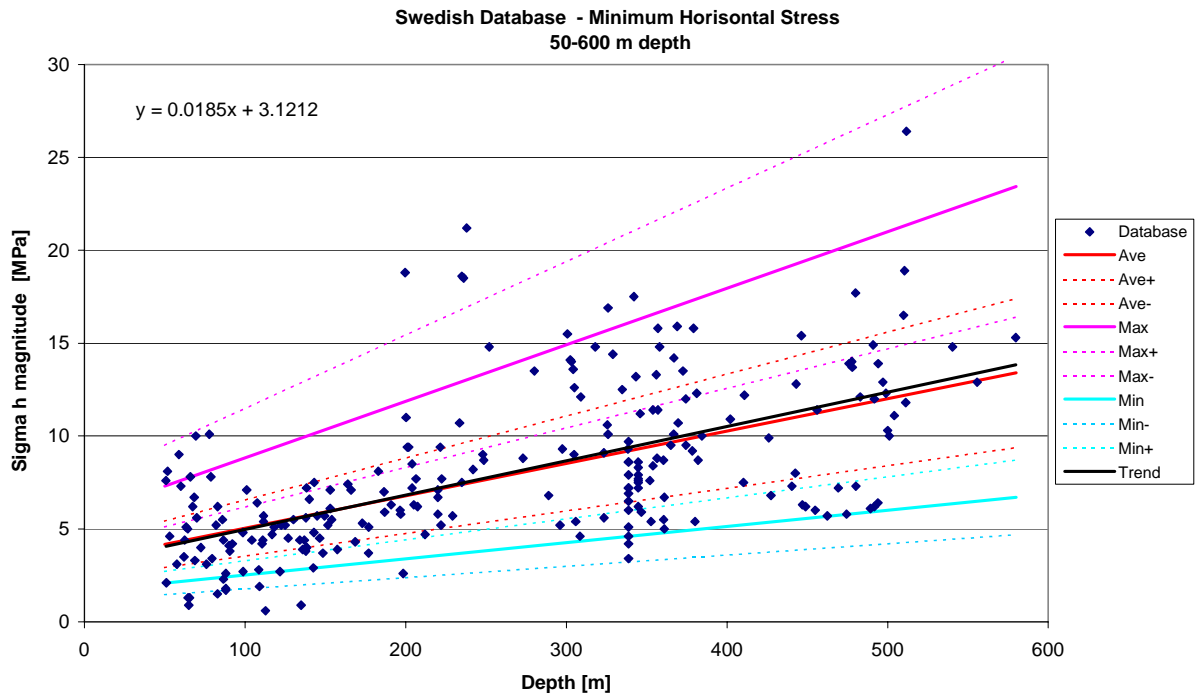


**Figure 5-2.** *Minimum horizontal stress vs. depth. Data from measurements in gneiss, granite and diorite, performed in 8 different boreholes at different locations in Sweden. Based on /Martin et al, 2001/.*

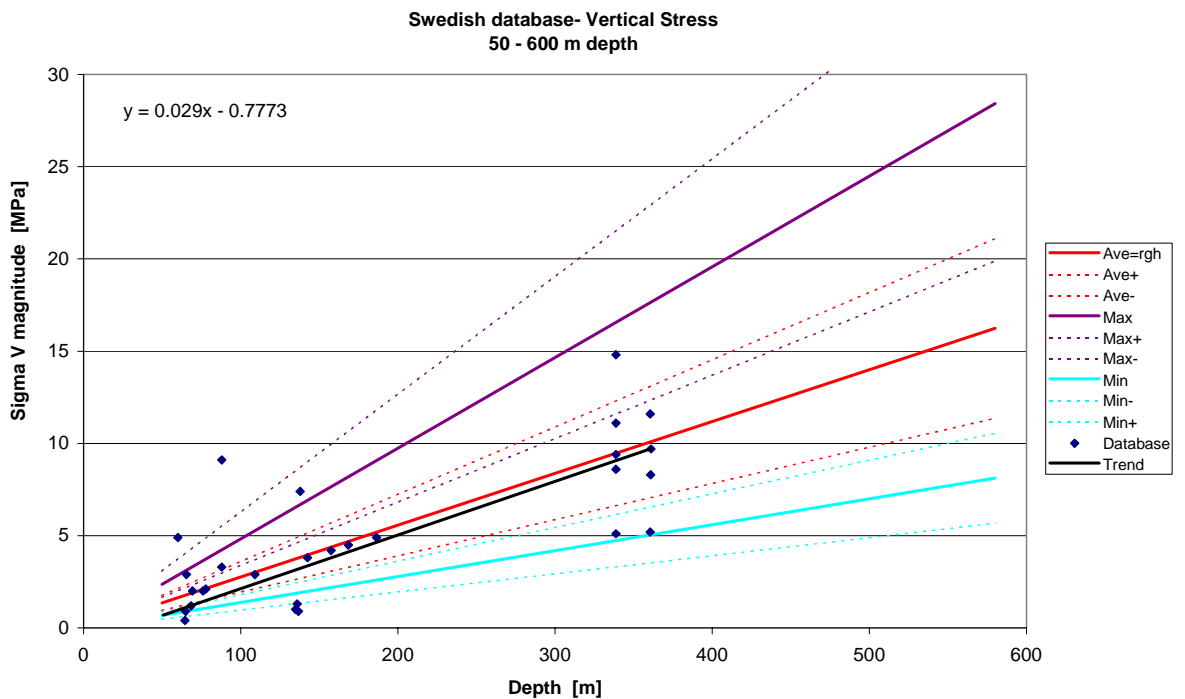


**Figure 5-3.** *Vertical stress vs. depth. Data from measurements in gneiss, granite and diorite, performed in 17 different boreholes at different locations in Sweden. Based on /Martin et al, 2001/.*

## Finnish database

Another source of information was a stress measurement database from Finland. Since Finland and Sweden are both located in the geological unit Fennoscandia, they are expected to have similar in situ stress conditions. In Figure 5-4 and Figure 5-5, Finnish data for the maximum and minimum horizontal stresses are shown, from /Martin et al, 2001/. Both the best-fit linear trend lines for these Finnish data and the best-fit linear trends from Swedish data are given in the diagrams. The comparison indicates that the differences are fairly small, supporting the assumption that a general database is appropriate for use as a first prediction.

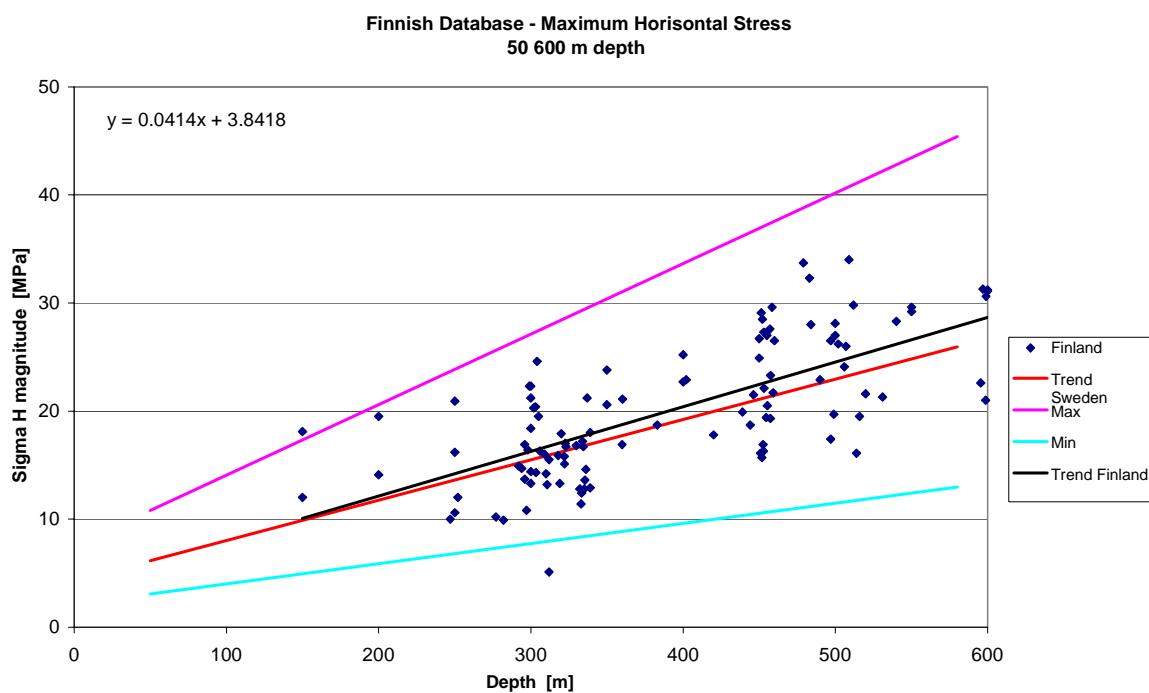


**Figure 5-4.** *Maximum horizontal stress vs. depth. Data from measurements in 15 different boreholes in Finland /based on Martin et al, 2001/.*

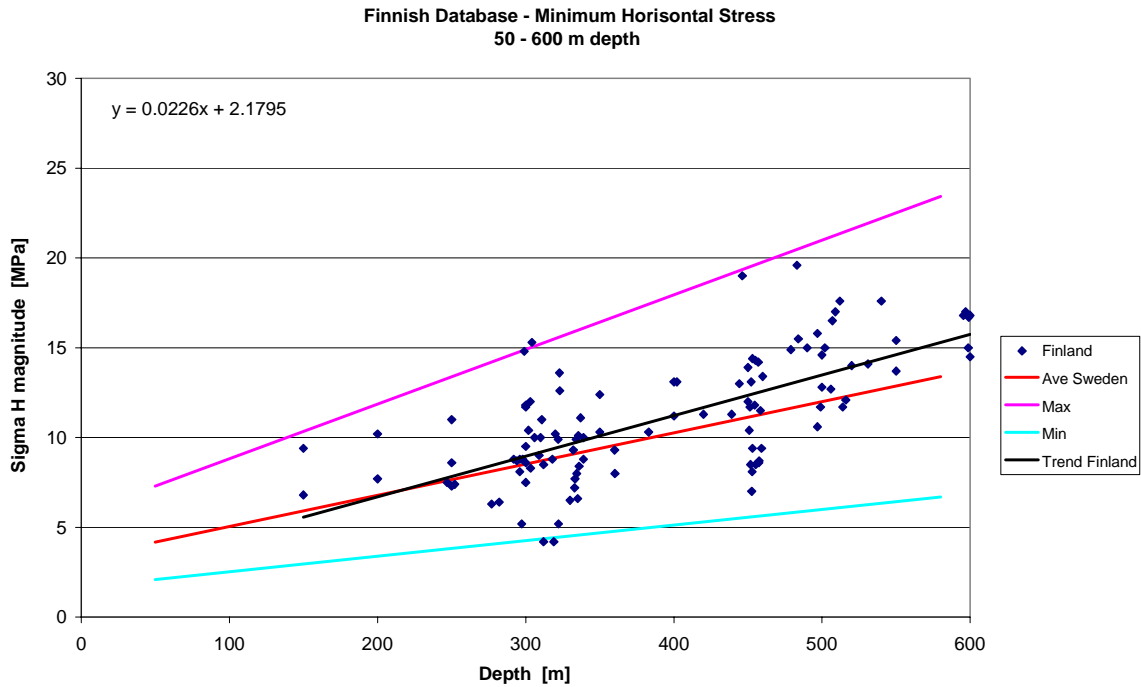


**Figure 5-5.** *Minimum horizontal stress vs. depth. Data from measurements in 15 different boreholes in Finland /based on Martin et al, 2001/.*

### 5.1.2 Stress orientations

The orientation of the maximum principal stress in Sweden has been estimated from a database published by /Stephansson et al, 1991/. Using a map they presented, the orientation for a few locations in SE Sweden was established. The orientation of the maximum horizontal stress varied between  $119^{\circ}$ – $136^{\circ}$  (degrees counted clockwise from magnetic north), corresponding to  $131^{\circ}$ – $148^{\circ}$  in the Äspö local co-ordinate system. This direction coincides with the general SE-NW stress direction of the maximum principal stress in Europe, and particularly for southern and central Fennoscandia as observed from stress measurements. Also, focal mechanism data from Sweden, Norway and Denmark indicated a SE-NW orientation of the maximum horizontal stress /e.g. Slunga et al, 1984; Bungum et al, 1991; Gregersen et al, 1991; Müller et al, 1992; cited in Ask, 1996/.

Another approach for estimating the most probable principal stress orientations, without using stress measurements from the site, was to relate the stresses to the orientation of water conducting fractures. It may be hypothesised that the maximum principal stress should be oriented parallel to such fractures, because the lesser normal stress on those fractures is an explanation for the higher conductivity observed.

Water conductive fractures have been identified in boreholes KAS02 and KAS06, based on borehole logs. The results are reported by /Sehlstedt and Strähle, 1991/. They classified the observed fractures in confidence classes 1–4. Only certain (class 4) water conducting fractures were used, which were 5 fractures, only found in KAS06 at 400

and 560 m depth. The average trend of these conductive fractures was  $120^\circ$  (assuming that this orientation is related to the true magnetic north). The Äspö local north is  $12^\circ$  west of magnetic north, and the corresponding orientation for the conductive fractures in the local system is thus  $132^\circ$ .

Since the two indications, from the database and from the core logs, fit fairly well with each other, the estimation of the average trend of the maximum horizontal stress was taken as the mean value  $136^\circ$  (in the Äspö local co-ordinate system), with an uncertainty of  $\pm 15^\circ$ . Locally, i.e. comparing different single measurements within the 550 m block, the orientation was expected to vary around the mean through about  $\pm 15^\circ$ . This variation was expected because of the influence of fractures of different sizes and the heterogeneity in mechanical properties within the block.

### **5.1.3 Description of uncertainty and spatial variability parameters**

Based on the measurement database from different locations in Sweden it was concluded that individual stress values deviate from the average trend. It was judged reasonable that most of the Swedish database values should fall inside the total uncertainty and variability span and a minimum of 95% of the data were selected as a reasonable criterion. The uncertainty,  $\pm u$ , and the spatial variability,  $\pm v$ , in the stress prediction were described using two ‘spans’ for each prediction as described below.

#### **The u parameter**

The u parameter should correspond to the uncertainty in the estimation of the mean stress in a rock unit, the uncertainty being calculated as a fixed percentage of the mean prediction. The reason for this was that, at least for overcoring measurements, the errors are dependent on the magnitude, i.e. the absolute measurement accuracy is less at large stress levels than at lower ones. For prediction of magnitude, the u parameter was selected to be 75% on the maximum side and 50% on the minimum side, for all principal stresses.

The choice of an uncertainty span that is proportional to the predicted mean value also corresponds to the idea of having a depth dependency in the predicted stress magnitude. If the depth-dependency factor is slightly wrongly estimated, this would cause a much larger absolute error for points at depth, compared to the error at shallower depths. Note that unknown spatial variability is included in the u parameter.

#### **The v parameter**

The second parameter, v, corresponds to the expected spatial variability of in situ stress around the mean (magnitude and orientation). The cause of a local variability of both stress magnitude and orientation is the inhomogeneous character of the rock mass on all scales. Even the most competent rock will include differences in the rock type and fractures of some kind.

The v-parameter is not meant to reflect the lack of knowledge or lack of data, but should reflect the expected actual variation in the parameter from point to point inside the volume it represents. Therefore, the value of the v-parameter will be dependent on the scale considered, i.e. how large a rock volume relates to each value. In a very large rock unit, the distance between different points may be larger and also the mechanical properties of the rock mass inside may be expected to vary more.

For the Test Case exercise it was assumed that the geological model provided a reasonable division into rock units that were homogeneous, i.e. that there was a similar degree of spatial variation inside. However, the RVS units representing deformation zones (fracture zones) were expected to be more inhomogeneous and the v-parameter has been given a higher value.

#### 5.1.4 Initial prediction for the 550 m block

For the initial prediction, a linear depth dependence was chosen for the stress magnitude, because there was no general knowledge at this stage of any mechanism that would suggest a different distribution. Also, the uncertainty estimations between different parts of the block were not varied at this stage.

The initial prediction included a linear variation with depth for all principal stresses. The same prediction equations corresponded to the whole 550 m block of the Test Case. The term ‘initial’ refers to predictions made at a stage when no measurement results from the site would be available and no geological geometrical model had been established. Thus, this prediction would be the same for any site in Sweden.

The initial stress prediction for the 50 – 550 m depth interval was as follows.

$$\begin{aligned} \sigma_1 &= 0.0373(-z)+4.3 \quad [\text{MPa}] && u_{\text{upper}} 75\%; u_{\text{lower}} 50\%; \text{ and } v 30\% \\ \sigma_2 &= 0.027(-z) \quad [\text{MPa}] && u_{\text{upper}} 75\%; u_{\text{lower}} 50\%; \text{ and } v 30\% \\ \sigma_3 &= 0.0174(-z) +3.3 \quad [\text{MPa}] && u_{\text{upper}} 75\%; u_{\text{lower}} 50\%; \text{ and } v 30\% \end{aligned}$$

#### 5.1.5 Initial prediction for the Target Block

The stress prediction model presented above for the 550 m block has been applied to the 380–500 level target volume for the Test Case and the results for the stress magnitudes are given in Table 5-1. Since the stress magnitudes are only dependent on the z-ordinate in this model, the predictions are given for four ‘cube groups’ corresponding to the four different cube levels in the target block.

In Table 5-2, the orientations of the estimated stresses in the target volume are presented. Since the three principal stresses are orthogonal at each point, only three parameters are needed to define the orientation. It was chosen to give trend,  $\phi$ , and plunge,  $\theta$ , for the maximum principal stress,  $\sigma_1$ , and the plunge of  $\sigma_2$ . From these values the trend of  $\sigma_2$  and the trend and plunge for  $\sigma_3$  may be determined. The values u and v correspond to uncertainty and variability estimates described in Section 5.1.3.

**Table 5-1. Principal stress magnitudes in the Target Block based on the initial stress model, from /Hakami et al, 2002/.**

Cube ID	Rock Unit	Cube Centre (z)	$\sigma_1$ (MPa)	Min–Max (u) (MPa)	$\pm v$ (%)	$\sigma_3$ (MPa)	Min–Max (u) (MPa)	$\pm v$ (%)	$\sigma_2$ (MPa)	Min–Max (u) (MPa)	$\pm v$ (%)
1–120	Any	–395	19.0	9.5–33.2	30	10.2	5.1–17.9	30	10.7	5.4–18.7	30
121–240	Any	–425	20.2	10.1–35.4	30	10.7	5.4–18.7	30	11.5	5.8–20.1	30
241–360	Any	–455	21.3	10.7–37.3	30	11.2	5.6–19.6	30	12.3	6.2–21.5	30
361–480	Any	–485	22.4	11.2–39.2	30	11.7	5.9–20.5	30	13.1	6.6–22.9	30

**Table 5-2. Principal stress orientations in the Target Block based on the initial stress model, from /Hakami et al, 2002/.**

Cube ID	Rock Unit	Cube Centre (z)	$\beta_1$	$\pm u$ (°)	$\pm v$ (°)	$\alpha_1$	$\pm u$ (°)	$\pm v$ (°)	$\alpha_2$	$\pm u^*$ (°)	$\pm v$ (°)
1–120	Any	–395	136°	15°	15°	0°	10°	15°	0°	45°	15°
121–240	Any	–425	136°	15°	15°	0°	10°	15°	0°	45°	15°
241–360	Any	–455	136°	15°	15°	0°	10°	15°	0°	45°	15°
361–480	Any	–485	136°	15°	15°	0°	10°	15°	0°	45°	15°

## 5.2 Site specific information

The information presented in Section 5.1 refers to generic ‘across Sweden’ information, and the initial predictions were formulated from principal stress magnitude-depth relations developed from this database. In this Section, the predictions are modified according to Äspö information.

### 5.2.1 Geological information from the Test Case site

It is known that fractures can locally affect the magnitude and orientation of the principal stresses. The geological model provided for the Test Case includes five major fracture zones inside the study volume. Relating the geological model and the RVS geometrically simplified model to the ‘550-m block’, it was noted that:

- 5 fracture zones intersect the Test Case block, dipping 70°–90°,

- the 550 m block in the RVS consists of 6 ‘rock mass units’ and 5 ‘units’ corresponding to the fracture zones.
- The 600 m × 180 m × 120 m Target Block is intersected by one fracture zone in the centre (NE2). Also, fracture zones EW1 and NE1 cut two opposite corners of the target block.

These fracture zones are all steeply oriented. Earlier investigations performed by /Talbot and Riad, 1987/ conclude that the fracture zones in the Simpevarp area (including Äspö) have experienced several reactivations of pre-existing faults. Both left and right-handed (dextral) strike-slips and dip and oblique slip faults have been observed. They further conclude that this indicates that such reactivations involved major changes in the direction of the stress field.

The description of the geological model of the Test Case refers to a report by /Munier, 1995/ stating that the latest detectable brittle movements in EW1 appear to be strike-slip dextral. The same information is given in /Nisca, 1987; Gustafson et al, 1989/, where it is written: “Once the steep EW penetrative fabric was established at least 1400 Ma ago, its anisotropy appears to have influenced all subsequent deformation of the rocks on Äspö. The bulk kinematics of the first ductile shears through the younger semi-ductile vein systems and still younger brittle fracture zones appear to have been remarkably similar in general location and geometry. Left-handed ductile shear movements changed to right-handed faults and fracture zones, but all regional displacements appear to have occurred along the same planar zones.”

The description of the geological model provided an indication of the fracture zone thickness. EW1a and EW1b are the widest, 45 m and 50 m, and NE1 and NE2 are allocated widths of 28 and 25 m, respectively. Fracture zone EW3 is modelled with a 14 m width. It should, however, be noted that these widths were the expected widths of the zones. Fracture zone NE2 is strongly undulating and the 25 m width refers to a span within which the zone is expected to be located. The actual zone itself is observed to be 0.6 – 6 m wide. For the other zones, the model unit widths were given the same width as that of the actual zone at the points where they have been observed (tunnels, outcrops, boreholes).

The fracture zone NE1 in the model was in fact only the north part of a wide zone with two strands. Of further importance for the estimation of the mechanical properties of this zone was the information that an approximately 8 m wide part of NE1 has open centimetre wide fractures and cavities and partly clay-altered rock. The central 1 m wide section is completely clay altered /Réhn et al, 1997/. Of course, stresses cannot be transmitted across those portions of the fractures that are open.

Since the model did not include any gently dipping structure, it was initially not expected to have any major abrupt stress magnitude changes with depth, but the stress field might still be influenced by the zones.

## 5.2.2 Stress measurement from the Test Case site

Within the Test Case exercise, stress measurement data were available from boreholes KAS02, KAS05 and KA3579G, *cf.* Section 3.4. Figure 5-6 shows the stress magnitudes for the maximum principal stress, from these three boreholes, as a function of the z-ordinate in the local co-ordinate system. Figure 5-7 shows corresponding diagrams

for the intermediate and minimum principal stress. To be able to judge whether these site-specific data conform to the overall stress pattern in Sweden, the best-fit linear trends from Figure 5-1 to Figure 5-3 and the estimated uncertainty spans (according to the initial prediction) have also been added to the diagrams.

It can be noted that the measured data, for all three principal stresses, fell within the total span of the initial estimate, i.e. the measurements were not remarkably different from those that have been seen at other locations in Sweden. In this sense, the site-specific data supported the suggested initial model.

It may be seen further in Figure 5-6 that the measurements in KAS02 gave lower stress values than the other measurements. The measurements in KAS02 were performed with hydraulic fracturing methods, and the other measurements with an overcoring method /Bjarnason et al, 1989; Klasson et al, 2001/.

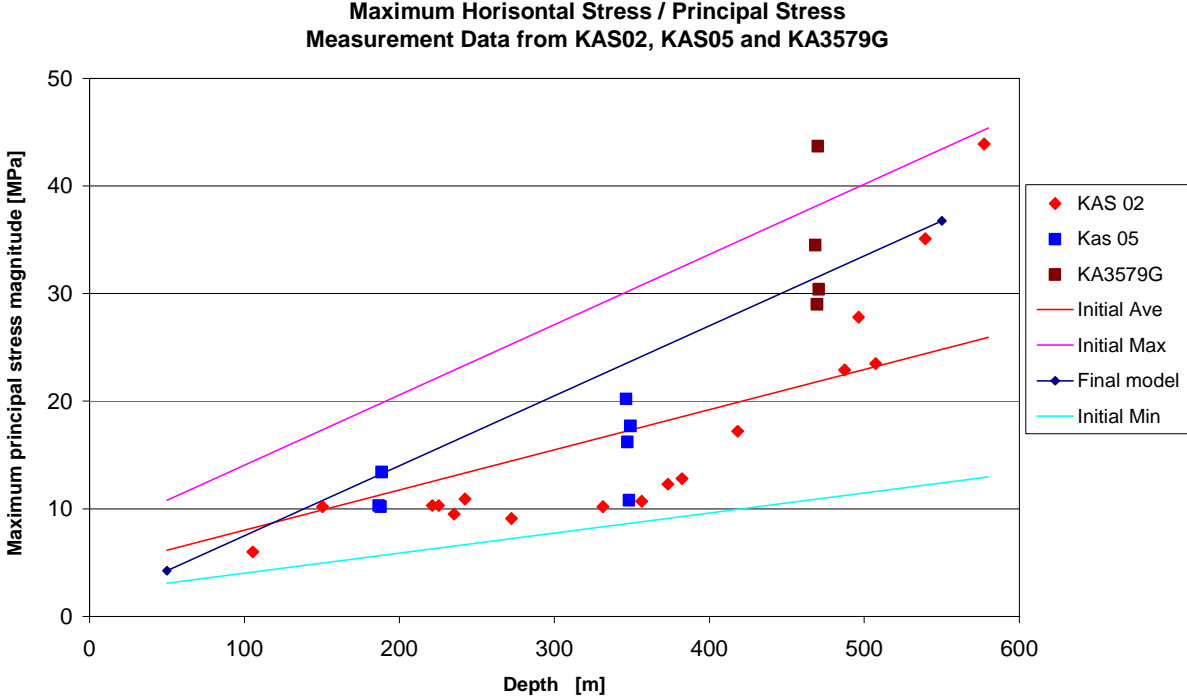


**Figure 5-6.** *Maximum principal stress,  $\sigma_1$  vs. depth. Data from measurements in three boreholes at ÄHRL. In KAS02, the measurement method was hydraulic fracturing and in KAS05 and KA3579G the method was overcoring. For KAS02, the maximum horizontal stress is assumed to correspond to the maximum principal stress, from /Hakami et al, 2002/ and based on work at Äspö HRL.*



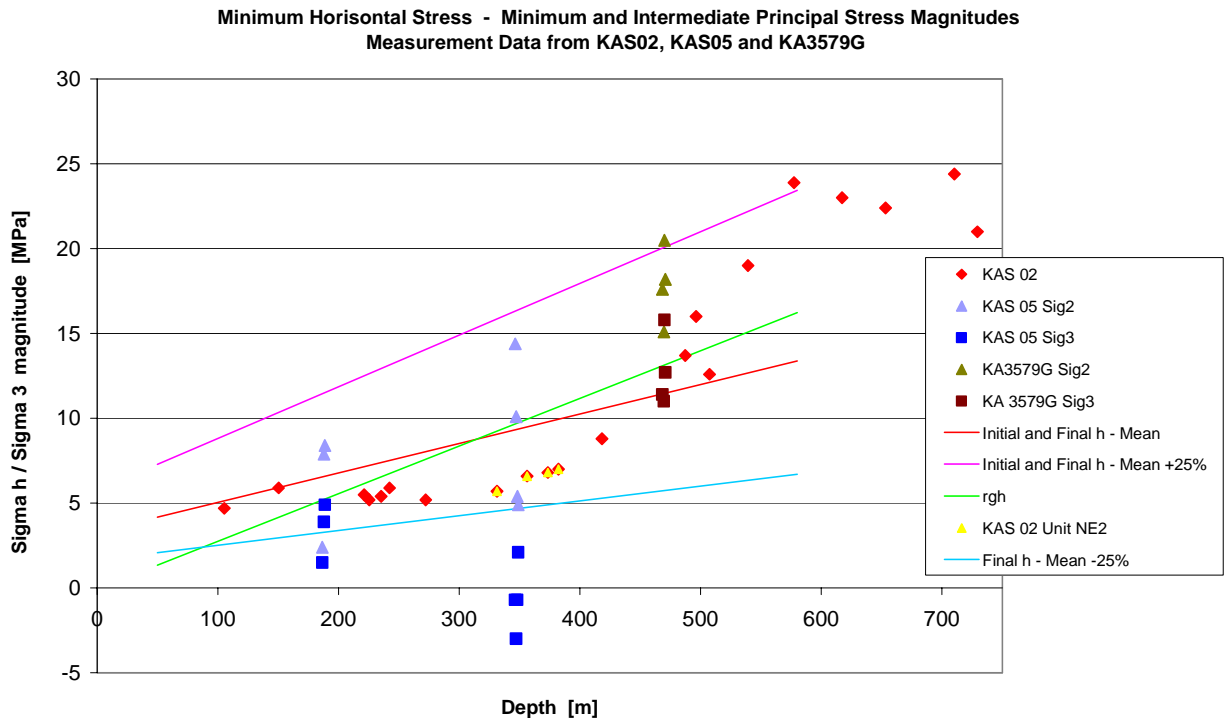


**Figure 5-7.** *Minimum and intermediate principal stress vs. depth. Data from measurements in boreholes at ÄHRL. In KAS02 the measurement method was hydraulic fracturing and in KAS05 and KA3579G the method was overcoring. (Using the hydraulic fracturing method, the minimum horizontal stress is here assumed to correspond to be the minimum principal stress, but the method gives no information on actual stress direction). The blue, red and green lines show the initial stress levels, from /Hakami et al, 2002/ and based on work at Äspö HRL.*

In Figure 5-8 to Figure 5.10, the orientation of the maximum horizontal stress and the maximum principal stress are presented. The direction is given in the local Äspö co-ordinate system. Since a sub-horizontal stress may have some slight variation in plunge, this means that trends, given as a single azimuth value, can be 180 degrees apart, such as the measurements in KAS05 at the 350 m level. The plunge of the maximum principal stress can be determined when using overcoring techniques, but is only assumed to be perfectly horizontal with hydraulic fracturing. Figure 5-9 shows measurement data for the plunge of the maximum principal stress.

The orientations of the intermediate and minimum stress are, by definition, in the plane perpendicular to the maximum principal stress. The plunge of the highest and lowest stress value in this plane may however vary. In Figures 5-10 and 5-11, the plunge determined at each overcoring measurement point are presented for the intermediate and the minimum stress, respectively.

It can be noted that the maximum principal stress seems to be fairly horizontal according to measurements in units H and I, but the measurements from the unit representing the fracture zone NE2 (unit J) give a large spread in the orientation results. This result may be explained by the fact that inside a fracture zone the stresses

should be expected to vary more than in the relatively homogenous blocks. Also, at these depths, the magnitudes of  $\sigma_2$  and  $\sigma_3$  are of the same order, thus giving large differences in calculated stress orientation (Figure 5-11). For the intermediate and minimum principal stresses, the orientation is not consistent for the two upper overcoring measurement levels but, for the lower level, the data indicate that the minimum principal stress is horizontal.

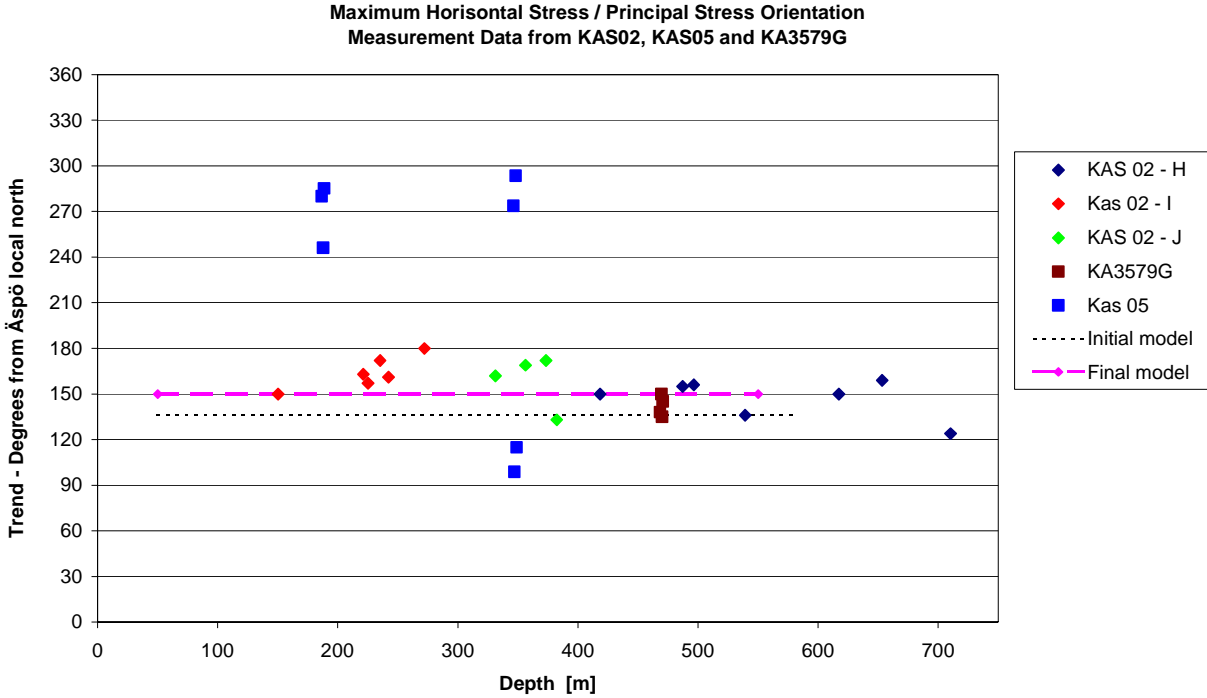


**Figure 5-8.** Trend of the maximum horizontal stress as determined from measurements from the Test Case site. I, J and H refer to the rock units in the geological model of the 550 m block, from /Hakami et al, 2002/ and based on work at Äspö HRL.

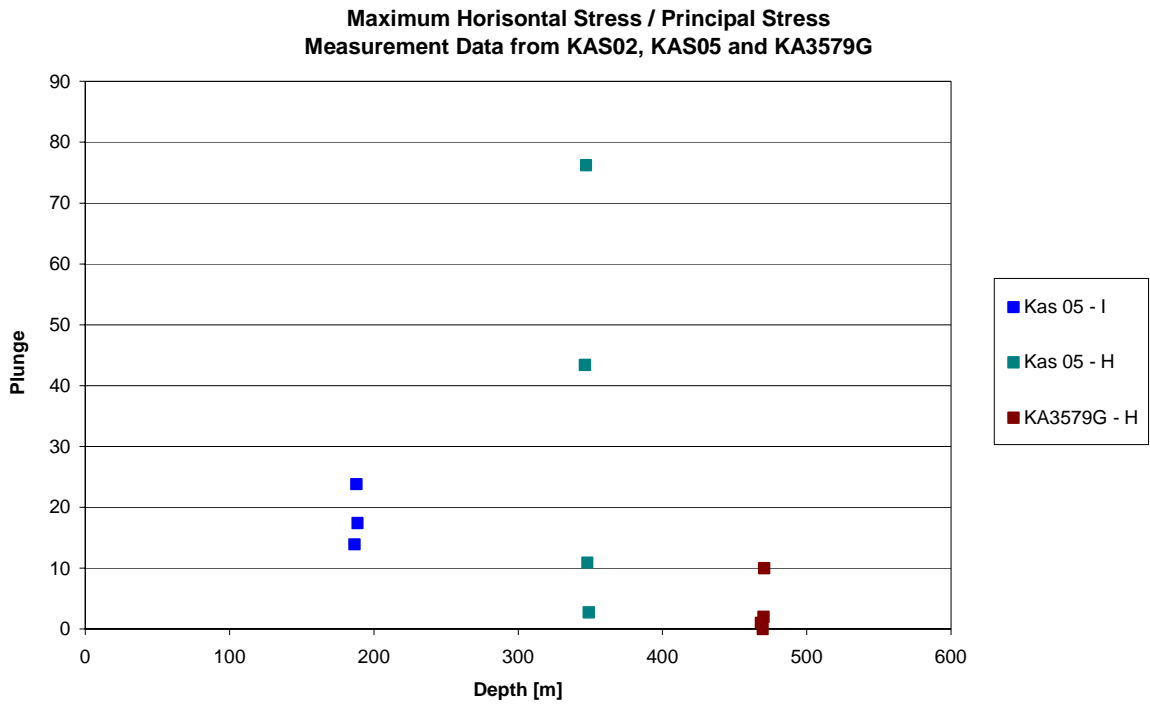


**Figure 5-9.** Plunge of the maximum horizontal stress data as determined from overcoring measurements in boreholes at the Test Case site, from /Hakami et al, 2002/ and based on work at Äspö HRL.

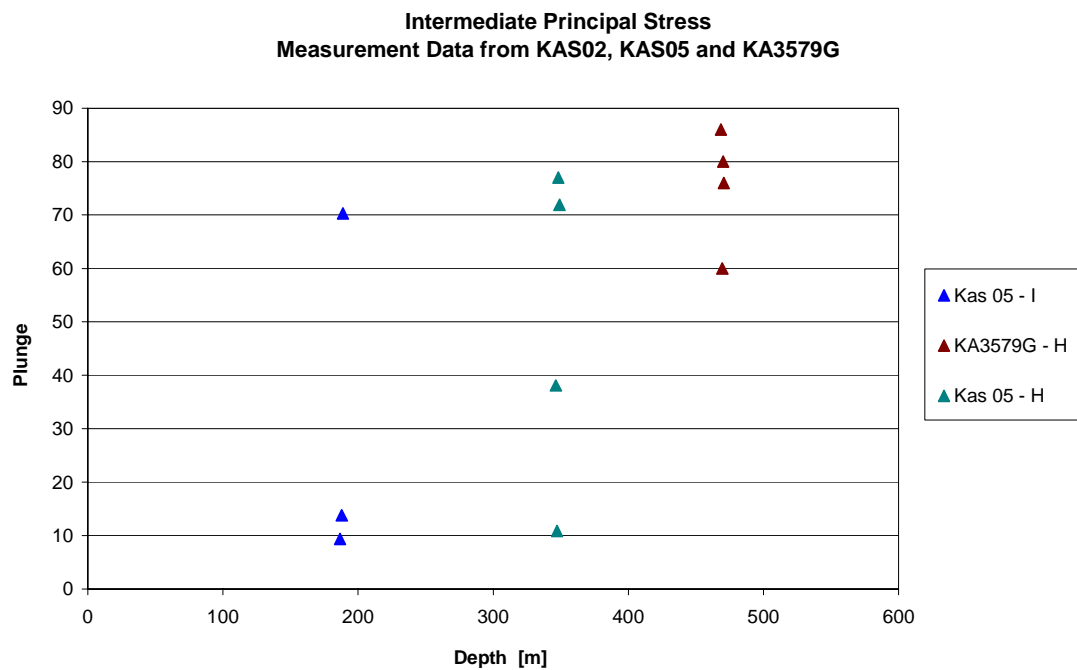


**Figure 5-10.** Plunge of the intermediate principal stress, as determined from overcoring measurements at the Test Case site, from Hakami et al, 2002 and based on work at Äspö HRL.

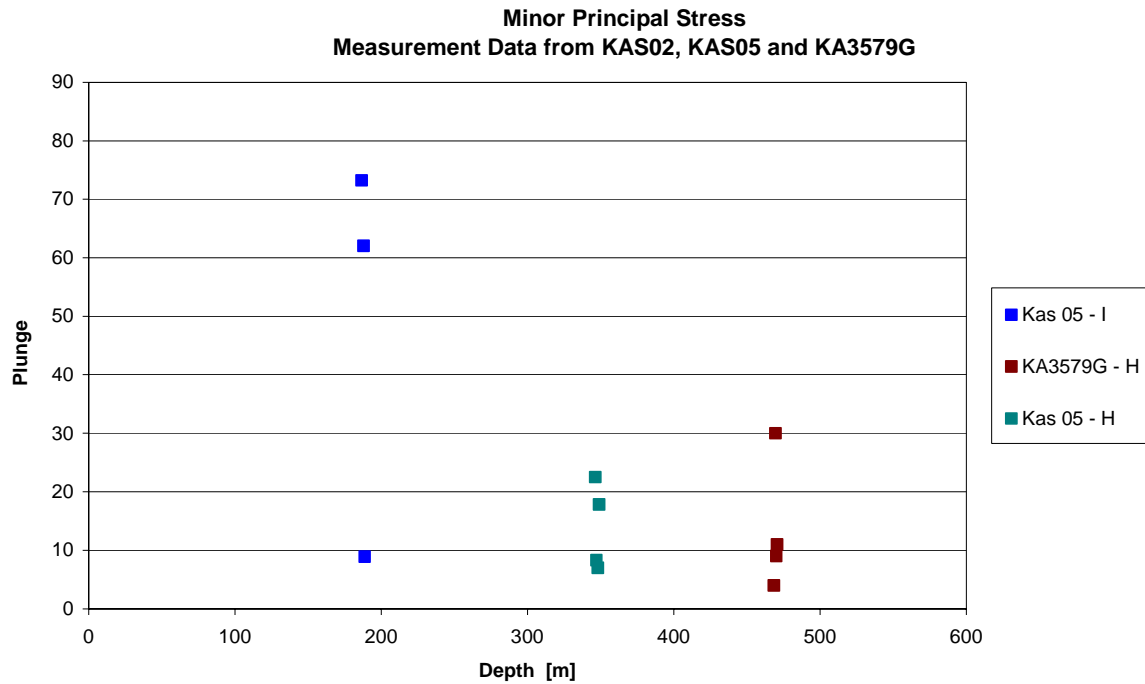


*Figure 5-11. Plunge of the minimum principal stress, as determined from overcoring measurements at the Test Case site, from /Hakami et al, 2002/ and based on work at Äspö HRL.*

### 5.3 Numerical analysis of in situ stress

In order to clarify how the stress magnitudes and orientations could be affected by fracture zones, numerical analyses were conducted using the 3DEC code. Complete details of the modelling are given in /Hakami et al, 2002/. The input data given to the teams has been summarized in Section 3.4.

#### 5.3.1 Geometry of the 3DEC model

##### Model size

In this project, in situ stress variation in the Test Case region as a result of mechanical response to regional loading of the rock was studied. Firstly, it was assumed that inside the 550 m block the effects from the closest fracture zones would dominate the stress variation, and the fracture zones far from this volume were not included specifically. It was further assumed that the volume and the surrounding rock was located in the same regional stress field, and thus had the same stress levels in general.

Also, on considering the regional map of the Äspö region, it was noted that the EW1 and NE1 fracture zones seem to have an extension in the order of 5 km, and that the 550 m block is also surrounded by fracture zones of even larger regional size. This may be taken as an indication that a block of side length in the order of 4 km may be regarded as a block with similar boundary conditions. The model size (side length 10 km) was selected because it gave a total size of the model that was about double the size of the largest structures. It was judged that the possible stress effects around the ends of zones would then not reach the boundaries of the model itself.

## Fracture zone geometry

Based on the idealized structural geological model of Äspö (the RVS model), five fracture zones were incorporated into the 3DEC model block. The natural fracture zones are geometrically modelled as thick plates in the RVS model. Such a plate has a thickness which encompasses a natural fracture zone that undulates along its length. However, in 3DEC, a fracture zone is modelled as a single planar surface with supposedly equivalent properties. The planar surfaces were placed in the 3DEC model as if they ran along the centre lines of the fracture zones included in the RVS-model.

Figure 5-12 shows how the fracture zones are oriented relative to each other. The zones NE2 and EW3 are smaller and terminate towards larger zones. The larger zones in the model were assumed to terminate as shown. Figure 5-13 gives a view of the 550-m block, again looking in the east direction. The volumes between the fracture zones were named within the project as shown. In the 3DEC model, the fracture zones do not have any thickness and therefore the RVS unit for deformation zones is not included.

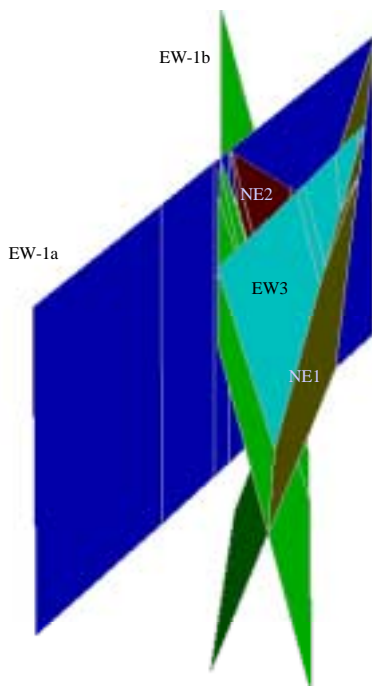


**Figure 5-12.** Fracture planes, representing the five major fracture zones, in the 3DEC models of the Test Case volume, looking eastwards.

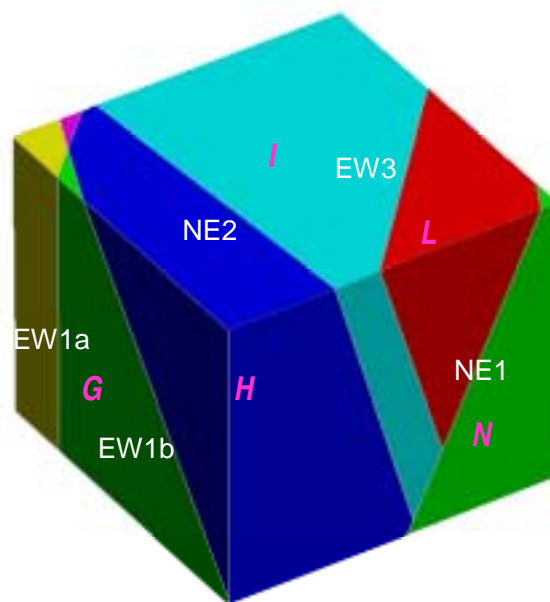


**Figure 5-13.** Fracture planes, representing the five major fracture zones, in the 3DEC models of the Test Case volume, looking eastwards.

From /Hakami et al, 2002/.

### 5.3.2 Examples of results from 3DEC models

Figure 5-14 shows a shear displacement plot for model TC8 with a  $15^\circ$  friction angle for the fracture zones. The arrows correspond to the shear displacements that have occurred on the model at a certain depth ( $-450$  m). The largest shear in the section is about 20 mm (see legends of the plots). Note that the lengths of the arrows in the figure correspond to the projected displacement vectors on the actual plane of the plot (with different scales), but the colouring code corresponds to the total shear displacement at the contact, independent of direction.

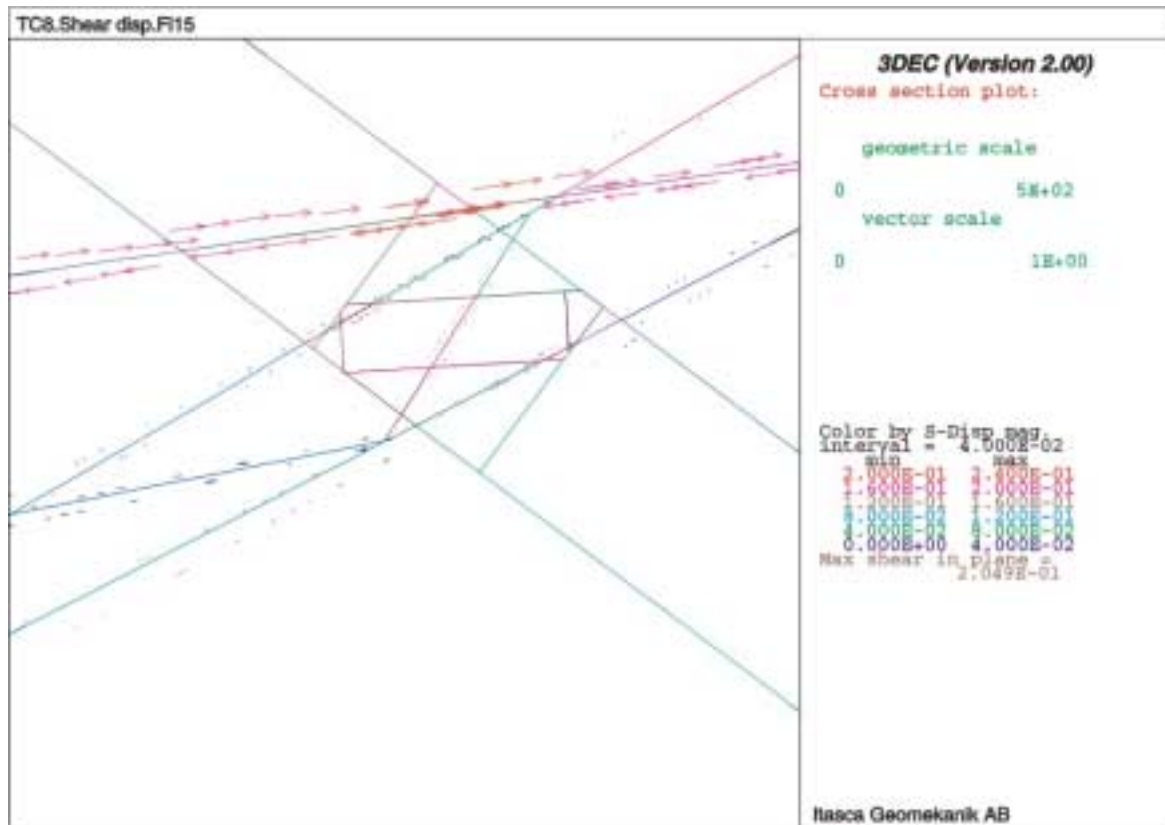


**Figure 5-14.** Shear displacement along fractures (simulating fracture zones) in 3DEC model TC8, which has a low friction angle on the fracture zones,  $15^\circ$ . The arrows are the components in the plane of the plot but the colour coding in the legend is the total shear displacement. The fracture zone that has sheared the most is zone EW1a and the maximum shear displacement in this section is 0.2 m. The movement of the zone has a dextral direction. From /Hakami et al, 2002/.

For modelling the Test Case target volume, results were considered along lines corresponding to the centre of cube rows with similar depth. An example, TC12, is shown in Figure 5-15, and the orientations of the stresses at the same locations are given in Figure 5-16. The points where a jump in values can be observed correspond to the move from one block to another, i.e. to the intersection of a fracture zone. (This will be different for the different cube rows.) The clearest effect is seen for the intermediate principal stress.

The general principal stress magnitudes of models TC33 and 34 resulted from the length of time the models were run. If the boundaries were moved a little more inwards, i.e. the model was a little further compressed, the levels would naturally have been higher. The selection of a certain level had to be based on measurement data. The model TC12 is an example of the modelling sequence with stress activation (not moving boundaries) and this explains the difference in stress magnitude compared to TC33 and TC34. Other models not shown here gave more or less similar results to the three examples shown. The magnitude and shape of the curves varied slightly with changing parameters. The models illustrated the expected variation in stress measured at a fracture zone, but the models are, of course, still simple idealizations of the real, even more complex, geometries at the fracture zone.

In the Target volume, particularly at deeper levels, the intermediate and minimum stresses were of similar magnitude and this made their orientation difficult to define. However, it should be possible to interpret the orientation of the maximum principal stress in the area, which is the information required for design needs.

Possible modelling alternatives could have included, for example, movement (e.g. relaxation) of the boundaries perpendicular to the minimum stress, and simulation of the overlying rock erosion. However, it was believed that more models, without further information on the stress state or on the geological and mechanical properties would not have resulted in significantly different conclusions for this Test Case.

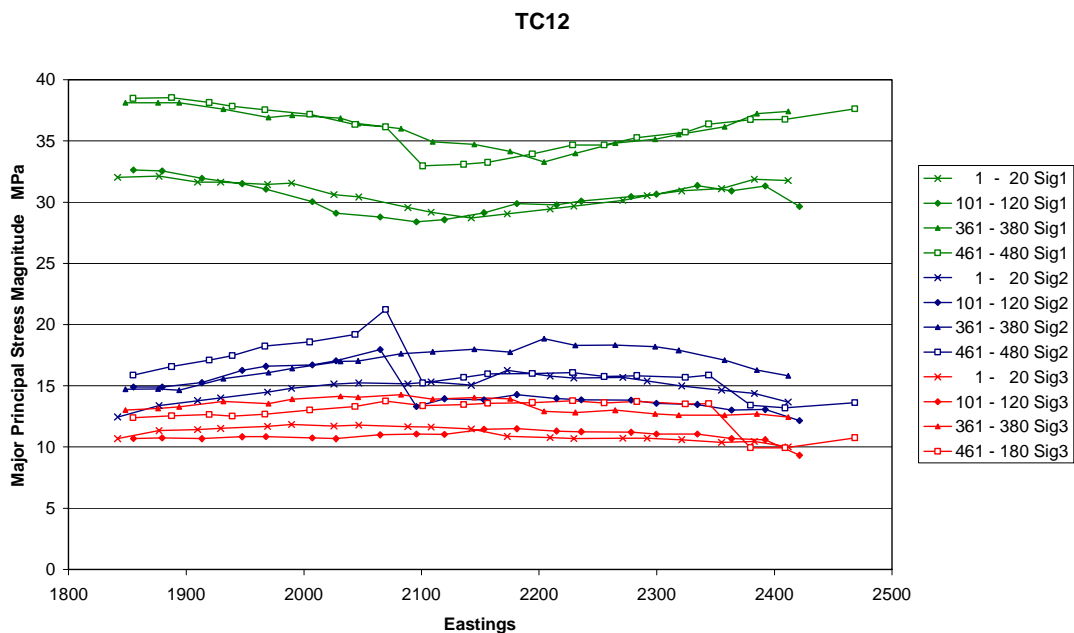


**Figure 5-15.** Calculated principal stresses for one model inside the Target volume of the Test Case. The numbers of the legends refer to the cube numbers. From /Hakami et al, 2002/.

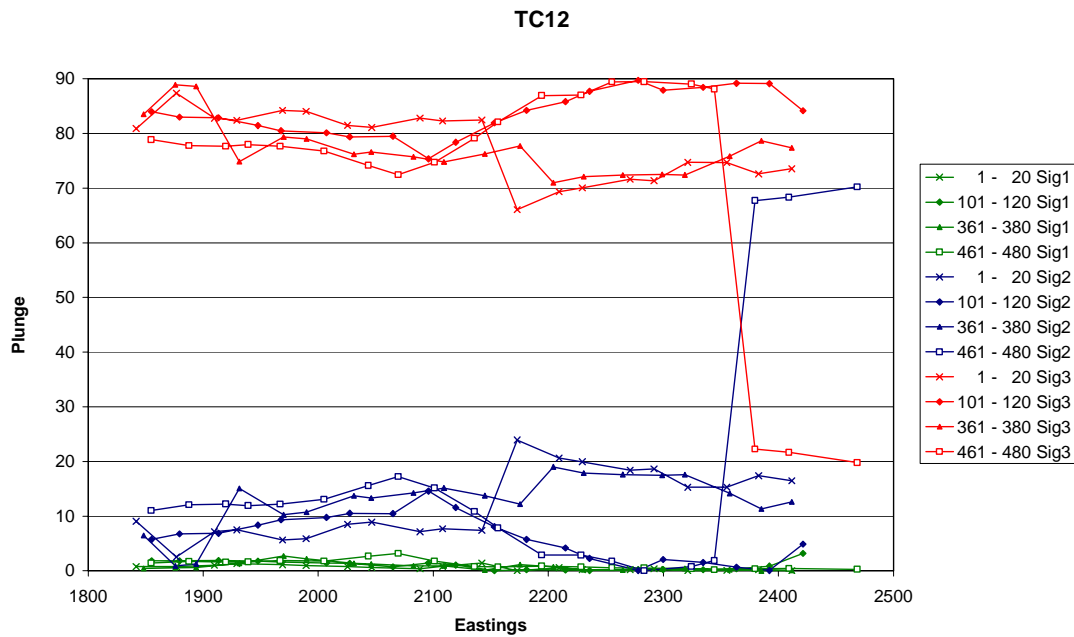


**Figure 5-16.** Calculated principal stress orientations for the same model as Fig. 5-15 inside the Target volume of the Test Case. The numbers of the legends refer to the cube numbers. From /Hakami et al, 2002/.

## 5.4 Final in situ stress prediction

### 5.4.1 Prediction of the stress field in the 550 m block

#### Principal stress magnitudes

The initial stress model was adjusted according to the site-specific information and the numerical modelling results. The final prediction, concerning principal stress magnitudes in the 550 m block, is presented in Tables 5-3 to 5-5. (The word ‘rock unit’ here refers to the geometrical units in the RVS model of the 550 m block of the Test Case).



**Table 5-3. Final prediction of  $\sigma_1$  stress magnitudes for Test Case 550 m block.**

Rock Unit	FZ Name	Mean $\sigma_1$ [MPa]		Uncertainty*	Variability*
		at z -500	Function of depth	u % of mean	v % of mean
A	EW1	33.5	$\sigma_1 = 0.065(-z)+1$	25	15
B C D E F		33.5	$\sigma_1 = 0.065(-z)+1$	25	50
G		33.5	$\sigma_1 = 0.065(-z)+1$	25	15
H		33.5	$\sigma_1 = 0.065(-z)+1$	25	15
I		33.5	$\sigma_1 = 0.065(-z)+1$	25	15
J		NE2	33.5	$\sigma_1 = 0.065(-z)+1$	25
K	EW3	33.5	$\sigma_1 = 0.065(-z)+1$	25	50
L	NE1	33.5	$\sigma_1 = 0.065(-z)+1$	25	15
M		33.5	$\sigma_1 = 0.065(-z)+1$	25	50
N		33.5	$\sigma_1 = 0.065(-z)+1$	25	50

\*For further explanation of the u and v parameters, see /Hakami et al, 2002/

**Table 5-4. Final prediction of  $\sigma_2$  stress magnitudes for Test Case 550 m block.**

Rock Unit	FZ Name	Mean $\sigma_2$ [MPa]		Uncertainty	Variability
		at z -500	Function of depth	u % of mean	v % of mean
A	EW1	13.5	$\sigma_2 = 0.027(-z)$	25	15
B C D E F		13.5	$\sigma_2 = 0.027(-z)$	30	50
G		13.5	$\sigma_2 = 0.027(-z)$	25	15
H		13.5	$\sigma_2 = 0.027(-z)$	25	15
I		13.5	$\sigma_2 = 0.027(-z)$	25	15
J		NE2	13.5	$\sigma_2 = 0.027(-z)$	30
K	EW3	13.5	$\sigma_2 = 0.027(-z)$	30	50
L	NE1	13.5	$\sigma_2 = 0.027(-z)$	25	15
M		13.5	$\sigma_2 = 0.027(-z)$	30	50
N		13.5	$\sigma_2 = 0.027(-z)$	30	50

**Table 5-5. Final prediction of  $\sigma_3$  stress magnitudes for the Test Case 550 m block.**

Rock Unit	FZ Name	Mean $\sigma_3$ [MPa]		Uncertainty	Variability
		at -500	Function of depth	u % of mean	v % of mean
A	EW1	12.0	$\sigma_3 = 0.0174(-z) + 3.3$	25	15
B C D E F		12.0	$\sigma_3 = 0.0174(-z) + 3.3$	30	50
G		12.0	$\sigma_3 = 0.0174(-z) + 3.3$	25	15
H		12.0	$\sigma_3 = 0.0174(-z) + 3.3$	25	15
I		12.0	$\sigma_3 = 0.0174(-z) + 3.3$	25	15
J	NE2	12.0	$\sigma_3 = 0.0174(-z) + 3.3$	30	50
K	EW3	12.0	$\sigma_3 = 0.0174(-z) + 3.3$	30	50
L	NE1	12.0	$\sigma_3 = 0.0174(-z) + 3.3$	25	15
M		12.0	$\sigma_3 = 0.0174(-z) + 3.3$	30	50
N		12.0	$\sigma_3 = 0.0174(-z) + 3.3$	30	50

### Principal stress orientations

The prediction of the stress orientation in the different rock units is presented in Table 5-6, in the same way as for the magnitudes.

**Table 5-6. Final prediction of principal stress orientations for the Test Case 550 m block.**

Rock Unit	FZ Name	$\sigma_1$ Trend			$\sigma_1$ Plunge			$\sigma_2$ Plunge		
		$\beta$ °	u °	v °	$\alpha$ °	u °	v °	$\alpha_2$ °	u °*	v °
A	EW1	150	15	15	0	10	15	0	10-45	15
B C D E F		150	30	25	0	20	30	0	10-45	30
G		150	10	15	0	10	15	0	10-45	15
H		150	10	15	0	10	15	0	10-45	15
I		150	10	15	0	10	15	0	10-45	15
J	NE2	150	30	25	0	30	30	0	10-45	30
K	EW3	150	30	25	0	30	30	0	10-45	30
L	NE1	150	10	15	0	10	15	0	10-45	15
M		150	30	25	0	20	30	0	10-45	30
N		150	15	15	0	10	15	0	10-45	15

\* Depending on depth. For  $z = 0$  to  $-100$ , u is 10; for  $z = -100$  to  $-400$ , u = 45; for  $z < -500$ , u = 10.

## 5.4.2 Stress prediction for the 380–500 level Target Block

### Principal stress magnitudes

The stress prediction model presented above for the 550 m block was applied to the target volume for the Test Case and the results for the stress magnitudes are given in Table 5-7. Since the stress magnitudes are only dependent on the z-ordinate in this model, the predictions are given for four ‘cube groups’ corresponding to the four different cube levels in the target block.

**Table 5-7. Principal stress magnitudes.**

Cube ID	Rock Unit	Cube Centre z	$\sigma_1$ MPa	Min–Max (u) MPa	$\pm v$ %	$\sigma_2^*$ MPa	Min–Max (u) MPa	$\pm v$ %	$\sigma_3^*$ MPa	Min–Max (u) MPa	$\pm v$ %
1–120	H	–395	26.7	18.7–34.7	15	10.7	8,0–13,3	15	10.2	7,6–12.7	15
1–120	I	–395	26.7	18.7–34.7	15	10.7	8,0–13,3	15	10,2	7,6–12,7	15
1–120	J	–395	26.7	18,7–34,7	50	10.7	7,5–13,9	50	10,2	7,1–13,2	50
121–240	H	–425	28.6	21.5–35.8	15	11.5	8,6–14,4	15	10.7	8,0–13,4	15
121–240	I	–425	28.6	21.5–35.8	15	11.5	8,6–14,4	15	10,7	8,0–13,4	15
121–240	J	–425	28.6	21.5–35.8	50	11.5	8,4–14,9	50	10,7	7,5–13,9	50
241–360	H	–455	30.6	22.9–38.2	15	12.3	9,2–15,4	15	11.2	8,4–14,0	15
241–360	I	–455	30.6	22.9–38.2	15	12.3	8,6–16,0	15	11,2	8,4–14,0	15
241–360	J	–455	30.6	22.9–38.2	50	12.3	9,2–15,4	50	11,2	7,9–14,6	50
361–480	H	–485	32.5	24.4–40.7	15	13.1	9,8–16,4	15	11.7	8,8–14,7	15
361–480	I	–485	32.5	24.4–40.7	15	13.1	9,8–16,4	15	11,7	8,8–14,7	15
361–480	J	–485	32.5	24.4–40.7	50	13.1	9,2–17,0	50	11,7	8,2–15,3	50

### Principal stress orientations

In Table 5-8 the orientations of the estimated stresses in the target volume are presented. Since the three principal stresses are orthogonal at each point, only three parameters are needed to define the orientation. It was chosen to give trend,  $\beta$ , and plunge,  $\alpha$ , for the maximum principal stress,  $\sigma_1$ , and the plunge of  $\sigma_2$ . From these values the trend of  $\sigma_2$  and the trend and plunge for  $\sigma_3$  may be determined. The values u and v correspond to uncertainty and variability estimates described earlier (Section 5.1.3).

**Table 5-8. Principal stress orientations.**

Cube ID	Rock Unit	Cube Centre z	$\beta_1$	$\pm u$ °	$\pm v$ °	$\alpha_1$	$\pm u$ °	$\pm v$ °	$\alpha_2$	$\pm u^*$ °	$\pm v$ °
1-120	H	-395	150°	10°	15°	0°	10°	15°	0°	45°	15°
1-120	I	-395	150°	10°	15°	0°	10°	15°	0°	45°	15°
1-120	J	-395	150°	10°	15°	0°	10	45	0°	45°	45
121-240	H	-425	150°	10°	15°	0°	10°	15°	0°	45°	15°
121-240	I	-425	150°	10°	15°	0°	10°	15°	0°	45°	15°
121-240	J	-425	150°	10°	15°	0°	10	45	0°	45°	45
241-360	H	-455	150°	10°	15°	0°	10°	15°	0°	45°	15°
241-360	I	-455	150°	10°	15°	0°	10°	15°	0°	45°	15°
241-360	J	-455	150°	10°	15°	0°	10	45	0°	45°	45
361-480	H	-485	150°	10°	15°	0°	10	15°	0°	45°	15°
361-480	I	-485	150°	10°	15°	0°	10	15°	0°	45°	15°
361-480	J	-485	150°	10°	15°	0°	10	45	0°	45°	45

\* The principal stress in this direction may in some cases be  $\sigma_3$  instead of  $\sigma_2$ .

## 5.5 Comparison with the ‘best estimate’ reference results

The comparison with the ‘best estimates’ of the stress states was only required for the 380–500 m level target volume. The ‘best estimate’ results, based on additional information ( *cf.* Section 3.4) are given in Table 5-9.

**Table 5-9. NGI estimates of ranges for the mean principal stress magnitudes for the four cube layers, from /Makurat et al, 2002/.**

Depth, m	$\sigma_1$ , MPa	$\sigma_2$ , MPa	$\sigma_3$ , MPa
Level 1: -380 – -410	8.0 – 30.5	5.2 – 15.1	2.9 – 9.9
Level 2: -410 – -440	16.1 – 31.2	9.4 – 16.6	5.8 – 10.8
Level 3: -440 – -470	21.9 – 37.4	12.8 – 20.1	8.0 – 13.1
Level 4: -470 – -500	22.1 – 45.6	14.1 – 24.4	8.7 – 16.0

Thus, the stress estimates made by the Stress Group are within the range supplied for the ‘best estimate’ reference case.

## 6 Conclusions

The conclusions and recommendations in this Chapter are presented in two parts. In Section 6.1, the overall and specific conclusions are presented. These follow directly from the Äspö HRL Test Case experience, as described in the earlier Chapters. In Section 6.2, further conclusions are presented in the context of the rock mechanics features of the Site Descriptive Model and to provide ‘lessons learnt’ advice for any future Test Case exercises of this kind.

At this stage, the content of the report and the conclusions and recommendations should not be interpreted as necessarily being SKB’s view of a recommended approach to the rock mechanics aspects of site characterization.

### 6.1 Test Case conclusions

The predictive aspects of the Test Case exercise were estimating the mechanical properties and estimating the state of stress for a large block of rock and a target volume within this block. The predictions were made by three teams: two working on the mechanical properties and one on the state of stress. A ‘best estimate’ of the actual conditions was then made by a fourth team. Quality Control procedures were used and the progress of the work was reviewed by both internal and external personnel. The overall conclusions relating to these activities are presented, followed by the specific conclusions relating to the mechanical property and stress predictions.

#### 6.1.1 Overall conclusions

1. The Test Case exercise was invaluable in forcing the generic approach to the Rock Mechanics Site Descriptive Strategy to become a specific approach for the Äspö HRL rock volume being considered. In asking the teams to make specific predictions, both individually and in combination, the strategy was translated into a pragmatic methodology. Many extra issues arose because of this and several of them were solved – thus significantly improving the approach. Also, the Test Case demonstrated the benefits of a combined, integrated approach.
2. A wide range of Quality Control instruments was used for the development of the approach to the Rock Mechanics Site Descriptive Model, and the use of Protocols in particular to structure the specific Test Case work was a crucial and successful component of the work. It is important to incorporate traceability throughout the process, including the conceptual assumptions.
3. The characterization and prediction methodologies were significantly enhanced by structured interactions between the teams involved, leading to improved understanding and a harmonization of approaches.

4. The differences between the predicted rock properties and the ‘best estimate’ reference rock properties in the Test Case were mainly due to different assumptions and the approaches used by the four teams involved in the work, rather than by the fact that the ‘best estimate’ predictions were based on additional data. This reinforces Point 2 above that traceability is required in the rock characterization process.
5. The predictions of the rock mass modulus between fracture zones made by the empirical and theoretical teams were similar and close to the ‘best estimate’ reference values.
6. The predictions of the rock mass modulus in fracture zones were more varied, because few data were available and hence there was greater choice in the assumptions necessary to make the predictions.
7. The empirical and theoretical teams’ predictions of the rock strength were also more varied, mainly because few data were available and different interpretations of rock mass strength were used.
8. The rock stress predictions, based on database information and numerical modelling, were satisfactory and helped to focus attention on the key factors involved. In particular, the use of numerical modelling assists in evaluating potential stress changes in the vicinity of fracture zones.
9. Methods of dealing with conceptual uncertainty and spatial variability of stress were successfully introduced into the rock stress characterization and predictive methodology
10. Aspects of the Test Case work that, with hindsight, could have been improved were:
  - better definition of the rock properties to be predicted;
  - more attention paid to difficulties in 3-D extrapolation, i.e. how to assign values to points distant from known information;
  - more rigorous application of the Quality Control instruments;
  - more encouragement of inter-team discussions; and
  - earlier implementation of external reviewing of the work.

### **6.1.2 Characterizing, modelling and predicting the mechanical properties**

An initial problem was to decide on the best ways of approaching this subject. There are two basic methods:

1. using rock mass classification and correlations of these values with rock properties in order to predict the rock properties; and
2. using numerical modeling procedures to estimate the rock mass properties from the component properties of the intact rock and the fractures.

For the Test Case, these approaches were used separately and in combination.

In both approaches for prediction and characterization, it is important to define the parameters – in this case, what is meant by the rock mass deformation modulus and strength, and to ensure that the failure criteria used in the model have been well thought through.

Both the empirical and theoretical approaches had to deal with uncertainties. The main uncertainties encountered related to the size and other properties of the fractures, the spatial distribution of mechanical properties, blocks with no information, rock types, 2-D versus 3-D modelling in the theoretical approach and the correlations between the classifications ratings and the mechanical properties in the empirical approach. However, the two approaches were fundamentally different and a summary of the conclusions for each approach is given below.

### **The empirical approach**

The Q and RMR rock mass classification systems were used to provide rating values. Correlation equations in the literature were used to estimate the rock mass modulus and the rock mass strength.

The conclusions relating to this aspect of the work are as follows.

- The empirical approach has been successfully used for general tunnelling, but the experience supporting the approach is limited for depths around 500 m. Also, by the very nature of an empirical approach, it cannot be checked against the basic laws of physics.
- Difficulties were encountered in the empirical systems with
  - exact definitions of the rock properties,
  - deciding on the borehole sample lengths for characterization,
  - how the stress and water factors should be dealt with in the Q approach,
  - subjectivity in deciding on the component ratings,
  - the fact that the classification values are directionally dependent.
  - the published correlations between rock mass properties and the empirical indices
- However, a successful approach was developed that overcame the problems and incorporated uncertainty considerations. Predictions were made that were in good general agreement with the ‘best estimate’ reference values.

### **The theoretical approach**

A Discrete Fracture Network (DFN) model was used to generate fractures for use in the 2-D Universal Distinct Element Code (UDEC). Modulus and strength values for the rock mass were estimated through numerical simulation of loading a rock block sample.

The conclusions relating to this aspect of the work are as follows.

- Sensitivity analyses proved to be most helpful for studying factors such as the influence of the boundary conditions, domain size, possible directional dependency, fracture distribution, failure criterion, etc. Also, using simple confidence levels (supported by data, interpolation, guess work) was a pragmatic way of dealing with uncertainties.
- The use of a 3-D fracture generation method to provide 2-D sections for UDEC was questionable, but considered useful if the 2-D section was in the weakest plane. The weakest planes might be the planes containing the major and intermediate principal stresses, but they also might be other planes; this depends on the geometry of the fracture network.
- Also, the use of a discrete fracture network model may not fully characterize the variation in fracture statistics over a large site.
- Again, a successful approach was developed that overcame the problems and incorporated uncertainty considerations, and predictions were made that were in good general agreement with the ‘best estimate’ values.

### **Harmonization of the empirical and theoretical approaches**

A Workshop was held to establish how the empirical and theoretical approaches could be combined to produce single predictions for the rock blocks being considered.

Conclusions from this Workshop were as follows.

- Groups with different approaches should interact to discuss how to extrapolate measured data into 3-D, and the overall support for the geological model of the site.
- Harmonization discussions should consider the need to characterise the site – not just how to carry out limited sets of analyses.
- Stress analysis provides justification for the stress levels used in the rock property modelling (but stress levels as measured are usually sufficient for the predictions).
- Conceptualisation of fracture zones needs to be co-ordinated and rock mechanics parameterisation of fracture zones needs to be established.
- Comparing predicted rock mechanics parameters for the same input using the theoretical and the empirical approaches can help to indicate which approach is more appropriate. For example, the empirical approach can be more sensitive to the properties of the minor fracture zones, whereas the theoretical approach tended to smooth these out. Which approach is the best depends on the characterization required.



### 6.1.3 Modelling and predicting the state of stress

Unlike the mechanical properties, the actual method of characterizing the stress state is not an issue: rock stress is a second order tensor, characterized by the magnitudes and orientations of the three principal stresses.

The conclusions for this aspect of the work relate to the Test Case simulating site investigation circumstances, and not to a case where a full stress measurement programme had been implemented.

- Good databases exist with information on the global, European and Swedish states of rock stress with depth. These enable estimates to be made of the magnitudes and orientations of the regional major principal stresses.
- Two important uncertainties relating to the in situ rock stress are
  - the fundamental uncertainty about whether the stress measurement data are correct,
  - the natural variability of the stress state in the rock mass, due mainly to inhomogeneities.
  - A method was developed for incorporating both these into the estimations.
- Predictions were refined by considerations of the fractures zones and some Äspö stress measurement data. In particular, 3-D numerical analyses were conducted to estimate the effect of the fracture zones in the 550 m and 380–500 m level target volume. It is important that the boundary conditions in such modelling are considered carefully (in terms of stress or strain) to avoid pre-judging the modelling output.
- At this stage, based on the information available to the stress model team,
  - the orientation and magnitude of the *major* principal stress can be estimated sufficiently accurately within the Table 3-1  $\pm 20\%$  acceptable estimation criteria.
  - the magnitudes of the *intermediate and minor* principal stresses can also be estimated sufficiently accurately.
- It is better to begin estimating the stress on a large scale and then to reduce the volume of interest. For this reason, the numerical modelling of the rock stress states was considered particularly successful because it provided an overview of the potential stress variations caused by the presence of the fracture zones and can be calibrated using measurement data.

### 6.1.4 The 'best estimate' of the actual conditions

The estimation of the actual rock mass conditions in the 380–500 m level target volume was based on all the information available, as described in Section 3.4. This comprised existing data in SKB reports and in the SKB data base SICADA, supported by information from the rock mechanics literature. Also, tunnel and tunnel borehole observations were also used – which were not available to the teams making the predictions.

The conclusions for this aspect of the work are as follows.

- The use of additional data to estimate the rock mass properties provides further characterization opportunities.
- However, a decision has to be made about how to incorporate additional data in the data processing structure.

## **6.2 Recommendations for general rock mechanics site characterization and Test Case work**

The following recommendations result directly from the Äspö HRL Test Case experience and it is hoped that they will be useful for any future exercises of this kind.

- 1 There is no standard method of characterizing a rock mass, nor any standard method of conducting a site investigation. Therefore, it is crucial to establish the purpose of the characterization – which data are required for what purpose and what accuracy is required?
- 2 It is important to establish Quality Control methods and to implement them rigorously.
- 3 All terms used should be defined before the work commences to avoid misunderstandings and different approaches
- 4 The methods used must be able to cope with the main features of rock masses – which are discontinuous, inhomogeneous, anisotropic and not elastic (i.e. DIANE in nature). In particular, data characterizing the rock fractures are required.
- 5 It is advantageous to use different approaches by different personnel to characterize the rock mass. This highlights problems and the procedure of harmonising the approaches significantly enhances the characterization process.
- 6 Stress modelling work should be conducted in association with the geological modelling to ensure compatible understanding and to provide the more detailed knowledge required for repository design.
- 7 The difficult task of predicting properties in deformation zones should be recognized and, if possible, data should be collected in the vicinity of the planned location of the excavations.
- 8 A Test Case provides an opportunity to test the methodology and smooth out problems that are highlighted by having to apply a general approach to a specific site.
- 9 The Äspö HRL can be used as a benchmark for crystalline rock conditions against which further Test Cases in different areas can be compared.

## 7 References

- Andersson J, Christiansson R, Hudson J A, 2002.** Site Investigations: Strategy for development of a Rock Mechanics Site Descriptive Model. SKB Technical Report TR-02-01. Svensk Kärnbränslehantering AB, Stockholm.
- Ask M S V, 1996.** In situ stress from borehole breakouts in Denmark. Licentiate thesis, Royal Institute of Technology, Stockholm, TRITA-AMI LIC 2012, ISBN 9171706682.
- Bjarnason B, Klasson H, Leijon B, Strindell L, Öhman T, 1989.** Rock stress measurements in boreholes KAS02, KAS03 and KAS05 on Äspö SKB International Progress Report IPR-25-89-17. Svensk Kärnbränslehantering AB, Stockholm.
- Bungum H, Alsaker A, Kvamme L B, Hansen R A, 1991.** Seismicity and seismotectonics of Norway and nearby continental shelf areas. *Journal of Geophysical Research*, 96, 2249–2265.
- Ericsson L O, 1988.** Fracture mapping study on Äspö island. Findings of directional data. SKB Progress Report PR-25-88-10. Svensk Kärnbränslehantering AB, Stockholm.
- Fredriksson A, Hässler L, Söderberg L, 2001.** Extension of CLAB – Numerical modelling, deformation measurements and comparison of forecast with outcome. Proceedings of the Eurock 2001 Symposium, Helsinki, Finland. Eds Särkkä P. and Eloranta P, 743–748.
- Gregersen S, Korhonen H, Husebye E S, 1991.** Fennoscandian dynamics: Present-day earthquake activity. *Tectonophysics*, 189, 333–344.
- Grimstad E, Barton N, 1993.** Updating the Q-system for NMT. Proceedings of the International Symposium on Sprayed Concrete. Fegernes, Norway, Norwegian Concrete Association, Tapis Press: Trondheim, pp. 46–66.
- Gustafson G, Stanfors R, Wikberg P, 1989.** Swedish Hard Rock Laboratory. Evaluation of 1988 year pre-investigation and description of the target area, the island of Äspö. SKB Technical Report TR-89-16. Svensk Kärnbränslehantering AB, Stockholm.
- Hakami E, Hakami H, Cosgrove J, 2002.** Strategy for a Rock Mechanics Site Descriptive Model: Development and testing of an approach to modelling the state of stress. SKB Report R-02-03. Svensk Kärnbränslehantering AB, Stockholm.
- Hermansson J, Stiggson M, Wei L, 1998.** A discrete fracture network model of the Äspö Zedex tunnel section. SKB Progress Report PR-98-29. Svensk Kärnbränslehantering AB, Stockholm.
- Hoek E, 1990.** Estimating Mohr-Coulomb friction and cohesion values from the Hoek-Brown failure criterion. *Int. J. Rock Mech. Min. Sci. & Geo. Abs.* 27, 3, 227–229.
- Hoek E, Brown E T, 1997.** Practical Estimates of Rock Mass Strength. *Int. J. Rock Mech. Min. Sci.* 34, 8, 1165–1186.

**Klasson H, Persson M, Ljunggren C, 2001.** Overcoring rock stress measurements at the Äspö HRL – Prototype repository: Borehole KA3579G (Revised data) and K-tunnel: Borehole KK0045G01. SKB Report (in press). Svensk Kärnbränslehantering AB, Stockholm

**Lanaro F, 2001.** Determination of the normal and shear stiffness of rock joints: geometry, normal and shear stiffness. SKB Technical Report.(in press). Svensk Kärnbränslehantering AB, Stockholm

**Makurat A, Løset F, Hagen A W, Tunbridge L, Kveldsvik V, Grimstad E, 2002.** Äspö HRL: A Descriptive Rock Mechanics Model for the 380–500 m level. SKB Report R-02-11. Svensk Kärnbränslehantering AB, Stockholm

**Martin C D, Christiansson R, Söderhäll J, 2001.** Rock stability considerations for siting and constructing a KBS-3 repository. Based on experiences from Äspö HRL, AECL's URL, tunnelling and mining. SKB Technical Report TR-01-38. Svensk Kärnbränslehantering AB, Stockholm.

**Müller B, Zoback M L, Fuchs K, Mastin L, Gregersen S, Pavoni N, Stephansson O, Ljunggren C, 1992.** Regional Patterns of Tectonic Stress in Europe. Journal of Geophysical Research, 97, No. B8, 11, 783–803.

**Munier R, 1995.** Studies of geological structures at Äspö. Comprehensive summary of results. SKB Progress Report 25-95-21. Svensk Kärnbränslehantering AB, Stockholm.

**Nisca D H, 1987.** Aeromagnetic interpretation. SKB Progress Report PR 25-87-23. Svensk Kärnbränslehantering AB, Stockholm.

**Nisca D H, 1988.** Geophysical laboratory measurements on core samples from KLX01, Laxemar and KAS02, Äspö. SKB International Progress Report IPR-25-88-06. Svensk Kärnbränslehantering AB, Stockholm.

**Nordlund E, Li C, Larsson B, 1999.** Mechanical properties of the diorite in the prototype repository at Äspö HRL. SKB, International Progress Report IPR-99-25. Svensk Kärnbränslehantering AB, Stockholm.

**Rhén I, Gustafson G, Stanfors R, Wikberg P, 1997.** Äspö HRL – Geoscientific evaluation 1997/5: Models based on site characterization 1986–1995. SKB Technical Report TR-97-06. Svensk Kärnbränslehantering AB, Stockholm.

**Röshoff K, Lanaro F, Jing L, 2002.** Strategy for a Rock Mechanics Site Descriptive Model: Development and testing of the empirical approach. SKB Report R-02-01. Svensk Kärnbränslehantering AB, Stockholm.

**Sehlstedt S, Strähle A, 1991.** Identification of water conductive oriented fractures in the boreholes KAS02 and KAS06 SKB. SKB International Progress Report IPR-25-91-11. Svensk Kärnbränslehantering AB, Stockholm.

**Serafim J L, Pereira J P, 1983.** Considerations of the geomechanical classification of Bieniawski. Proceedings of the International Symposium on Engineering Geology and Underground Construction, Lisbon, 1, II. 33–42.

**SKB, 2000b.** Geoscientific programme for investigation and evaluation of sites for the deep repository. SKB Technical Report TR-00-20. Svensk Kärnbränslehantering AB, Stockholm.

**SKB, 2001a.** Integrated account of method, site selection and programme prior to the site investigation phase. SKB Technical Report TR-01-03. Svensk Kärnbränslehantering AB, Stockholm.

**SKB, 2001b.** Site investigations: investigation methods and general execution programme. SKB Technical Report TR-01-29. Svensk Kärnbränslehantering AB, Stockholm, Sweden.

**Slunga R, Norrman P, Glans A-C, 1984.** Baltic Shield seismicity, the result of a regional network. *Geophysical Research Letters*, 11, (12), 1247–1250.

**Staub I, Fredriksson A, Outters N, 2002.** Strategy for a Rock Mechanics Site Descriptive Model: Development and Testing of the Theoretical Approach. SKB Report R-02-02. Svensk Kärnbränslehantering AB, Stockholm.

**Stephansson O, Ljunggren C, Jing L, 1991.** Stress measurements and tectonic implications for Fennoscandia. *Tectonophysics*, 189, 317–322.

**Stille H, Olsson P, 1989.** First evaluation of rock mechanics. SKB Progress Report 25-89-07. Swedish Nuclear Fuel and Waste Management Co, Stockholm, Sweden.

**Stille H, Olsson P, 1990.** Evaluation of rock mechanics. SKB Progress Report PR-25-90-08. Svensk Kärnbränslehantering AB, Stockholm, Sweden.

**Sundberg J, Gabrielsson A, 1999.** Äspö Hard Rock Laboratory – Laboratory and field measurements of thermal properties of the rocks in the prototype repository at Äspö HRL. SKB International Progress Report IPR-99-17. Svensk Kärnbränslehantering AB, Stockholm, Sweden.



**Test Case Protocol 4B for Individual Model Predictions**

**TEST CASE**  
**PROTOCOL 4B: INDIVIDUAL MODELLING PREDICTIONS**

**Objectives**     1. *To establish the methodology and obtain the predictions from the individual modelling teams.*

**Procedures**

1. *Use the work being conducted for the Theoretical Model, Empirical Model and Stress Model.*
2. *Use of the principles and procedures established in Protocols 1–3.*
3. *Each modelling team develops and documents their own protocol for making the predictions.*
4. *Each of the teams makes their own predictions.*
5. *Each team submits their predictions using a protocol (see following text).*

**Format for submission**

*It is suggested that the output for inter-comparison is submitted as Excel tables. However, it should be remembered that all teams are expected to deliver any additional output they feel is needed/interesting in a format decided by themselves.*

**Co-ordinates**

*In general, predictions (the estimates and some uncertainty value) are given for each 30 m × 30 m × 30 m cube in the detailed 380–500 level model. (For stress this may not practical).*

*In order to facilitate inter-comparison, it is necessary to adopt common domain locations, etc. The following should be noted:*

- *The corner co-ordinates of the detailed 380–500 m level model domain are provided by SKB.*
- *NGI has introduced a cube numbering for identifying each individual cube. All teams should strive at using this numbering system. The numbering has been handed out to all teams. (It should be straightforward to implement in the local system of each team).*

- 
- *All teams (including NGI) should provide the centre co-ordinates of each cube when they deliver their predictions. The information will be used for consistency checks and for simplifying plots etc.*

*For the later inter-comparison, it would also be of great importance to separate cubes in the rock unit, in different fracture zones, in the general rock unit or in the “greenstone unit” (if these exist).*

*Some cubes may cover more than one rock unit (e.g. ‘ordinary rock unit’ and a fracture zone unit, see Figure 0-1). Furthermore, within a fracture zone unit, the actual fracture zone may be less than the width of the unit (also see Figure 0-1), i.e. such cubes may contain both ‘fracture zone’ and ‘ordinary’ rock. The data file of cubes should indicate if the cube contains such a mixture of units (i.e. all cubes marked with x in Figure 0-1).*

*When predictions are made for cubes with several possible conditions (e.g. the x-marked ones), they should not be averaged between rock types. Instead, different values will be given for each rock unit which may exist within such a cube (i.e. for all the x-marked cubes, two sets of values will be given – one for the fracture zone properties and one for the other rock properties). Similar divisions should be made if there are other different rock units (i.e. greenstone, and not-greenstone).*

*The predictions are provided for each cube. Furthermore, if a cube has more than one rock unit, a full line of prediction should be provided for each unit. In particular, one should note that rock mass properties may also be provided for a rock cube inside an RVS fracture zone rock unit, since only part of it contains the real fracture zone (see Figure 0-1). The same principle will later apply if teams decide to divide the rock into sub-units based on rock mechanics properties.*

## **Representation of uncertainty**

*The following principles apply:*

- *Most parameters should be predicted with an uncertainty measure. In order to simplify matters, uncertainties will be given as an interval (value  $\pm$ unc). However, teams with a more precise prediction of uncertainty may also provide these, but all should provide the simple  $\pm$ unc ‘range measure’. The range measure could be interpreted as the 5/95 percentiles of the distribution if it is known.*
  - *Teams are encouraged to divide uncertainty into i) uncertainty in the mean value (or trends) for the specified rock unit (due to all sources of uncertainty) and ii) spatial variability (at the 30 m scale) within the rock unit – then two different columns should be used for this.*
-



- 
- *Teams should indicate their level of confidence in the prediction given by using the following scale (flags),*

*1 = value supported by local data or other reasons for a high confidence prediction,*

*2 = value produced by interpolation/reasoning,*

*3 = value based only on generic information.*

*It should be noted that different cubes in the domain may have different confidence levels.*

- *All uncertainty predictions and uncertainty values should be justified in written text.*

*If teams have more elaborate ways of expressing uncertainty, such information should be provided in addition to the information asked for above.*

---

**Product**

**Deformation modulus and rock mass strength**

*The focus for inter-comparison regarding deformation will be the deformation modulus,  $E_m$ , and some measure of its uncertainty. In addition, the 'best estimate' team will provide  $Q$ , RMR, and  $v$  values. The other teams should also provide these parameters, where possible. For a possible submission table, see Table 0-1*

*The focus of inter-comparison regarding rock mass strength will be the intact rock strength  $\sigma_c$  (and some measure of its uncertainty). In addition, the 'best estimate' team will also provide the rock mass strength  $\sigma_m$  as estimated by the  $Q$ -relation. If available, the other teams should also provide this as well as the other parameters ( $m$ ,  $s$  and  $a$ ) in the Hoek and Brown criterion. For a possible submission table, see Table 0-2. (The table can be divided into two component tables, i.e. one for deformation modulus and one for strength).*

**Stress**

*The focus for inter-comparison regarding stress will be the value of the principal stresses  $\sigma_1$ ,  $\sigma_2$ ,  $\sigma_3$ , and the directions (i.e. trend<sub>1</sub> and plunge<sub>1</sub> of sigma-1 and the plunge<sub>2</sub> of sigma2). This defines the six-component stress state. Measures of uncertainty should also be provided. Other parameters used in deriving the stress (if any) may also be provided. It is suggested that stresses are also delivered according to a format similar to Table 0-1. A possible submission format is outlined in Table 0-3.*

---

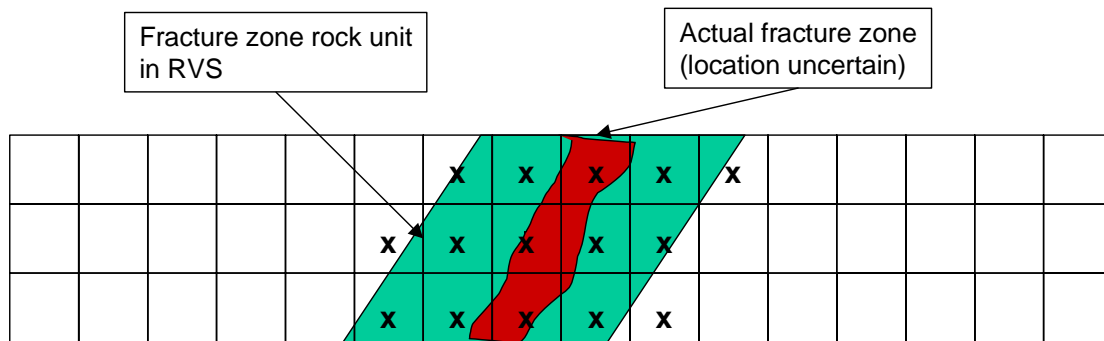


**Figure 0-1.** A cube may contain more than one rock unit. For example all cubes marked with x may contain the fracture zone (red) with unknown location within the fracture zone rock unit (green). For all x-marked cubes, teams should provide both rock mass and fracture zone properties.

**Table 0-1. Possible format for submission of deformation modulus and related parameters. The predictions are provided for each cube. Furthermore, if a cube contains more than one rock unit, a full line of prediction should be provided for each unit (i.e. there may be more than one prediction for a single cube). (Table 0-1 and Table 0-2 may be combined).**

<b>Cube ID</b>	<b>Rock Unit</b>	<b>Location</b>	<b><math>E_m</math></b>	<b>Uncertainty in <math>E_m</math></b>	<b>Confidence</b>	<b>Q, RMR, <math>\nu</math></b>
According to the 'best estimate' team's numbering system	The coding system used in the SKB RVS model should be adopted.	Co-ordinate of cube centre (x, y, z)	in GPa	Uncertainty in $E_m$ provided as a $\pm$ error value (or 5/95 percentiles if these are known).	1=value supported by local data or otherwise high confident prediction, 2= value produced by interpolation/reasoning,	If available. One column for each parameter (and another for uncertainty in parameter)
If the cube has more than one feature type, a full line of prediction should be provided for each type				The uncertainty may also be divided into spatial variability (on the 30 m scale) and other uncertainty. Then two different columns should be used.	3=value based only on generic information.	

**Table 0-2. Possible format for submission of rock mass strength and related parameters. The predictions are provided for each cube. Furthermore, if a cube contains more than one rock unit, a full line of prediction should be provided for each unit (i.e. there may be more than one prediction for a single cube). (Table 0-1 and Table 0-2, may be combined).**

<b>Cube ID</b>	<b>Rock Unit</b>	<b>Location</b>	$\sigma_c$	<b>Uncertainty in <math>\sigma_c</math></b>	<b>Confidence</b>	$\sigma_m, m, s, a$
<i>According to the 'best estimate' team's numbering system</i>	<i>The coding system used in the SKB RVS model provided should be adopted.</i>	<i>Co-ordinate of cube center (x, y, z)</i>	<i>Intact rock strength <math>\sigma_c</math> in H-B criterion</i>	<i>Uncertainty <math>\sigma_c</math> provided as a <math>\pm</math>error value (or 5/95 percentiles if these are known).  <i>The uncertainty may also be divided into spatial variability (in the 30 m scale) and other uncertainty. Then two different columns should be used.</i></i>	<i>1=value supported by local data or otherwise high confident prediction,  2= value produced by interpolation/reasoning,  3=value based only on generic information.</i>	<i>If available. One column for each parameter (and another for uncertainty in parameter)</i>
<i>If the cube has more than one type a full line of prediction should be provided for each type</i>						

**Table 0-3. Possible format for submission of stress predictions. The predictions are provided for each cube. Uncertainty in a parameter is noted by  $\pm u$ . Trend is noted by  $\alpha$  and plunge by  $\beta$ .**

<b>Cube ID</b>	<b>Rock Unit</b>	<b>Location</b>	$\sigma_1$	$\pm u$	$\sigma_2$	$\pm u$	$\sigma_3$	$\pm u$	$\alpha_1$	$\pm u$	$\beta_1$	$\pm u$	$\beta_2$	$\pm u$
<i>See Table 0-1</i>	<i>See Table 0-1</i>	<i>See Table 0-1</i>	<i>MPa</i>	<i>MPa</i>	<i>MPa</i>	<i>MPa</i>	<i>MPa</i>	<i>MPa</i>	<i>°</i>	<i>°</i>	<i>°</i>	<i>°</i>	<i>°</i>	<i>°</i>